Department of Civil Engineering,
University College,
Cork.

Soil Moisture and Stream-flow Modelling of an Intensively Grazed Grassland with a 30 Minutes Time Increment

By

Yan Lacaze

A Thesis submitted to the National University of Ireland
In part candidature for the Degree of Master of Engineering Science

October 2002

To my Family

Acknowledgements

The author wishes to express his thanks to the following people :

Prof. Ger Kiely, my supervisor, for his guidance and his encouragements.

Prof. John Albertson, from Duke University for his enthusiasm and helpful advice.

Prof. J.P.J. O'Kane, for use of the facilities of the Department of Civil Engineering, U.C.C

Dr. Michael Creed, for his enthusiasm for international relationships.

Fidelma Horgan, **Dermot Moynahan** and **Charlotte Le Bris**, for their permanent support and friendship.

Brendan Keenan, for his help and encouragements for my coming in Ireland.

Cécile Delolme, for her time and interest all along the year.

All the members of the Pourrissage Corp. for their support.

Abstract

A new parameterization of soil vegetation atmosphere transfers is described. The scheme uses a three-soil layer configuration to simulate the soil moisture, as it was found to give a more robust response compared to a two-layer soil scheme. The hydrological processes leading to the stream-flow simulation are based on the response of the soil moisture model. It consists of a ponding water storage which creates surface runoff. The moisture state of soil dictates a subsurface runoff, and a third component adds base-flow. The parameterization has been implemented with the intention of keeping the complexity low and making the calibration easier. The short time step used (30 minutes) made the calibration difficult but the results reflect the quick variability of the site (a gently sloping small grassland catchment (15 ha), near Cork, Ireland).

A simple phosphorus module was then combined to the existing model in order to simulate a phosphorus budget from soil to water, thus reproducing the impact of the management of the site on the stream water quality. This module has been developed from a hydrological viewpoint. To process this balance, three phosphorus pools are used. The most active one is the soil solution which is split between the first two soil layers. A second reservoir contains Morgan's P, and a third large storage contains a slowly reactive phosphorus. Uptake by plants takes place in the root zone. The discharge in the stream is simulated by two components draining the soil solution : one from the simulated surface runoff and the other from the simulated subsurface runoff.

Good simulations with a short time increment are more difficult to obtain, but once calibrated and validated, the model gives a more accurate representation of the site and still provides satisfactory results when increasing the time-step, whereas it is not true for the opposite process. The model is useful in predicting the P loss to the stream.

Table of contents

Chapter 1

Introduction

Chapter 1
Introduction

1-1 Introduction

1-1-1 The land surface

In recent years, the knowledge of the transfers of water and heat between the soil, the vegetation, and the atmosphere is improving. Climate modelling scientists have paid more and more attention to the processes occurring at the interface between the earth's surface and the atmosphere. Indeed the land surface plays an important part that has drawn an increasing attention for the past decades. It acts as a lower boundary for the atmosphere, exchanging heat, momentum and moisture. Many experiments have shown the influence of the soil nature and the vegetation coverage on the atmospheric circulation. Although the land may be less important as a forcing boundary than the oceans, it is more changeable and variable. Most remarkable is the water balance over the land surface. When the soil is wet it can exchange water with the atmosphere rapidly, but when, on the contrary, the soil is dry, it provides no water. Indeed the surface is much more responsive to the net radiation from the atmosphere than the oceans, which implies quicker responses with regard to the evaporation. Besides the land system is characterized by a wide range of heterogeneity, which explains the great development of studies dealing with the transfers between the land surface and the atmosphere. Different types of vegetation or different soil types mean different response to the forcing of the atmosphere, and so totally different processes can be observed.

But the land surface is also of crucial importance on a human point of view. The human being constantly faces the consequences of the inference between the land surface and the atmosphere. Floods, soil freezing, drought periods, erosion, pollution transport are only few examples as a consequence of human activities of the number of phenomena forced by the atmosphere.

1-1-2 The modelling effort

The only quantitative tools available for predicting the different mechanisms and for assessing the possible risks are climate models and their components of land surface simulation. A land surface parameterization intends to simulate the exchanges of heat, water and momentum over a given area. A hillslope model can be used for both research purposes and for application-oriented studies at hillslope scale, in collaboration with other scientific disciplines such as geotechnics, geochemistry, environmental impact studies, etc. Many Soil-Vegetation-Atmosphere Transfers (SVAT) models have therefore been developed for different purposes. Nowadays some SVAT models succeed in simulating well some variables dealing with the energy budget and the water balance, such as the evaporation and the soil moisture. But many questions arise when working on a simulation tool. How detailed must the parameterization be ? Which concepts and mechanisms should be included in the scheme and which ones should be neglected ? What level of complexity is required ? What are the relevant spatial and temporal scales ? What are the forcing conditions of the model and what does the model simulate ? What is the acceptable error in the simulation and how to assess the reliability of the parameterization ? and many others.

1-2 Objectives and methods of this study

1-2-1 Objectives

Within the context of physically based hydrological modelling, the objective of this study is to provide a suitable representation of a small grassland catchment area of 15 ha. This parameterization was initially thought for research with the goal to understand the processes occurring at the surface. The study site is considered homogeneous and the small size of the catchment area led our interest to a one-dimensional investigation of the processes. Our point of view for this study in terms of modelling is the point of view of the hydrologist. This study thus emphasizes the energy budget and the water balance of a column of soil and of atmosphere of one metre square. Biochemical processes or microscopic mechanisms are not explicitly represented. The parameterization is also guided by the concern to describe the processes on a physical basis with low complexity. This study includes a parameterization of the energy budget at the surface, describing the main fluxes. The equation that solves the energy budget is :

$$G = R_n - H - LE \qquad [\mathrm{W.m^{-2}}], \tag{1.1}$$

where G is the heat storage rate in the soil-vegetation medium, R_n is the net radiation at the surface, H is the sensible heat flux and LE is the latent heat flux.

The water balance is based on the simulation of the soil moisture profile using a three conceptual soil layer configuration. The flow of the adjacent stream is represented by simulating three components. The surface runoff or overland flows represents the quick response flow to rain events. A subsurface runoff or storm-flow constitutes the fast response of the soil to forcing precipitation, whereas the base-flow component is simulated using drainage.

The site is monitored by continuous measurements at thirty minutes intervals. A very good data set is available at a thirty minutes time increment for all the computations.

Finally, since the site is an intensively grazed grassland, it was interesting to see the effect of the site management in terms of water quality. A module of prediction of phosphorus discharge in the stream was then added.

The ultimate objective of this parameterization would be to change from a research scheme to a management strategies oriented application.

1-2-2 Methods

The development of this SVAT parameterization was carried out in a progressive way. First of all the energy budget was solved and a first scheme for the soil moisture simulation was studied. The soil moisture constitutes one of the main component of the scheme. Indeed it plays a part in the energy budget through the evaporation and controls the components that generates the stream water. Attention was thus paid to simulate correctly the soil moisture. The initial two soil layer configuration was improved by the addition of a third soil layer. Then, in order to assess the impact of the number of soil layers defined in the models and to investigate the role of different flow components, we used several formulations for surface runoff, subsurface runoff, diffusion, drainage and base-flow, adapted from recent SVAT models found in the literature. This study led us to take into account the principle of ponding water in the scheme. Likewise a subsurface runoff controlled by the soil moisture seemed to provide a suitable representation of the hydrological mechanisms on the catchment. However we had to investigate a way to represent the increase of the groundwater during long and intense rain events. The idea of macropores and preferential pathways adapted from literature provided an adequate answer for the completion of an acceptable simulation of the hydrograph.

As for the phosphorus module, it was developed in collaboration with Jean Noël Vidal as a final year project of the Ecole Polytechnique in France. It is based on a simplistic approach of the transfers of phosphorus occurring in soil, and focuses on the behaviour of the different forms of phosphorus under hydrological forcing conditions. The aim being to simulate the total phosphorus content in stream.

1-3 Structure of this thesis

This thesis is made up of five chapters, a list of references and a glossary of terms commonly used about the land surface modelling. A detailed presentation of the study catchment area is given in Chapter 2. It includes a presentation of the topography, the meteorological conditions over the area and the instrumentation on the site that provided the data. Chapter 3 details the progression in the modelling effort of the energy budget and of the soil moisture. It presents the different models tested and the conclusions we drew to achieve the SVAT parameterization. The final scheme is presented in chapter 4, including the description of the phosphorus module. Chapter 5 gives a summary and conclusions of this thesis, and mentions recommendations for further research.

Chapter 2

Description of the studied catchment area

Chapter 2
Description of the studied catchment area

2-1 Field site

2-1-1 Topographic data about the site

The research area is located in Donoughmore, 30 km Northwest of Cork, in the Southwest of Ireland. It is a 15 ha grassland catchment area (approximately 3003500 m, 210 m above mean sea level) nested in a larger sub-catchment of the Dripsey river that supplies the river Lee flowing through Cork.

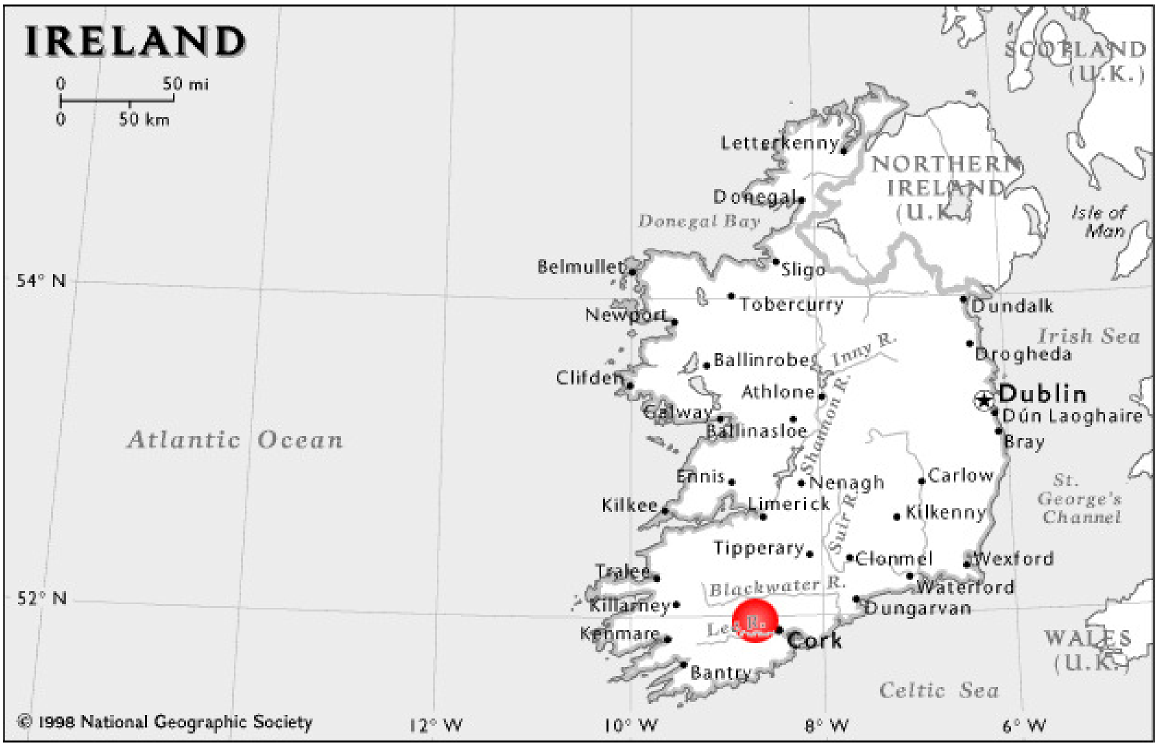

Figure 2-1 Location of the study area in Ireland.

This small catchment area is considered homogenous with respect to soil type, vegetation cover and atmospheric forcing data. It is gently sloping from 3 to 5 percent grade to a small stream. (see figure 2-2).

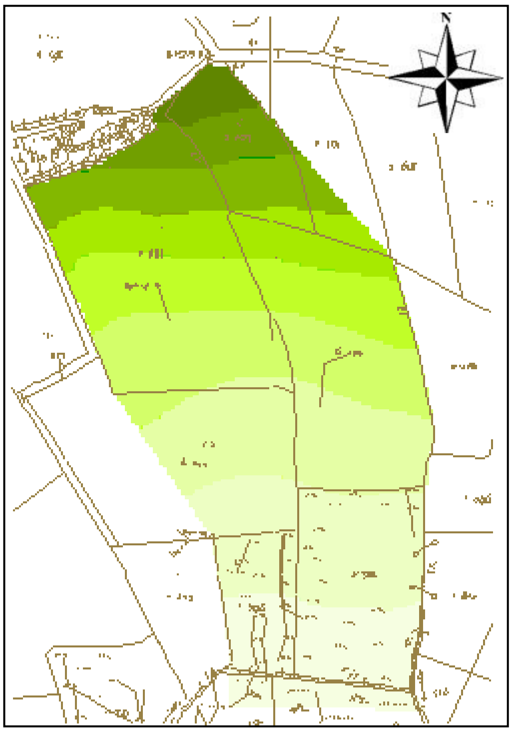

Map
Site 1
190.855 - 194.224
194.224 - 197.592
197.592 - 200.961
200.961 - 204.329
204.329 - 207.698
207.698 - 211.067
211.067 - 214.435
214.435 - 217.804
217.804 - 221.172
No Data

Figure 2-2 Elevation of the 15 ha catchment in m above mean sea level.

2-1-2 General meteorological data

The climate is temperate and humid, influenced partially by the Gulf Stream of the North East Atlantic. The mean annual temperature is around 12 degrees Celsius. Mean annual precipitation in the Cork region is about 1200 mm, as shown by figure 2-3. However the study period, which covers the period between July 2001 and July 2002, was especially wet, as one can notice, since the value of 1000 mm was reached approximately a hundred days before the other years. The rainfall regime does not follow a well-defined pattern. Long duration events occur at any time of the year with variable intensity. Events with high intensity and short duration occur mainly in summer. (see figure 2-4 and figure 2-5). As for the study period, 20% of the days recorded no rainfall (figure 2-6). Among the 80 % of rainy days of the study period, rainfall of 3 mm or less occurred 57 % of time (see figure 2-7).

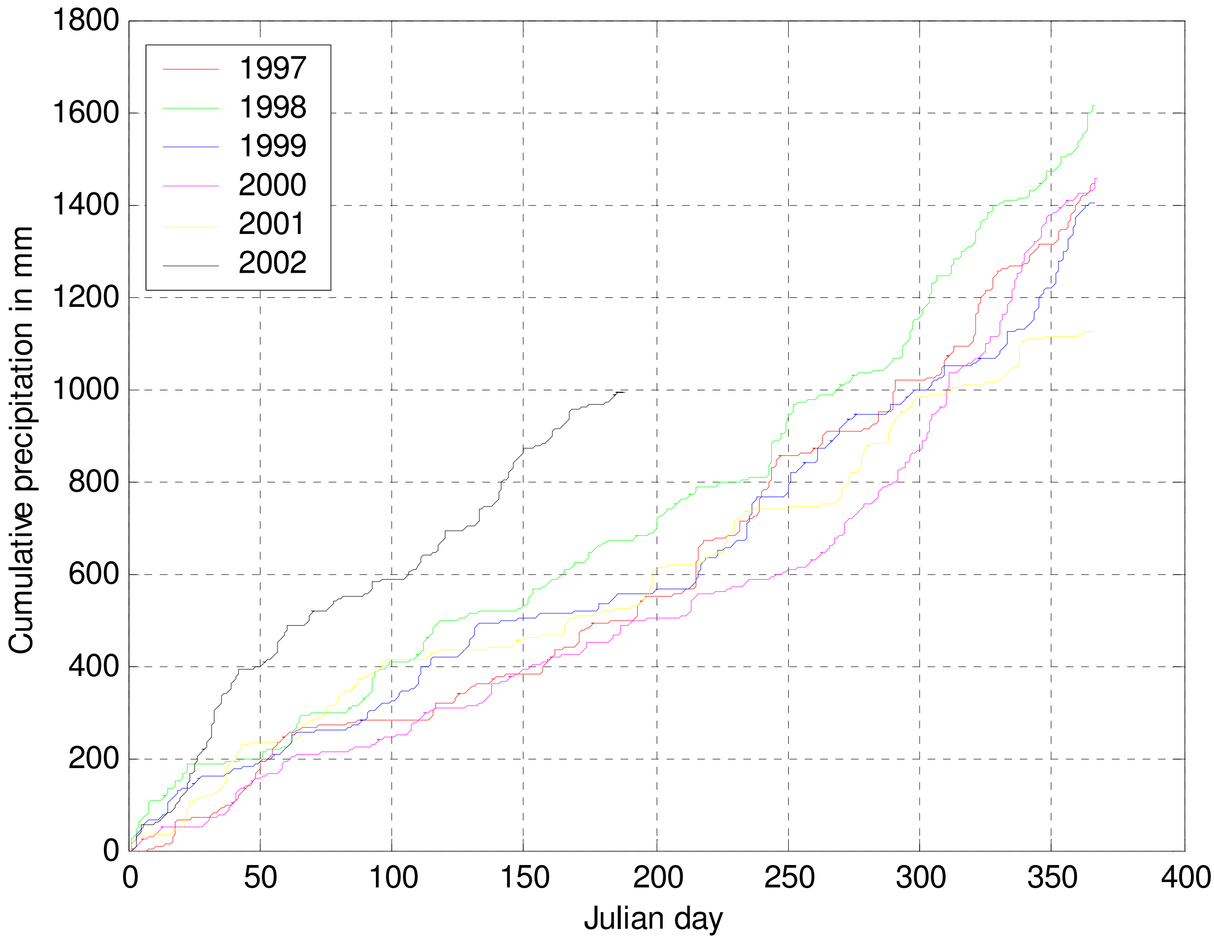

Figure 2-3 Cumulative precipitation over one year from 1997 to 2001 compared to 2002

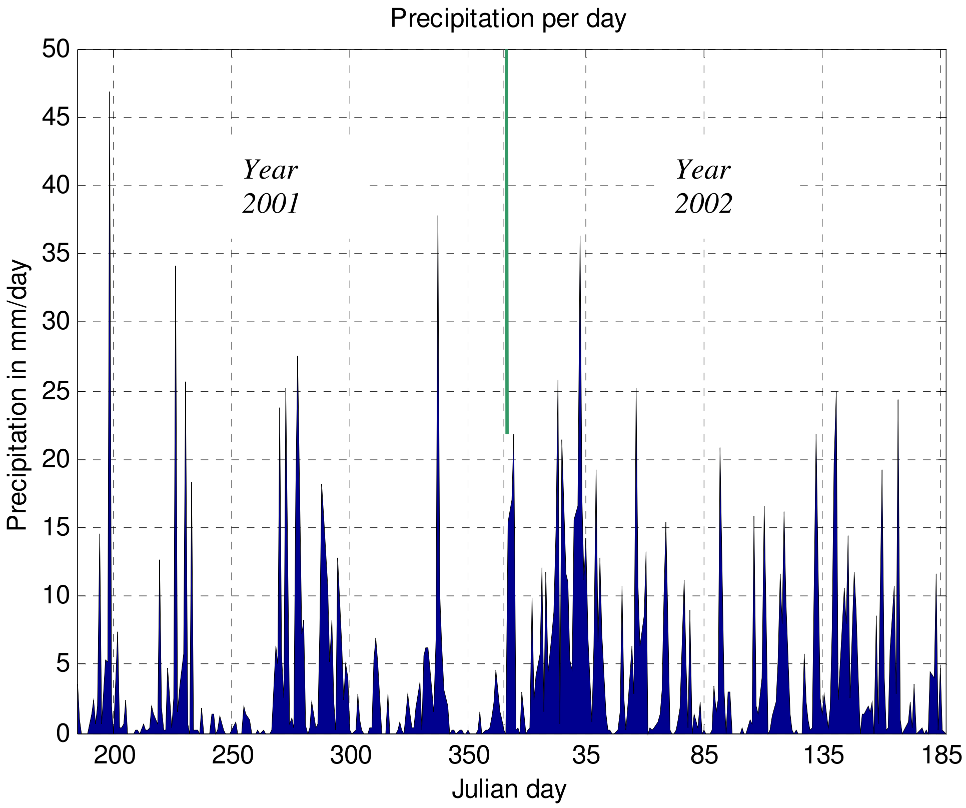

Figure 2-4 Precipitation per day during the study period. The maximum is slightly less than 50 mm/day

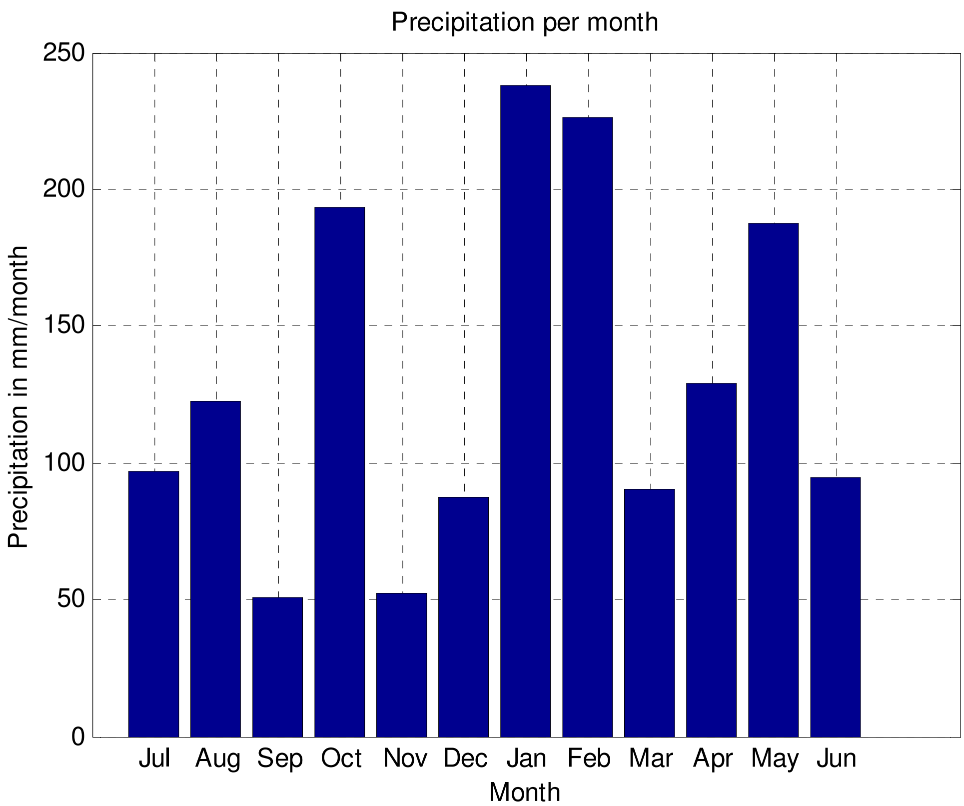

Figure 2-5 Precipitation per month. Even if January and February are wetter, there is no real “wet” and “dry” season.

Some statistical data are useful to try to characterize the rainfall events, and give a better comprehension of the atmospheric conditions.

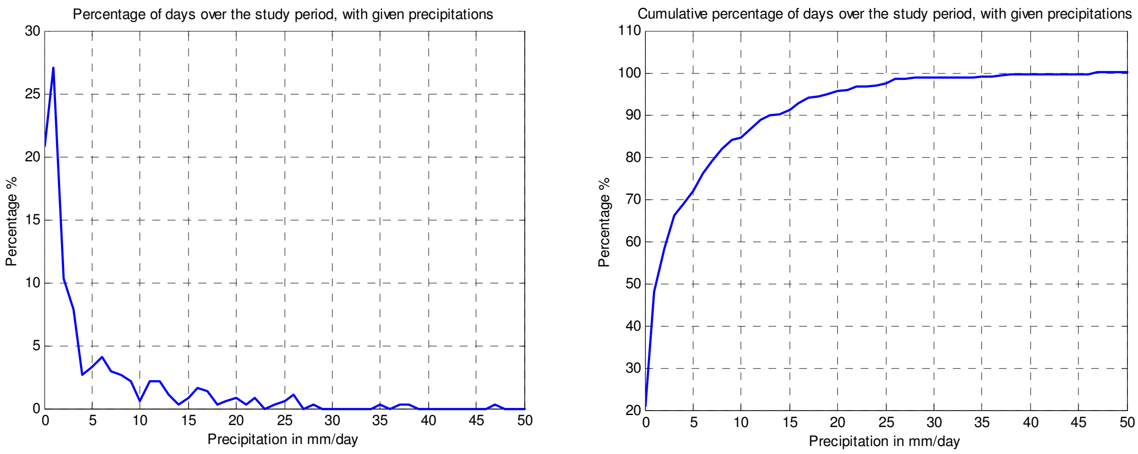

Figure 2-6 Distribution curves of precipitation over the study period, including dry days.

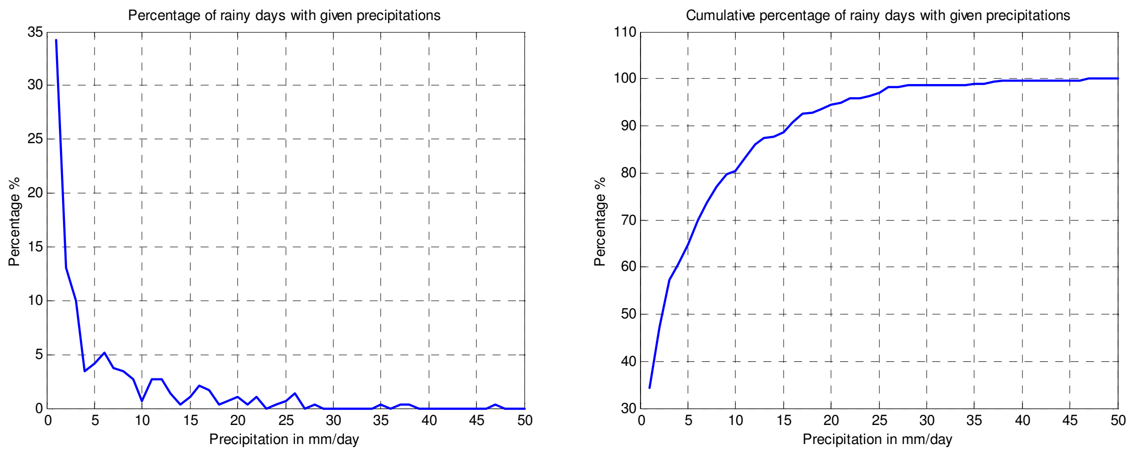

Figure 2-7 Distribution curves of precipitation dealing only with rainy days.

The influence of the Atlantic Ocean as a regulation is visible in the mean range of temperatures. Both soil and air temperature are not subjected to large variations. The monthly average air temperature range of 8 degrees, and the monthly mean temperature varies from a low 8°C to a high 20°C. (figure 2-8)

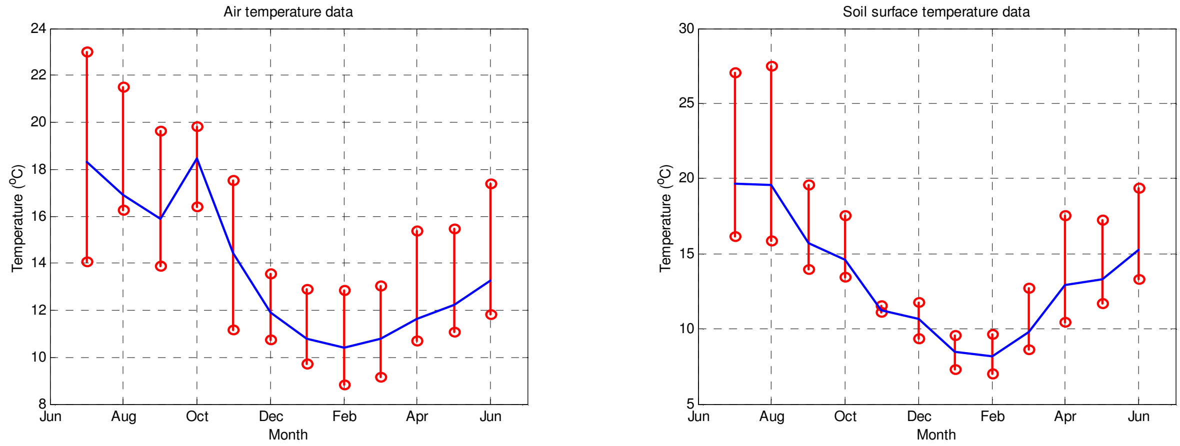

Figure 2-8 Monthly mean temperature of air and of soil surface, with the minimum and maximum temperature that occurred during the month. Note : there is a gap in data for the soil surface temperature in November.

It is also interesting to look at wind data, as far as wind is an important factor in the evaporation. Globally, the site could be described as open so that the airflow circulates with few constraints. As one can assume from the location of the site, the wind mainly blows from the Southwest. It is a moderate breeze but almost permanent. The mean wind speed at 10 m high over the study period is about 4.5 m/s (16 km/h), reaching peaks up to 16 m/s (57 km/h).

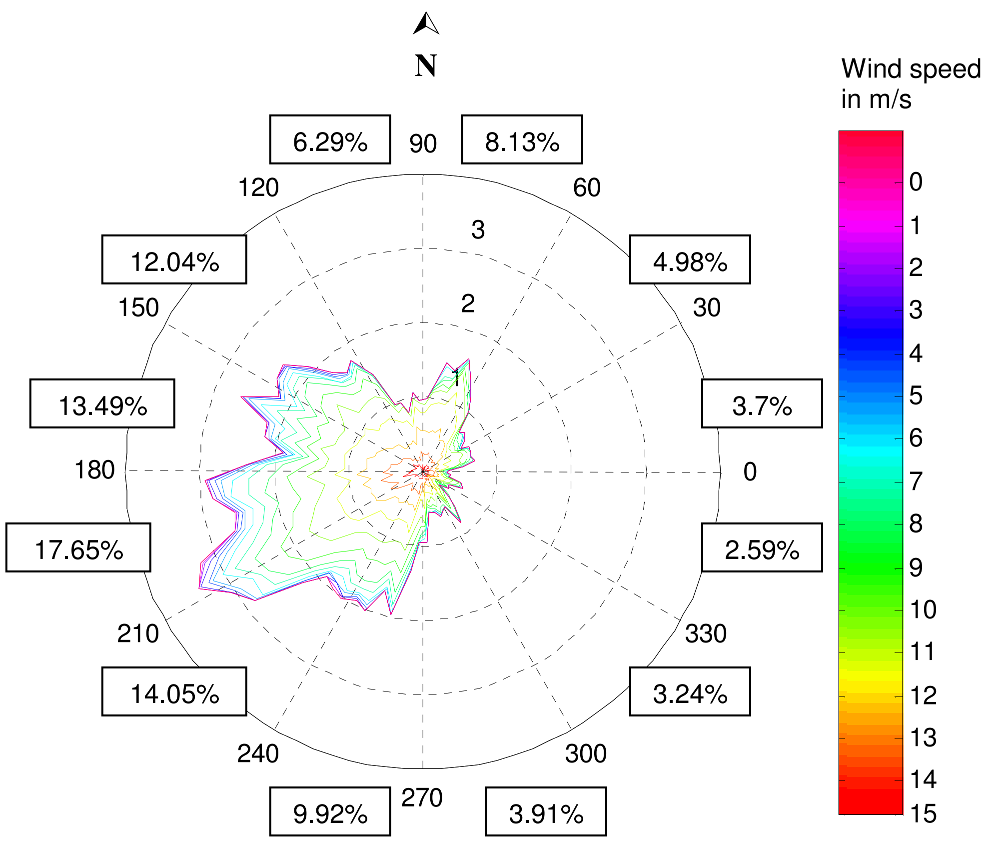

Figure 2-9 Wind rose indicating the percentage of occurrence of a wind direction at 5° intervals. Different colours correspond to different wind speeds. The boxed percentage are given for portions of 30°. (~75% comes from Western hemisphere).

2-1-3 Vegetation cover

The site is an intensively grazed grassland representative of the land use and vegetation in this part of the country. The management of the site follows the same pattern every year. Cattle graze alternatively on the three fields surrounding the study area and on the site itself, between February and April and between July and December. Cows are moved from one field to another every week. Between April and July, the grass is cut after 6 weeks of growth. The grass height on this good quality pasture land varies from a low 5 cm to a high 50 cm approximately. The grass is cut as silage two times per year and fertiliser is spread with the same time interval. Finally, in winter, between December and February there are no cattle grazing the field. But there are on occasions slurry applications.

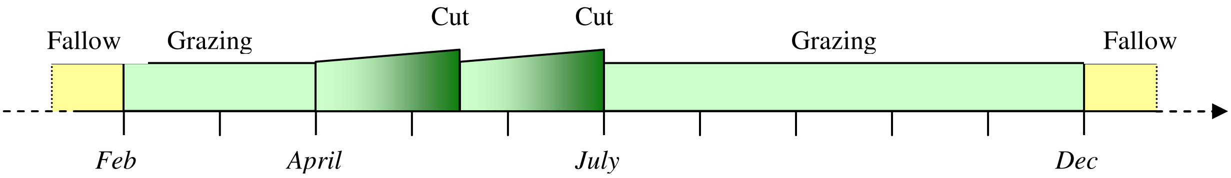

Figure 2-10 Typical field history. Note : months are shown for information only.

2-1-4 Soil description

The soil profile can be indented as follows : the top 5 cm make up a first layer of organic soil. It overlies a dark brown A horizon of sand texture to a depth of 20 cm. Then a yellowish brown B horizon of sand texture progressively changes into a brown gravely sand at about 30 cm deep which constitutes the parent material. A particle size analysis may also be useful to characterize the soil properties. Soil particles are arbitrarily separated into different categories of size. The results obtained for a sample taken on the field are presented below.

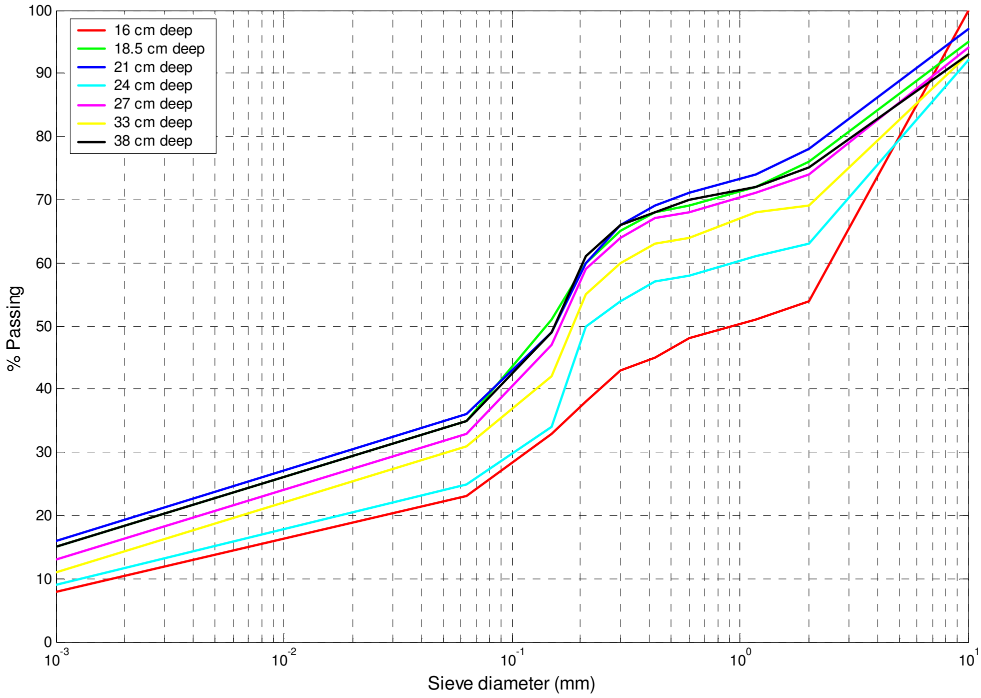

Figure 2-11 Soil particle distribution at different depths

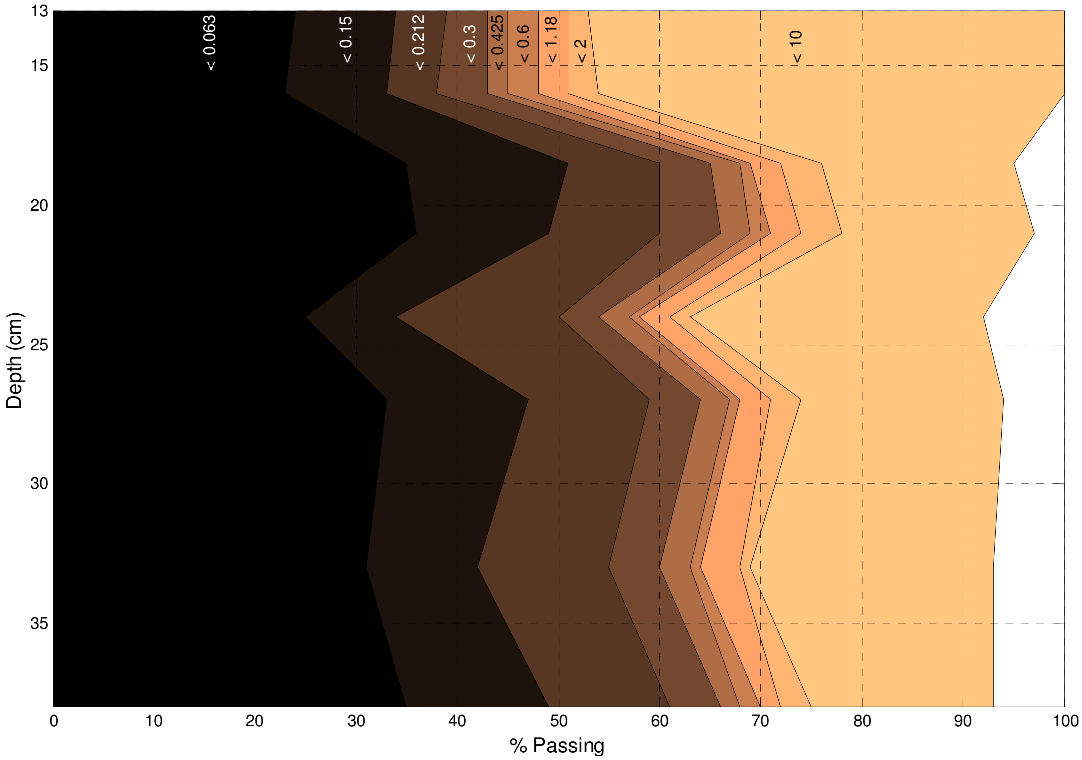

Figure 2-12 Soil particle distribution with depth. The sieve sizes are given in mm

We distinguish three main textural classes, depending on the size : sand, silt and clay, which can be further subdivided as shown in Table 1-1. A textural class corresponds to a range of particle size distributions with the same behaviour. The soil textural class can be determined through the U.S. Department of Agriculture (USDA) soil textural triangle (Figure 1-12). It allows us to conclude that the soil is mostly sandy loam. The knowledge of the soil textural class gives information about the behaviour of the soil, notably as far as infiltration and water diffusion is concerned.

Fraction name	Diameter (mm)
Sand	2.00 to 0.05
-Very coarse	2.00 to 1.00
-Coarse	1.00 to 0.50
-Medium	0.50 to 0.25
-Fine	0.25 to 0.10
-Very fine	0.10 to 0.05
Silt	0.05 to 0.002
-Coarse	0.05 to 0.02
-Medium	0.02 to 0.005
-Medium	0.005 to 0.002
Clay	< 0.002
-Coarse	0.002 to 0.0002
-Fine	< 0.0002

Table 2-1 Size fractions of soil particles according to the U.S. Department of Agriculture (USDA).

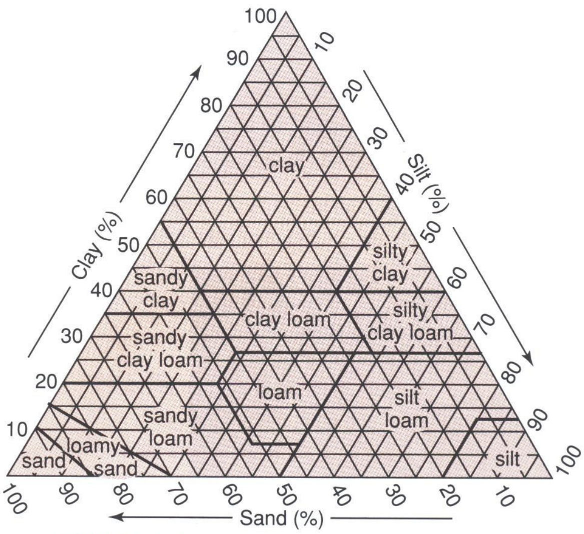

Figure 2-13 The USDA texture triangle. The percentage of clay is read horizontally from left to right. Silt is read diagonally down from the right. The two lines intersect in the texture class.

2-2 Monitoring the site

2-2-1 Introduction

Data about a specific environment constitute the basis for all kinds of studies. Data are collected from the field by an automatic weather station. The purpose of setting up a tower is multiple. First and foremost the interpretation of collected data gives a better knowledge of the nature of the site it concerns. The response of the field to forcing meteorological data can be better understood. One can then be interested in the modelling aspect. In that case data from field measurements are used in two ways. On the one hand they are the input of the hydrological model. On the other hand they are used to assess the performance of the model, whatever for calibration or validation purpose.

The tower that provided data for this study was set up in the middle of a field, in order to get the most representative data for the grassland. Measurements must indeed be carried out in an open field with a minimum of obstacles for data not to be distorted by irrelevant elements for the study. The tower is 10 metres high. It is thus influenced as far as main fluxes are concerned in a radius of less than 100 metres (*H.P.Schmid 1997*). It consists of a set of weather sensors connected to a central data logger which controls the measurements, the data processing and the digital storage of the sensors outputs.

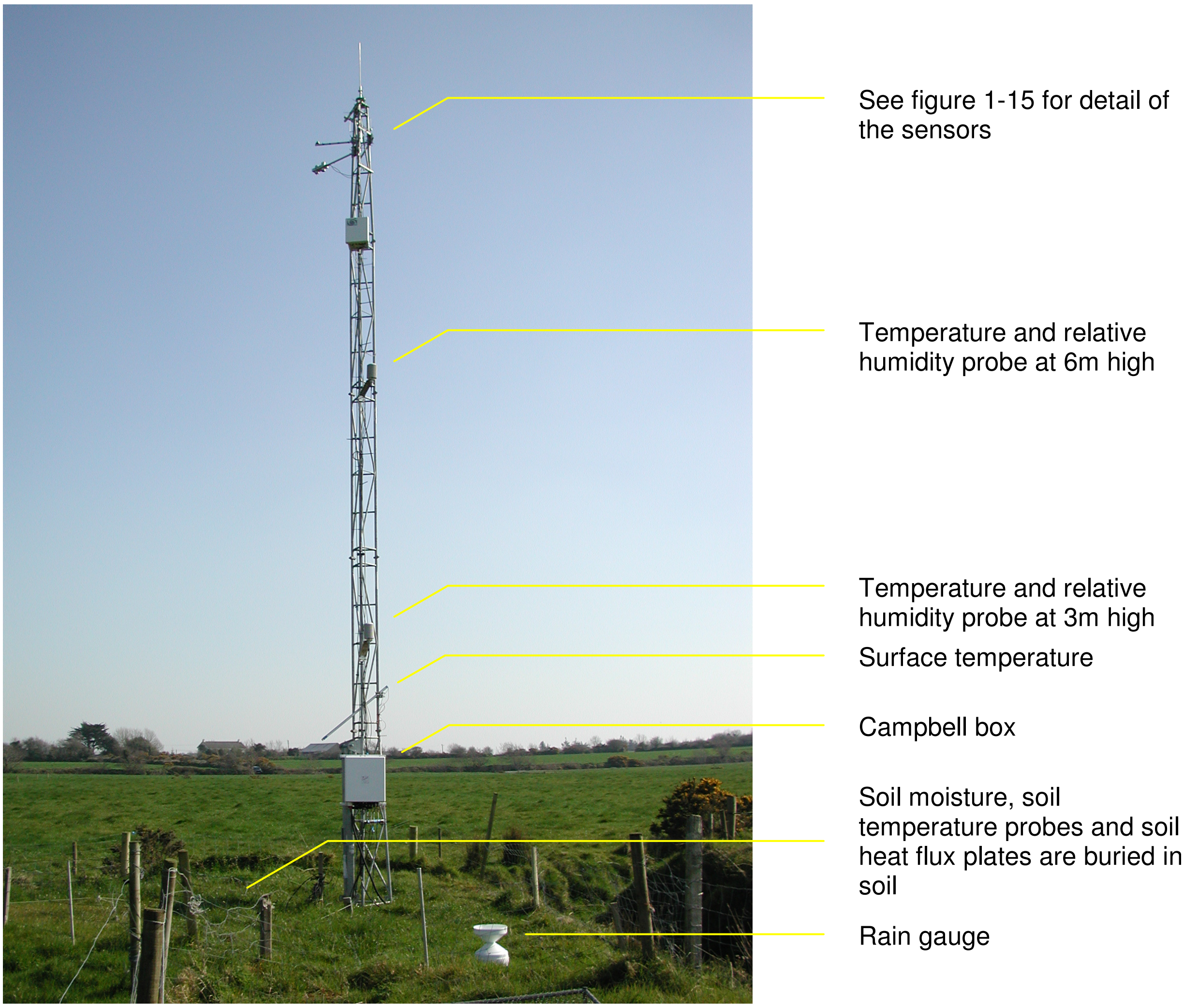

Figure 2-14 The 10m high tower and some of the weather sensors

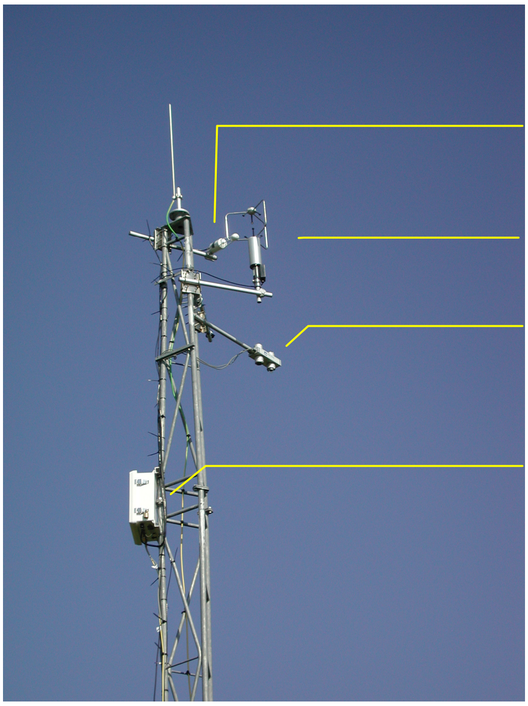

Figure 2-15 Instruments of the top of the tower

The Campbell box represents the active core of the tower. Indeed it shelters the instruments that process and store data, i.e. the data logger, the multiplexer as well as a modem telephone connection.

Moreover a barometric pressure sensor is protected in this box.

The instruments are concisely described below.

2-2-2 Precipitation

Precipitation being the main forcing parameter of hill slope processes, its measurement is crucial for the accuracy of the study. The most widely used rain gauge is a tipping bucket type rain gauge. Its principle is the following : precipitation is collected by the funnel and falls in one of the two buckets located at either end of a balance arm. When a bucket is full, the arm tips under the weight, thus emptying the bucket and positioning the second under the funnel. The tipping process repeats as long as rain continues to fall. Each tip corresponds to a fixed quantity of rainfall (0.2 mm). The rain gauge is connected to a data logger recording the number of tips in a time interval. In this site the time interval is 30 minutes.

Globally the accuracy of a tipping bucket rain gauge is good. However a degradation in accuracy can occur during very windy rain events, or heavy rainfalls.

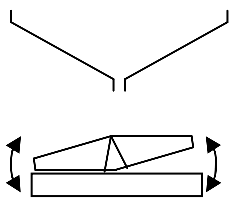

F igure 2-16 The tipping bucket principle

2-2-3 Temperatures

Air temperature is measured by a HMP45C temperature and relative humidity probe by Campbell Scientific. Two of these combined probes are located at 3 and 6 metres high. In order to perform accurate measurement the sensing element is shielded from direct or reflected solar radiation and from rainfall. The accuracy of this sensor is good and there is no need for recalibration. The temperatures that can be measured range from –40°C to 60°C, with a mean accuracy of 0.2°C.

An other kind of temperature probes is used to measure the soil temperature at different depths. It is the 107 temperature probe by Campbell Scientific. Three probes of this type are buried in soil. Two at 2.5 cm deep, and one at 7.5 cm deep. The accuracy and the range of temperatures measured are the same as for the HMP45C probe. The soil temperature is useful when studying the energy budget.

2-2-4 Relative air humidity

As mentioned before two HMP45C temperature and relative air humidity probes by Campbell Scientific are set up on the tower at 3 and 6 metres high. The measurements can range from 0.8 to 100 % with accuracy varying from 62 % to 63 % when relative humidity is greater than 90 %. The dependence with temperature is very low and the long term stability is better than 1 % per year.

2-2-5 Barometric pressure

Atmospheric pressure is recorded at regular time intervals like the other parameters with a PTB101B barometric pressure sensor, protected from humidity in the Campbell box. Pressure influences evaporation since it is related with the air humidity. This sensor gives the real pressure at the weather station whereas most barometers measurements are referred to sea level.

2-2-6 Wind speed and wind direction

In order to measure wind speed and wind direction a model 81000 ultrasonic anemometer from Young meteorological instruments is used.

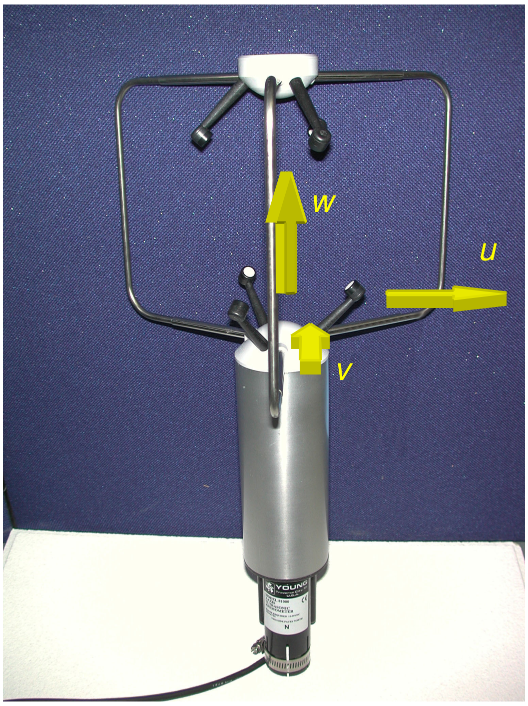

The principle to measure wind speed is based on the transit time of ultrasonic signals sent between three transducers. If air flows between the transducers, it alters the time that the sound waves take to normally travel along all three paths. The sonic anemometer measures the transit time and thus calculates speed of sound and wind velocity in all three dimension. The wind velocities are then transformed into orthogonal wind components *u*, *v*, *w* respectively in x, y and z direction. Positive *u* values indicate a wind blowing from the East, positive *v* values for a wind from the North and positive *w* values for a wind from below. The sonic anemometer measures at 10 Hz but averages are logged at 30 minutes intervals.

Figure 2-17 The sonic anemometer with the 3 computed orthogonal wind components

2-2-7 Radiation

- Description

The energy budget and the balance of radiation analysis are performed thanks to data collected by a CNR1 net radiometer from Kipp & Zonen. One of the features of this instrument is to measure separately four radiation components. It measures two components of solar radiation with two sensors (two CM3 pyranometers), one facing upward for the incoming solar radiation from the sky and one facing downward for the reflected solar radiation. They cover a spectral range from 0.3 to 3 micrometers. Likewise two sensors (two CG3 pyrgeometers) measure far infrared radiation from the sky and from the soil surface. The spectral range for it is between 3 to 50 micrometers. The sensors are designed to measure on either side the energy from the whole hemisphere (180°). Applications are then straightforward knowing the four components.

- Calculation of the albedo

Albedo is the ratio of incoming and reflected solar radiation. Its value is between 0 and 1. As for the grassland, the averaged albedo during the study period is around 0.23.

$$\text{Albedo} = \frac{\text{Irradiance from lower CM3}}{\text{Irradiance from upper CM3}} \tag{2.1}$$

- Calculation of the net solar radiation

Net solar radiation is the difference between the incoming solar radiation and the reflected solar radiation. It represents the solar radiation that is absorbed by the earth's surface.

$$\text{Net solar radiation} = (\text{Irradiance from upper CM3}) - (\text{Irradiance from lower CM3}) \tag{2.2}$$

- Calculation of the net far infrared radiation

Net far infrared radiation is the part that contribute to heating or cooling of the earth's surface.

$$\text{Net far infrared radiation} = (\text{Irradiance from upper CG3}) - (\text{Irradiance from lower CG3}) \tag{2.3}$$

- Calculation of the net (total) radiation

The advantage to measure separately four components of the radiation is here emphasised. The measurement of the four components allow to control the possible sources of errors.

$$\text{Net radiation} = \text{Net solar radiation} + \text{Net far infrared radiation} \tag{2.4}$$

Figure 2-18 The net radiometer from above, showing from left to right a pyrgeometer and a

pyranometer. The principle of these sensors called thermopiles is based on the properties of black bodies

Figure 2-19 The four sensors of the net radiometer

2-2-8 CO_2 Flux

The last instrument of the top of the tower to be described is a LI-COR's CO_2/H_2O gas analyser. The LI-7500 open path gas analyser measures densities of carbon dioxide and water vapour in air. These data used with those collected by the sonic anemometer allow to determine the CO_2 and H_2O fluxes by the eddy covariance technique. The flux of CO_2 is obtained from the vertical wind speed and the concentration of CO_2.

The LI-COR's gas analyser performs an open path measurement. No pumping is required. The principle is based on the property of carbon dioxide to retain a part of the infrared radiation emitted by the source housed in the body of the instrument.

An application of this instrument is to work on the carbon dioxide yearly budget.

Figure 2-20 The LI-7500 sensor head

2-2-9 Soil heat flux

Soil heat flux, often referred as G in literature, appears in the energy balance at surface. Even though this flux has a small magnitude compared to the other energy terms, it participates in the evaporation process and therefore must not be neglected. It is monitored on the site by two HFP01 heat flux plates from Campbell Scientific. They are buried at a depth of 50 mm below the surface. The sensors generate a signal depending on the temperature gradient.

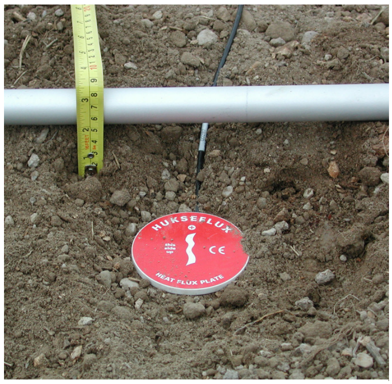

Figure 2-21 A soil heat flux plate at 5 cm below surface

2-2-10 Soil moisture

The volumetric water content of soil is measured with 6 water content reflectometers of model CS616-L. The probe consists of two 30 cm steel sticks connected to a circuit board. A reflectometer uses time-domain reflectometry (TDR) theory. It is based on the characteristics of the propagation of electromagnetic waves. The propagation velocity of an electromagnetic wave in a medium depends on the dielectric permittivity. The dielectric constant of water is 2 orders of magnitude higher than other materials, so that the change in this constant for a soil can be directly related to soil moisture content. The soil moisture occupies an important part of this study and the measurements carried out at different depths allow a detailed comprehension of water transfer processes. Indeed 6 probes are connected to the tower. Two probes are set up vertically, measuring volumetric water content. One from surface to 30 cm deep, the other from 30 to 60 cm deep. In addition four probes are set up horizontally at 5, 10, 25 and 50 cm deep. The probes are

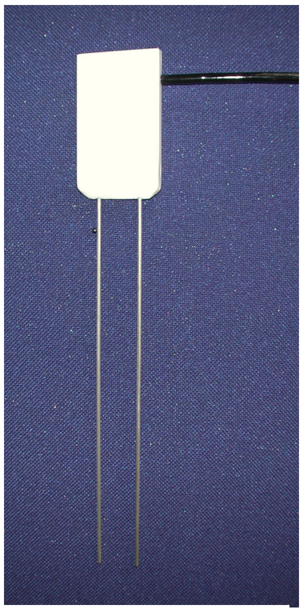

Figure 2-22 A TDR-probe

calibrated by a standard calibration considered suitable for sandy loam soil. However it is the relative rather than the absolute soil moisture content that is required.

2-2-11 Stream flow

A study about the water balance could not be carried out if one of its major components with rainfall was not monitored. The flow of the small stream adjacent to the catchment is monitored by measuring the height of water at a 90° V notch section weir with a Thalimedes device. The catchment area defined at this outlet is 15 ha. Data are collected every 15 minutes. Given that all data from the tower are recorded every 30 minutes, the flow is converted to this time increment.

Figure 2-23 The V-notch weir.

The flow is then computed knowing the height of water by the following formula :

$$Q = 1.390 \times h^{2.5} \qquad \text{with } Q \text{ in m}^3.\text{sec}^{-1} \text{ and } h \text{ in m} \tag{2.5}$$

2-2-12 Eddy correlation technique

Fluxes apparently difficult to measure on the field can be measured with an acceptable error with this method (for example the sensible heat flux or latent heat flux). This technique is based on the measurement of fluctuations in wind speed. These fluctuations produce no net vertical movement.

Let u, v and w, the orthogonal components of the wind velocity. At any time, these velocities can be written as the sum of an average term (e.g. $\overline{u}$) and a turbulent term (e.g. u'):

$$u = \overline{u} + u' \qquad v = \overline{v} + v' \qquad w = \overline{w} + w' \tag{2.6}$$

Other parameters can be separated in the same way, depending on the variable considered. Thus temperature T and air specific humidity q can be written as :

$$T = \overline{T} + T' \qquad \text{and} \qquad q = \overline{q} + q' \tag{2.7}$$

By definition, the average of the turbulent parts are null :

$$\overline{u'} = \overline{v'} = \overline{w'} = \overline{q'} = \overline{T} = 0 \tag{2.8}$$

Considering the wind speed as a volume flux per unit area, the vertical mass flux of moist air is the product of the air density ρ_a, and the vertical wind speed w. It is then straightforward to get the sensible heat flux, relating this product to specific heat of air per unit mass. The average sensible heat flux is :

$$H = \overline{\rho_a.c_p.w.T} \qquad (W.m^{-2}) \tag{2.9}$$

Likewise, the average latent heat flux can be written as :

$$\lambda E = \overline{\lambda.\rho_a.q.w} \qquad (W.m^{-2}) \tag{2.10}$$

If we assume that the wind components have been taken such as u is in the direction of the mean flow, then $\overline{v} = \overline{w} = 0$ and $\overline{u} \neq 0$. Moreover ρ_a can be considered as a constant, so that, in combining these assumptions with the previous equations, we get :

$$H = \overline{\rho_a.c_p.w.T} = \rho_a\overline{w'.(c_p.T)'} \qquad (W.m^{-2}) \tag{2.11}$$

$$\lambda E = \overline{\lambda.\rho_a.q.w} = \lambda.\rho_a\overline{w'.q'} \qquad (W.m^{-2}) \tag{2.12}$$

Chapter 3

Review of models

Chapter 3

Review of models

3-1 Introduction

3-1-1 Context of the modelling

The aim of this study was to develop a landsurface parameterisation scheme. But this notion is vague if the frame of the project is not defined more precisely. It is first interesting to know what is meant by the landsurface.

The landsurface is the interface where the incoming radiant energy is processed and converted into living material (by means of the photosynthetic activity), into evaporation or more generally into evapotranspiration and into heat. All the physics at this interface tackle different topics that cannot be separated or ignored from the landsurface. Human activities continuously face the potential of the landsurface (floods, eutrophication, pollution dispersion, etc.). Depending on the activities and the area of interest, the landsurface is considered from different points of view. Meteorologists, hydrologists or ecologists have different perceptions of the relative importance of the phenomena occurring at this interface, their time constants or the main physical laws.

A landsurface parameterisation scheme intends to describe the energy, mass and momentum exchange at the earth’s surface. Recent years have seen an increased interest in landsurface parameterisation. The knowledge of transfers of water and heat between the soil, vegetation, and the atmosphere has greatly been improving. Soil-Vegetation-Atmosphere Transfers (SVAT) models have known a rapid expansion on a theoretical point of view as well as for their applications. Nowadays such schemes operate within global climate models, for atmospheric weather predictions, as hydrological models for water resources or ecological models…). Landsurface schemes are developed depending on the intended application, and so, include different concepts, at different levels of complexity. But whatever the purpose of the model, it is necessary for the landsurface to be realistic to improve the predictive capability.

The treatment of the landsurface processes is largely determined by the spatial and temporal resolution adopted. As far as this study is concerned, it concentrates on a hydrological point of view. As underscored by A. Henderson-Sellers (1995), the emphasis for hydrological models must be set on a good simulation of the cycle of surface and subsurface moisture. Detailed parameterisation of surface energy and momentum fluxes are slightly less important. As for both temporal and spatial scales, the choice was mainly led by the availability of data. Data being the gold of research, we had the great opportunity to deal with good continuous measurements at 30 minutes intervals, on the small catchment described in chapter 2. The spatial scale was dictated by the size of the catchment. The short time increment used for measurements represented an interesting challenge on a modelling point of view, so that the 30 minutes time step was used as temporal scale. These choices led us to face difficulties to reliably represent the processes, since the shorter the time step and the smaller the scale, the more detailed the mechanisms must be.

3-1-2 Main characteristics and summary

The interest of this study only concerns one dimensional landsurface parameterisation schemes. The aim is to predict the state of some variables by modelling a column of soil, vegetation and atmosphere of 1 m², and generalising the outputs for the whole catchment area (15 ha). Soil moisture being of critical importance to the physical processes at the land/air boundary. (Shao et al. 1994), emphasis is put for its simulation. Thus, configuration of soil layers is of fundamental importance and the effect of some configurations are explored. In order to assess the impact of the number of soil layers defined in the models, we have used several formulations for surface runoff, subsurface runoff, diffusion, drainage and base-flow, adapted from recent SVAT models (ISBA, SEWAB, LAPS). A two-layer soil hydrological configuration developed by Albertson and Kiely (2001) was used as a basis for the different schemes. The ISBA model (Noilhan et al. 1999) has been used as a first attempt for the water budget. We have improved the results by adding a third soil layer as advocated by A. Boone et al. (1999). In parallel with that, we tested the SEWAB model (Mengelkamp et al. 1999) and the LAPS model (Mihailović 1996) in their three-layer and multi-layer soil configurations.

3-2 The initial SVAT model

3-2-1 Variables and parameters

The initial SVAT model was mainly inspired by the Simple Parameterization of Land Surface described by J. Noilhan and S. Planton (1989). Their parameterisation was guided by the concern to keep as low as possible the number of parameters and to conserve the main mechanisms that control the energy and water balance at the surface. The vegetation for example is simply described.

This scheme takes into account the wide range of properties of soils under temperature and water stress. Heat and water transfers are dependent upon the soil texture and the soil moisture content. Vegetation reproduces the main water exchanges at the interface between ground surface and atmosphere, such as interception, transpiration, direct evaporation and the influence on bare soil evaporation. The soil moisture content and the processes governing the changes are computed for two soil layers : an upper thin layer and a deeper one, using a force restore method. It computes five prognostics variables listed below :

- Surface temperature T_s, used to describe the energy exchange at the land cover surface.
- Mean surface temperature T_2.
- Surface volumetric water content w_g.
- Mean volumetric water content w_2.
- An interception water reservoir for canopy W_r.

The parameters aim to put a figure on the properties of soil and vegetation. They are derived from Clapp and Hornberger (1978) who used the USDA classification.

The main parameters for the physics of water transfer are :

- the saturated volumetric water content w_{sat}.
- the wilting point volumetric water content w_{wilt}.
- the saturated hydraulic conductivity K_{sat}.
- the slope in the retention curve b. see Clapp and Hornberger 1978.

The hydraulic conductivity is related to the volumetric water content w by the formula :

$$K = K_{sat}.\left(\frac{w}{w_{sat}}\right)^{2b+3} \tag{3.1}$$

Since soil is divided into two layers, we must fix an arbitrary lower boundary for calculations. This depth is referred as d_2, and represents the depth at which water fluxes in soil become negligible for a period of one week. In this first model d_2 is thus deeper than the root zone. Vegetation is numerically parameterised by a coefficient *veg* that represents the fraction of vegetation protecting the ground from solar radiation. The Leaf Area Index (LAI) also characterises vegetation. Moreover a resistance parameter R_S, controls the transfer of water from the root zone to the leaves. When the soil is easily supplied with water, a minimum resistance R_{Smin} only depends on the kind of leaves, since it is related to the stomatal resistance. Finally the albedo, the emissivity and the roughness length are also parameters appearing in the parameterisation.

3-2-2 The surface fluxes

The energy budget considered is given by the following equation :

$$G = R_n - H - LE \qquad [\mathrm{W.m^{-2}}], \tag{3.2}$$

where :

G is the heat storage rate in the soil-vegetation medium.
R_n is the net radiation at the surface.
H is the sensible heat flux.
LE is the latent heat flux.
The water vapour flux E is the sum of the evaporation from the soil surface E_g and the vegetation evapotranspiration E_v.

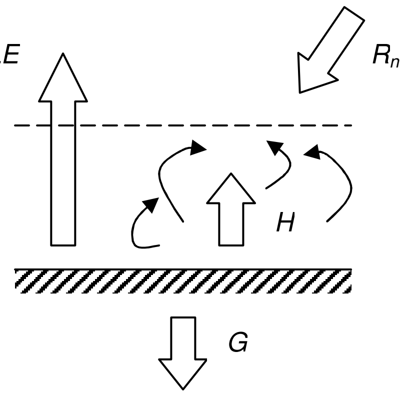

Figure 3-1 The energy budget

The net radiation at the surface is the sum of the absorbed fraction of incoming solar radiation R_{sw} and of the infrared radiation R_{lw} to which we subtract the emitted infrared radiation :

$$R_n = R_{sw}.(1 - \alpha) + \varepsilon.(R_{lw} - \sigma.T_S^4) \tag{3.3}$$

where α is the albedo (about 0.23 for the grassland). ε is the emissivity (about 0.98) and σ the Stefan-Boltzmann constant.
The sensible heat flux H is calculated by means of a classical formula we can find in Garrat 1994 for example :

$$H = \rho_a.c_p.C_H.V_a.(T_S - T_a) \tag{3.4}$$

where c_p is the specific heat capacity of air, equals 1005 J.kg^{-1}.K^{-1} .
ρ_a is the air density = 1.29.
V_a is the wind speed and T_a is the air temperature.
C_H is the drag coefficient of which a description can be found in Brutsaert 1984.

$$C_H = \left(\frac{k}{\ln\left(\frac{z_1}{z_0}\right)}\right)^2 \tag{3.5}$$

where k is von Karman constant = 0.378, z_1 the height of measurements and z_0 the roughness length.

The evaporation has two components. The evaporation from soil surface E_g and the evapotranspiration E_v. They are calculated as follow :

$$Eg = (1\text{-}veg).\rho_a.C_H.V_a.(h_u.q_{sat}(T_S) - q_a) \tag{3.6}$$
$$E_v = veg.\rho_a.C_H.V_a.(h_v.q_{sat}(T_S) - q_a) \tag{3.7}$$

where $q_{sat}(T_S)$ is the saturated specific humidity at temperature T_S., and q_a is the atmospheric specific humidity (see Appendix for details).

h_u is the relative humidity at the ground surface. It depends on the soil moisture in the first thin layer w_g, and the field capacity w_{fl} (see Appendix).

As for the evapotranspiration, the coefficient h_v takes into account the direct evaporation E_r from the fraction δ of vegetation covered with the intercepted water.

$$Er = veg.\frac{\delta}{Ra}.(q_{sat} - q_a) \tag{3.8}$$

In this equation, R_a is the aerodynamic resistance.

We then calculate $G = R_n - H - (E_v+E_g).L_v$. This leads to the computation of the soil surface temperature T_S and its mean value T_2 over one day τ. The equations below are in the linearised form in which they are applied :

$$\frac{T_S(t+dt)-T_S(t)}{dt} = C_T.G - \frac{2\pi}{\tau}.(T_S(t)-T_2(t)) \tag{3.9}$$

Diurnal forcing ⮥ ⮤ This term tends to restore T_s to T_2

$$\frac{T_2(t+dt)-T_2(t)}{dt} = \frac{1}{\tau}.(T_S(t)-T_2(t)) \tag{3.10}$$

The coefficient C_T is taken from Garrat. (see Appendix).

3-2-3 The soil water

The equations that simulate the soil water content are presented in this section. The model computes three variables for the soil water treatment w_g, w_2, and Wr. w_g is the soil moisture in the first thin layer. w_2 is the volumetric water content in a column of soil of depth d_2. W_r is a reservoir for water retained on the vegetation. Thus when precipitation occurs, it is first partially stored on the vegetation, in W_r. What falls through is then processed to update the soil moisture in both layers by equations based on a force restore method. The behaviour of the reservoir W_r follows the equation :

$$\frac{\partial W_r}{\partial t} = veg.P - E_r - R_r \tag{3.11}$$

where P is the precipitation rate, so that $veg.P$ is the intercepted water on leaves. R_r is the runoff from the interception reservoir occurring when W_r exceeds a maximum value.

This maximum water content on the foliage is $Wrmax = 0.2.veg.LAI$. (3.12)

$$\frac{\partial w_g}{\partial t} = \frac{C_1}{\rho_w.d_1}.(P_g-E_g) - \frac{C_2}{\tau}.(w_g-w_{eq}) \ , \ 0 \le w_g \le w_{sat} \tag{3.12}$$

Influence of the atmospheric fluxes ⮥ ⮤ Diffusion of water through soil

$$\frac{\partial w_2}{\partial t} = \frac{1}{\rho_w.d_2}.(P_g - E_g - E_r) - K \ , \quad 0 \le w_2 \le w_{sat} \tag{3.13}$$

where P_g is the precipitation reaching the ground, ρ_w the density of water. d_1 and d_2 are depths set respectively to 10 cm and 30 cm. C_1, C_2 are diffusion coefficients and w_{eq} is an equilibrium value of moisture content, taking into account gravity (see Appendix for details). Equation (3.13) for the soil moisture w_2 in the second layer differs from the one in Noilhan

Planton (1989) to include a drainage at the bottom of the layer. This drainage is $K.dt$, where K is the hydraulic conductivity defined with equation (3.1).

3-2-4 Results and comments

The results of the simulation with this model are presented briefly in this section. The main idea about this model is that it gives a first approach of a one dimensional parameterisation of the catchment and thus gives an idea of the processes occurring at the land surface.

The energy budget derives from commonly accepted equations. The parameterisation used for R_n and H are widely held up in literature. The evaporation is still the object of a lot of research to improve the simulation of the latent heat flux. However the results obtained with this set of equations are satisfactory, as long as they respect the seasonal and diurnal trends. The energy budget allows an acceptable simulation of the soil temperature.

Figures below present a comparison of the simulated variables and the measured values.

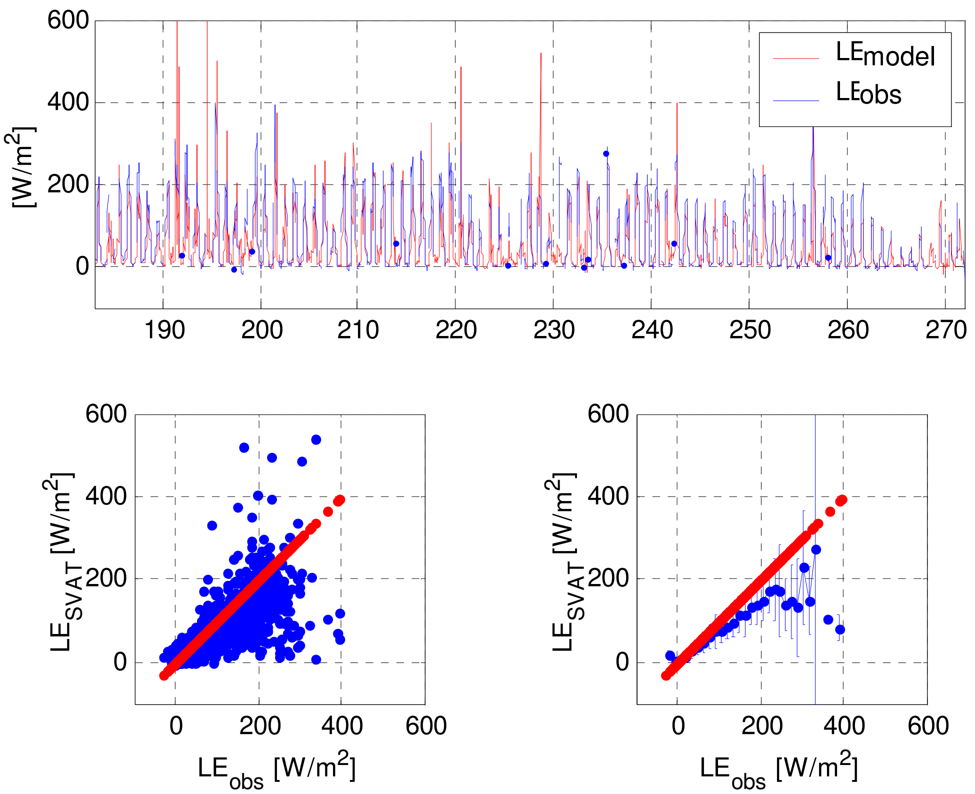

Figure 3-2 Example of results of the simulation of the latent heat flux. The magnitude and the diurnal variations are correctly simulated.

The latent heat flux enters in both the energy budget and the water balance. Although the quantity of water involved in evaporation is not as important as the other terms of the water balance equations, its simulation influences the quality of the results for soil moisture.

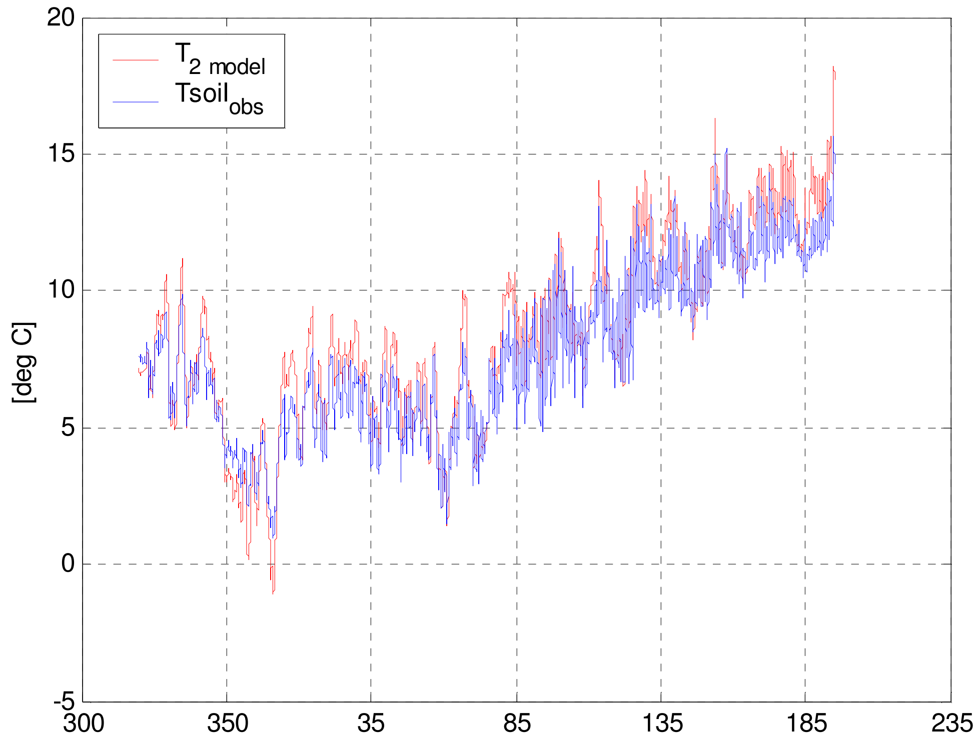

Figure 3-3 The soil temperature simulation over a long period shows that the seasonal trend, as well as the magnitude, is respected by the model.

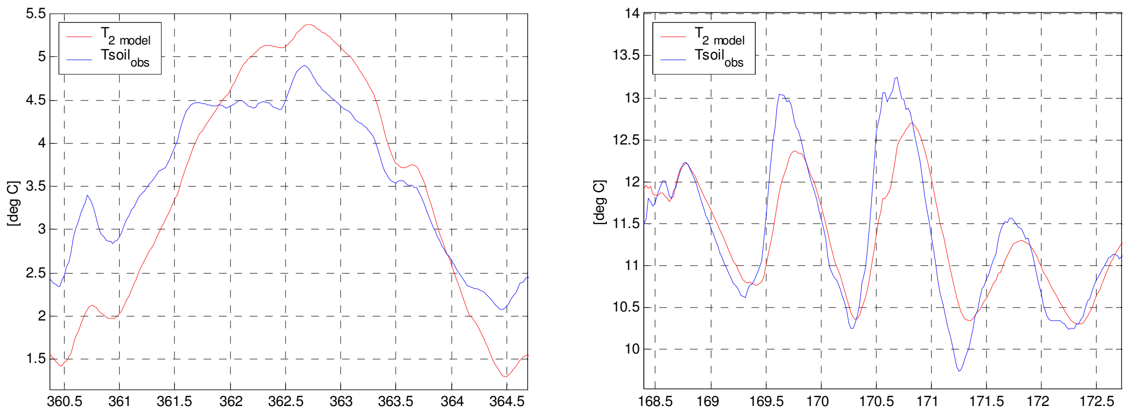

Figure 3-4 A detail of a few days in winter and in summer. Generally the variation is respected, even if the magnitude differs of about 1 °C.

The results obtained for the energy budget are satisfactory. One the one hand because the simulated curves fit approximately the observed values, and on the other hand because the budget considered is quite simple, and the equations involved are not heavily parameterised. This is a very positive aspect. Indeed the benefit on the simulations that could bring a more detailed parameterisation would not balance the increase in complexity and in the numbers of parameters required. It is interesting to note that the results presented above were obtained based on parameters values found in literature, without any calibration or adjustment.

The results of the simulations of the volumetric soil water content are presented hereunder. Initially, we mainly focus on the simulation of the deeper layer including the root zone. This layer is indeed the most representative of the state of soil. It is the centre of the processes governing the water balance. That is the reason why we first focus on getting a good and robust simulation of the soil moisture in this layer. Inappropriate results would stop the progress to a realistic stream flow simulation. As for the first layer, it is very sensitive and is for the moment only used as an interface between soil and atmosphere.

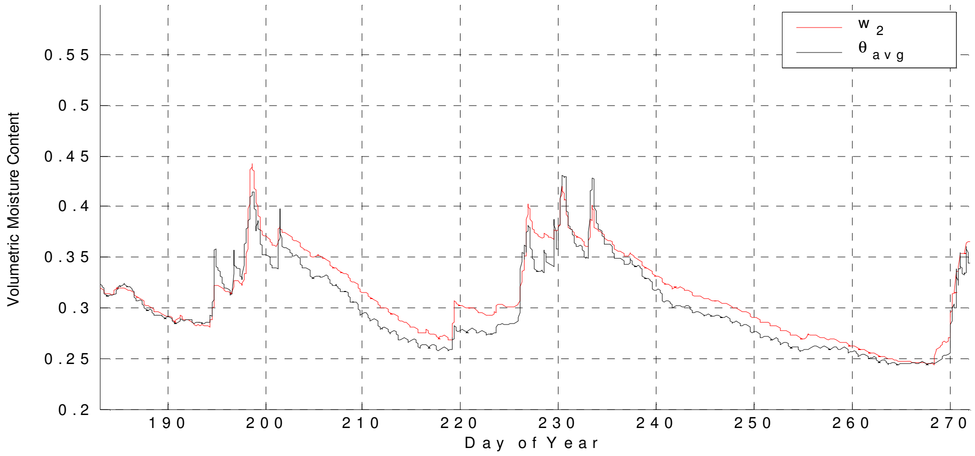

Figure 3-5 A comparison of the simulated moisture in soil at a depth of 30 cm (red line) and a calculated mean soil moisture observed at this depth (black line). This period corresponds to the period of calibration.

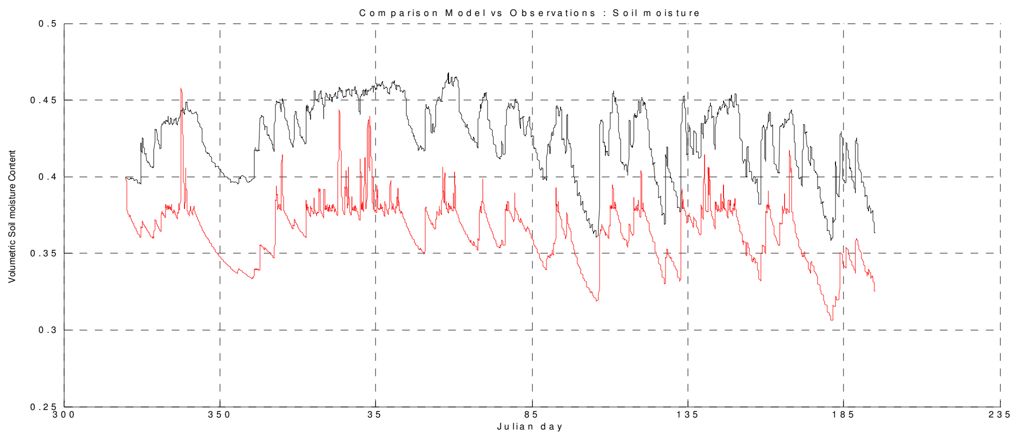

Figure 3-6 This figure shows a simulation (red) compared to the observations (black). The simulation was run with the same set of parameters for this period as the parameters used in figure 3-5. This simulation was aimed to validate the model. However the results are clearly underestimated, even if the response of the model follows the same pattern as the observations.

The results presented in the previous figures show two aspects of the model. The positive aspect is that, the model has the possibility to simulate correctly the soil moisture (figure 3-5) in the second layer, if calibration is correct. The negative aspect is that the model is not robust, as seen by the poor results obtained for the period of validation (figure 3-6). So that the next step in this study was to reinforce the robustness of the model in order to keep its capability of prediction and improve the representation of the water processes in soil.

3-3 Improvement of the soil moisture simulation

3-3-1 Method

A workshop about soil moisture as part of the Program for the Intercomparison of Land surface Parameterisation Schemes (PILPS) allowed great progress on this topic, and made a rich source of possibilities to investigate in order to improve the model. (Shao et al. 1996, Henderson-Sellers et al. 1995, Desborough et al. 1996). Many SVAT schemes use three soil layers for computing the soil water content evolution. Generally the organisation of the layers starts at the top with a thin surface layer including bare soil, then the second subsurface layer corresponds to the root zone and the third layer constitutes a deeper soil reservoir, a sub-root layer, often down to the water table. (e.g. Land Air Parameterization Scheme (LAPS) (Mihailović 1996), Best Approximation of Surface Exchanges scheme (BASE) (Desborough and Pitman 1998), Biosphere Atmosphere Transfer Scheme (BATS) (Dickinson et al. 1993)).

The idea to improve the soil moisture simulation is to distinguish a root extraction layer and a base-flow layer. This distinction aims to capture the diversity of moisture with depth. Moreover this distinction renders better the physical reality of the different processes and their time constants. The root zone must produce a more rapid time response in terms of changes in soil moisture compared to the deeper soil layer, whose water content produces a more attenuated time series with precipitation. (Betts et al. 1993, Albertson et al. 2001).

Thus, we have improved the model by adding a third soil layer as advocated by Boone et al. (1999), to the existing model.

3-3-2 New configuration

The new soil configuration includes three soil moisture reservoirs. The energy budget equations and all the previous equations governing variables other than soil moisture have been kept to calculate the fluxes of heat, the time evolution of soil temperatures and the water interception storage. The governing equations of soil moisture evolution with time are written as :

$$\frac{\partial w_g}{\partial t} = \frac{C_1}{\rho_w . d_1} . (P_g - E_g) - D_1 \tag{3.14}$$

$$\frac{\partial w_2}{\partial t} = \frac{1}{\rho_w . d_2} . (P_g - E_g - E_r) - K_2 - D_2 \tag{3.15}$$

And for the third layer :

$$\frac{\partial w_3}{\partial t} = \frac{d_2}{(d_3 - d_2)} . (K_2 + D_2) - K_3 \tag{3.16}$$

All the gravitational drainage is represented by K and the vertical diffusion of soil moisture is represented by D. C_1 is a dimensionless coefficient used in the surface force restore equation. As previously, ρ_w is the density of water and d_1 is the depth of the surface layer. However d_2 has a more physical sense than previously, since it represents the depth of the root zone only. d_3 is the total modelled depth of soil. The definition given by Boone et al. (1996) for d_3 is that d_3 is the depth at which the soil moisture change with respect to time can be neglected in comparison to the time step used. This information, that can be deduced from measurements, was not available for this study. However the water table is assumed to be around 2 metres deep. That gives an upper limit for its value. The average water contents in the surface layer, the root zone and the deep soil layer are respectively w_g, w_2 and w_3. These variables are limited to a water content at saturation called w_{sat}. It represents the maximum quantity of water the soil can retain. As noticeable in the equations, the root zone overlaps the surface layer, while the deep soil layer starts at the base of the root zone.

The drainage K and vertical diffusion terms D are given by :

$$D_1 = \frac{C_2}{\tau}(w_g - w_{eq}) \tag{3.17}$$

$$D_2 = \frac{C_4}{\tau}(w_2 - w_3) \tag{3.18}$$

$$K_2 = \frac{C_3}{\tau}\frac{d_3}{d_2}\max(0, (w_2 - w_{fc})) \tag{3.19}$$

$$K_3 = \frac{C_3}{\tau}\frac{d_3}{(d_3 - d_2)}\max(0, (w_3 - w_{fc})) \tag{3.20}$$

w_{fc} is the field capacity volumetric water content. The force restore soil hydrological parameters C_1, C_2, C_3 and C_4 are estimated according to parameterization depending on the soil texture properties and moisture developed by Noilhan and Planton (1989), and Mahfouf and Noilhan (1996).

The two different soil configurations are presented in figure 3-7 :

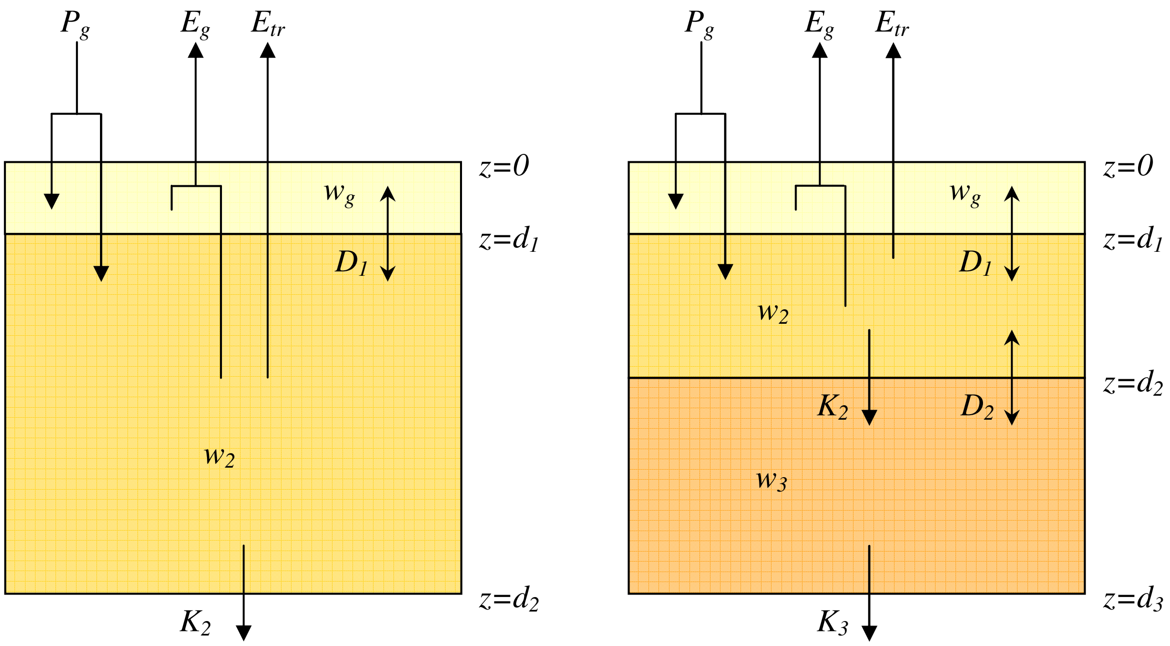

Figure 3-7 The soil configurations of the model. On the left the first version used to compute the soil water content. On the right the improved version with an additional soil layer. the direction of the fluxes (diffusion (D), drainage (K), infiltration (P_g) and evapotranspiration (E)) is indicated by arrows. The soil depth is increasing downward.

In both models P_g is the precipitation rate reaching the ground. However when the surface layer soil moisture exceeds the soil porosity, during very intense rain events, P_g would be written as $P_g = P_{through} - R_{sfc}$, where $P_{through}$ would be the effective precipitation flowing through vegetation and R_{sfc} a direct surface runoff.

3-3-3 Results and discussion

Figure 3-8 shows a simulation of soil moisture with the new configuration for the period between November the 16th 2001 (day 320 of year 2001) and March the 6th 2002 (day 430). The improvement of the simulation of the soil moisture in the root zone layer had impacts on the simulation of the first layer. After calibration the model was able to predict reasonably well the surface layer water content. This allows us to assume that the flux of water (diffusion combined with drainage) between these two layers is correct.

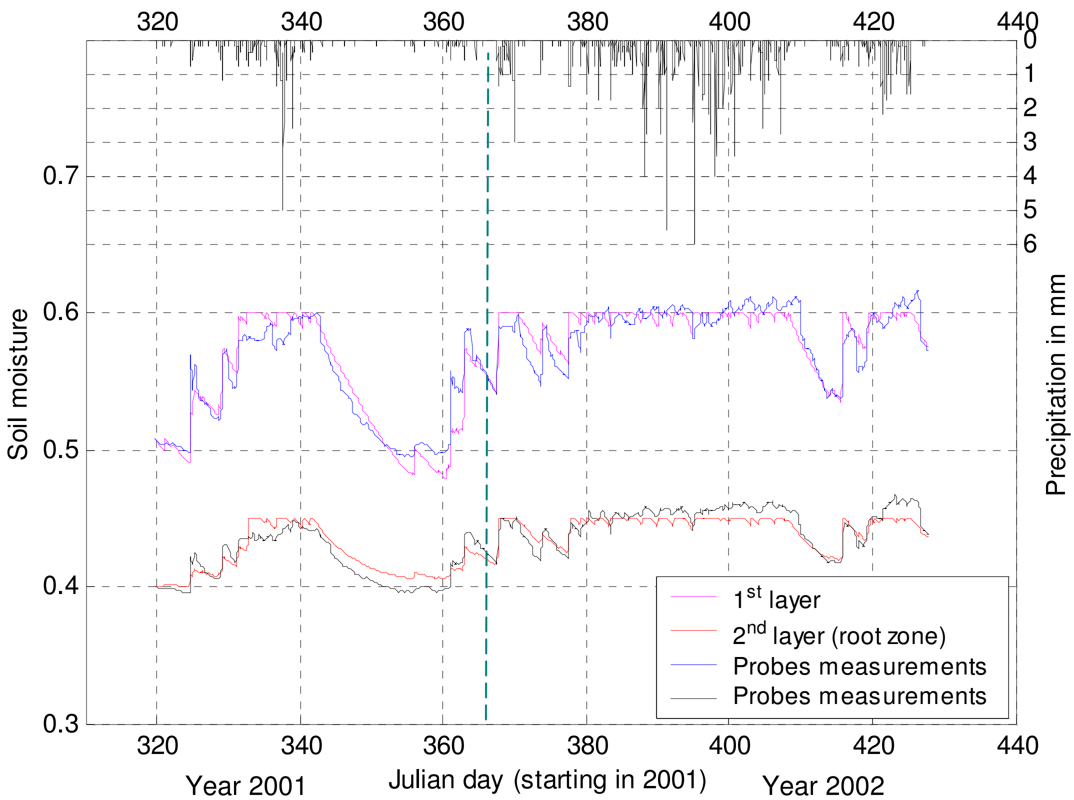

Figure 3-8 Comparison of measured versus modelled root-zone and surface layer soil moisture time series. Precipitation is displayed inverted on the top of the figure.

Thus, the inclusion of a third layer makes the root zone more robust in terms of simulation. Figure 2-8 does not show the time series for the deeper soil layer, because no observations are available for this depth.

It is however visible on figure 2-9. This is to emphasise the shape of the time series of w_3. At the depth at which w_3 is simulated, the effects of rainfall are clearly smoothed. The evolution of the soil moisture at this depth is slow and progressive although it is the result of an almost continuous stimulation by precipitation. We can assume from the slow response to the different events that the hypothesis made on the depth of the third layer is correct. We had set d_3 = 1 metre.

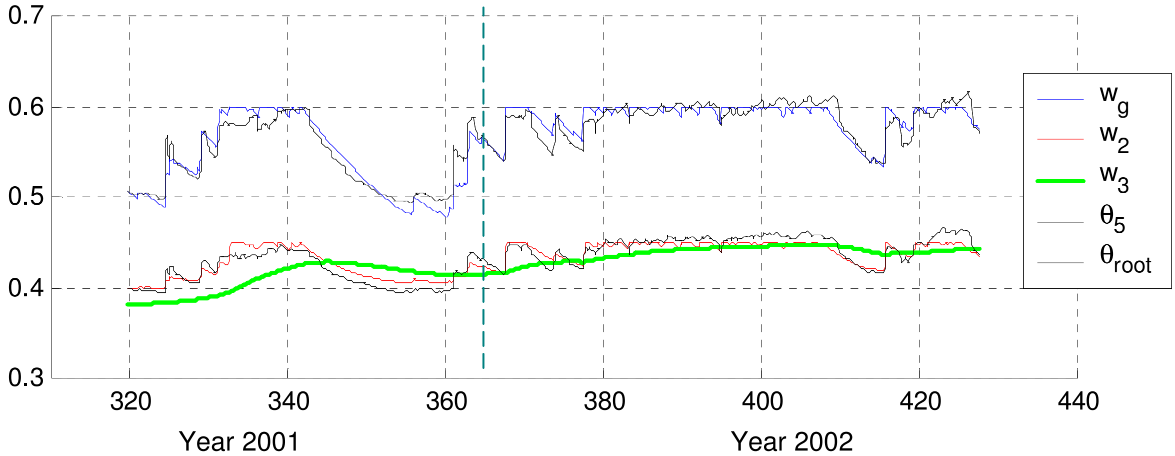

Figure 3-9 Time series of the simulated soil moisture at different depths. w_g, w_2 and w_3 are the volumetric water content representing respectively the surface layer of depth 10 cm, the root zone of depth 30 cm and a deeper soil layer of depth 1 m.

The purpose of the third layer is to give a clearer characterisation of the root zone in the soil. It allows a separation of the water fluxes in the soil profile. The deep soil layer may provide water to the system by capillary rises. The shape of the time series corresponds more adequately to the evolution of a deep soil reservoir. Thus the gravitational drainage occurring at the base of this layer is assumed to create a more realistic component of the base-flow. This is a positive point in the effort to simulate the stream-flow.

3-4 Simulation of stream-flow

3-4-1 Procedure

In order to model stream-flow and to assess the impact of each component of the water balance, we carried out a comparison of formulations for surface runoff, subsurface runoff, drainage and base-flow. The description of these components are borrowed from recent SVAT schemes. This study starts with the first version of the ISBA we implemented with two layers. The soil moisture was calibrated again for the period for which we studied the stream discharge. We used this configuration again in order to see if this simple soil layer configuration could lead to a reliable stream-flow modelling. In case of positive results the robustness of the soil moisture simulation would be to improve because soil moisture and stream-flow are closely linked. (Shao et al. 1996, Chen et al. 1997, Henderson-Sellers 1996). Then different configurations were tried in the order of increasing complexity.

The results were presented at the EGS conference held in Nice in 2001 at a poster session. The following sections take up in more details the results presented in the poster.

3-4-2 The ISBA flow model

In a recent study the ISBA surface scheme was coupled to a hydrological model at a regional scale. (Habets et al. 1999). In their study the authors validated the model of the water budget with mean observed daily stream flow of a large basin. We were interested in seeing the effect of the scale on the equations. Could this large scale model, computing the daily cycle of energy balance and water budget be applied for a small catchment and with a short time increment ? As long as the study site is homogeneous with regard to soil and vegetation we could focus on the one dimensional application of this scheme. Thus, what corresponded to a grid cell in ISBA was actually 1 m² in our model, extended to the whole catchment area.

ISBA generates two flow components to reproduce the stream flow : a surface runoff and a gravitational drainage. The model was first studied in its two soil layers configuration and then in its three soil layers version. The number of layers for this model influences mainly the gravitational drainage. The detailed characteristics are presented for the two layer configuration for clarity.

The fluxes of water for the hydrological application of ISBA are described as follows :

The gravitational drainage K_2 is defined as a restore term to the field capacity :

$$K_2 = \frac{C_3}{\tau} \max\left[0, \left(w_2 - w_{fc}\right)\right] \tag{3.21}$$

C_3 is a soil dependent coefficient representing the time for the water to drain. Mahfouf and Noilhan (1996) proposed a relationship to express C3 as a function of the fraction of clay :

$$C3 = 5.3273 Clay^{-1.043} \tag{3.22}$$

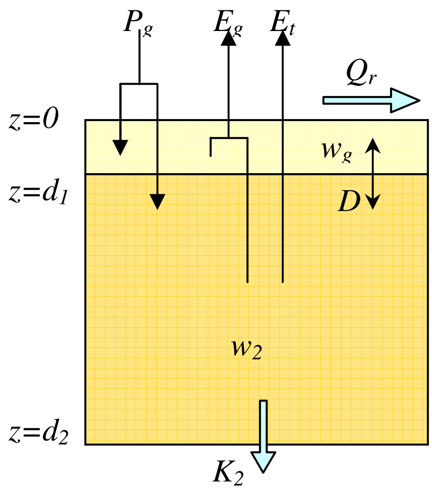

Figure 3-10 Sketch of the fluxes in ISBA. The blue arrows show the components for stream-flow modelling.

The surface runoff follows the Variable Infiltration Capacity scheme (Dümenil and Todini 1992). This scheme allows surface runoff to occur before the entire considered area is saturated. This is to represent the possible heterogeneity of the catchment in terms of response to rainfall. Following this principle the fraction of the area that is saturated and will generate surface runoff changes with the infiltration capacity. The infiltration capacity can be defined as the total amount of water that could be stored in the soil for a given moisture in soil. Thus if the whole area is saturated, the infiltration capacity is maximum. The fraction of area for which the infiltration capacity is less than i is :

$$A(i)=1-\left(1-\frac{i}{i_m}\right)^B \tag{3.23}$$

where B is a shape parameter.

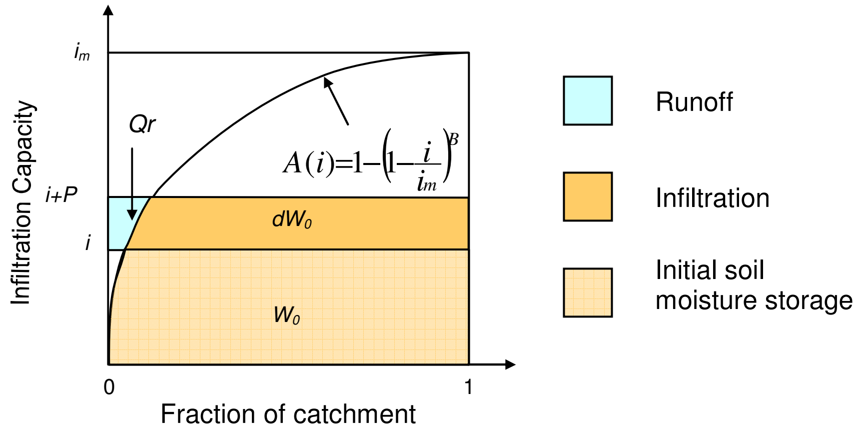

Figure 2-11 The runoff parameterisation deriving from the Variable Infiltration Capacity. (Dümenil and Todini 1992, Habets et al. 1996)

The calculations for surface runoff are included in this theory, which leads to the following expression of the surface runoff Q_r for an amount of precipitation P :

$$\begin{aligned}
&\text{If } \; P \exists (1+B)(w_{sat}-w_{wilt})\left(1-\frac{(w_2-w_{wilt})}{(w_{sat}-w_{wilt})}\right)^{(1/B+1)} \\
&\qquad \text{then } \; Q_r=P-(w_{sat}-w_2)d_2 \\
&\text{If } \; P \leq (1+B)(w_{sat}-w_{wilt})\left(1-\frac{(w_2-w_{wilt})}{(w_{sat}-w_{wilt})}\right)^{(1/B+1)} \\
&\qquad \text{then } \; Q_r=P-(w_{sat}-w_2)d_2+d_2(w_{sat}-w_{wilt})\left[\left(1-\frac{(w_2-w_{wilt})}{(w_{sat}-w_{wilt})}\right)^{(1/B+1)}-\frac{P}{(w_{sat}-w_{wilt})(1+B)}\right]^{1+B}
\end{aligned} \tag{3.24}$$

3-4-3 Hydrological components of SEWAB

The second scheme tested was the parameterization of the Surface Energy and Water Balance (SEWAB) (H. T. Mengelkamp et al. 1999, 2001). The energy budget is solved with the scheme presented in chapter 3-3-2. Soil moisture is simulated by a three soil layers configuration. In this model stream flow simulation comprises surface runoff (R_s), subsurface runoff (R_k) and base-flow. Surface runoff is created from the discharge of a ponding storage. When the precipitation rate (P) is greater than the infiltration rate (I), rainfall water accumulates at the surface as ponding water. Water then flows from this ponding storage depending on the height of ponded water at the surface. If the maximum allowed height allowed is exceeded (h_{0max}), the excess water creates instantaneous runoff. Otherwise, surface runoff corresponds to a linear discharge from the ponding storage. Subsurface runoff is a flow which is linearly dependent on soil moisture, between field capacity and saturation. Base-flow is generated from two reservoirs so as to model a slow and a fast component.

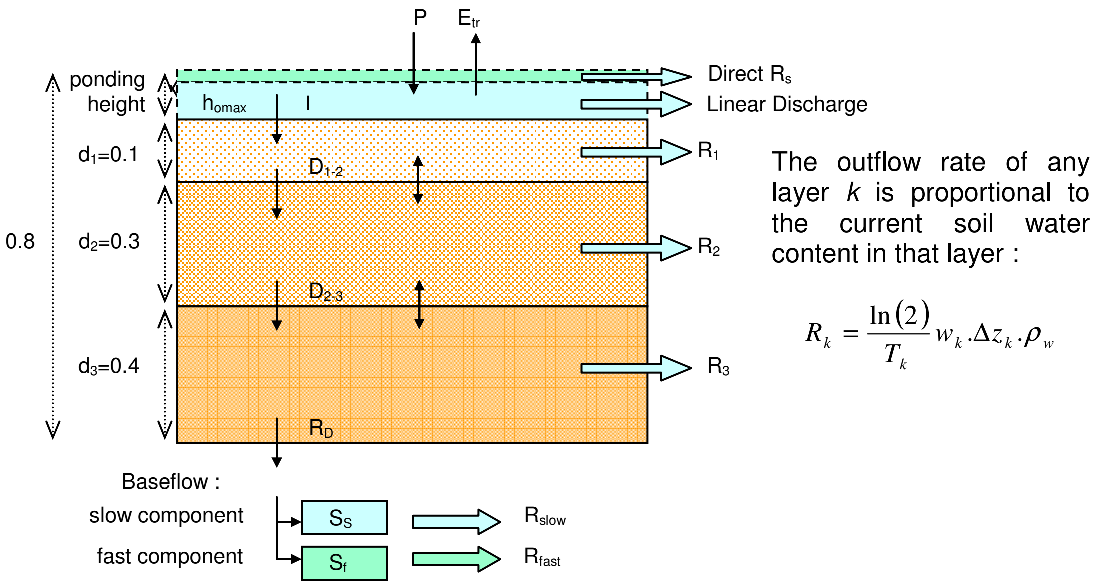

Figure 3-12 Vertical configuration of SEWAB with the different hydrological components indicated by solid arrows.

The difference between the amount of water falling onto the ground and the actual infiltration rate (I_{act}) is added to the ponding storage. So that for a time step of duration Δt, the height of the ponding storage at time $n+1$ is given by :

$$h_0^{n+1}=h_0^n+\left(\frac{P}{\rho_w}-I_{act}\right)\Delta t \tag{3.25}$$

The discharge from the ponding storage is expressed as a linear function of the height of water stored :

$$R_{pond}^{n+1}=\frac{\ln(2)}{T_{pond}}h_0^{n+1}\rho_w \tag{3.26}$$

Subsurface runoff is formulated for a volumetric water content contained between field capacity and saturation, for each soil layer. For layer k, this outflow is written as :

$$R_k=\frac{\ln(2)}{T_k}w_k.\Delta z_k.\rho_w \tag{3.27}$$

In equations (2-26) and (2-27) T_{pond} and T_k are time constants. As the response of surface runoff to rain events is quicker than the response of subsurface flows, T_{pond} is much smaller than T_k. Moreover the deeper the layer, the longer it is for the soil moisture profile to evolve so that we have this relationship between the different time constants : $T_{pond} \leq T1 \leq T2 \leq T3$.

Base-flow is modelled using two reservoirs that flow linearly as a function of the amount of water stored. They are filled by the drainage (R_D) at the bottom of the last layer which is partitioned between the two reservoirs by a coefficient $0 \leq \gamma \leq 1$. The stored water at time step $n+1$ is expressed by $S_{s/f}^{n+1}$, whether it is the slow component (s) or the fast one (f).

$$R_{s/f}^{n+1} = \min\left(\frac{\ln(2)}{T_{s/f}}\left(S_{s/f}^{n} + \delta.R_D.\Delta t\right), \frac{S_{s/f}^{n} + \delta.R_D.\Delta t}{\Delta t}\right), \tag{3.28}$$

$$\text{where } S_{s/f}^{n+1} = S_{s/f}^{n} + \left(\delta.R_D - R_{s/f}^{n+1}\right)\Delta t \tag{3.29}$$

and $\delta = \gamma$ for slow component (s)

$\delta = (1-\gamma)$ for fast component (f)

3-4-4 The hydrological partitioning of the LAPS

We are considering in this section the Land-Air Parameterization Scheme (LAPS) based on papers by D. T. Mihailović et al. (1996, 1998) to explore new aspects of the modelling of stream-flow components. The LAPS computes the same type of hydrological components as the SEWAB scheme. It includes surface runoff, subsurface runoff as lateral flow for each layer and base-flow. However the formulations for these flows are different. It is interesting in terms of general overview of the modelling possibilities to detail this model to.

The version presented hereunder includes four soil layers, even though a configuration with three layers was also examined.

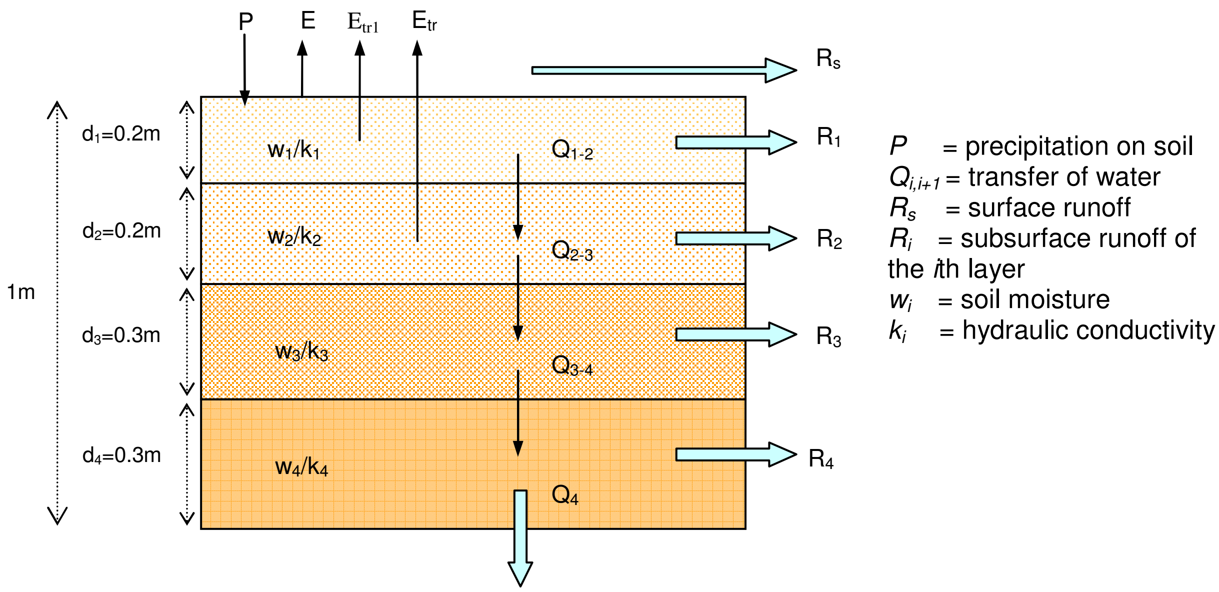

Figure 3-13 Schematic diagram for the four soil layer configuration of the LAPS. As previously, the modelled components that simulate the stream-flow are represented with solid arrows.

An interesting aspect of the LAPS is to refer to the hydraulic conductivity of each layer as a dominant parameter. Indeed the hydraulic conductivity is used as a limit to initiate the runoff. The surface runoff R_S is computed by :

$$\begin{aligned} &R_S = P - min(P,\ k_{sat1}3dt) \qquad if\ w_1 < w_{sat1} \\ &R_S = P \qquad when\ the\ 1^{st}\ layer\ is\ saturated \end{aligned} \tag{3.30}$$

Subsurface runoff is calculated in two steps for each layer. The first condition relies on the drainage capacity if the layer. After computation of the diffusion ($Q_{i,\ i+1}$) between layers i and $i+1$, the flux is compared to the hydraulic conductivity of the layer. The amount of water that could have been diffused in excess of the hydraulic conductivity forms a first lateral subsurface flow $R_i^{(1)}$. Equation (3.31) is the mathematical expression of it :

$$R_i^{(1)} = Q_{i,\ i+1} - min(Q_{i,\ i+1},\ k_{sat_i}3dt) \tag{3.31}$$

At the end of a time step, after computation of the soil moisture, a second condition is tested for subsurface runoff. If the possible subsurface runoff $R_i^{(2)}$ is positive then it is added to $R_i^{(1)}$ and the sum becomes the subsurface runoff of layer i.

$$R_i^{(2)} = d_i \times \left(w_i + \frac{(Q_{in} - Q_{out})}{d_i} - w_{fc} \right) \tag{3.32}$$

where w_{fc} is the field capacity.

Finally the gravitational drainage Q_4 is calculated by equation (3.33) :

$$Q_4 = k_{sat,4} \times \left(\frac{w_4}{w_{sat,4}} \right)^{2b+3} \times \sin(x) \tag{3.33}$$

where x is the mean slope angle, which is around 3 % for the study site.

3-5 Comparison and interpretation

3-5-1 General characteristics

As seen in the section 2-1 in the description of the field, the study site is an interesting catchment area for model testing. Indeed its homogeneity regarding vegetation and soil, limits the uncertainty about the parameters characterising them. The number of parameters is also reduced as long as only one grid cell of 1 m² is to be calibrated to represent the whole catchment. There is need of subdividing the catchment area in several subcatchments depending on their properties, and calibrate them separately. This kind of process is common for 2-D hydrological models (e.g. Soil Water Assessment Tool SWAT). The problem in that case is that it considerably increases the complexity, particularly for calibration. Moreover the small size of the site pushes the models like SWAT to size scales they might not have been designed for. The study site has indeed a quick response to rain events. The duration of some peaks in the hydrograph may not exceed 3 hours. So that it is interesting to see if the models are able to follow variations so close in time. This leads us to the question of the time scale. Is the short time step used for the simulations (30 min.) suitable for all the models ?

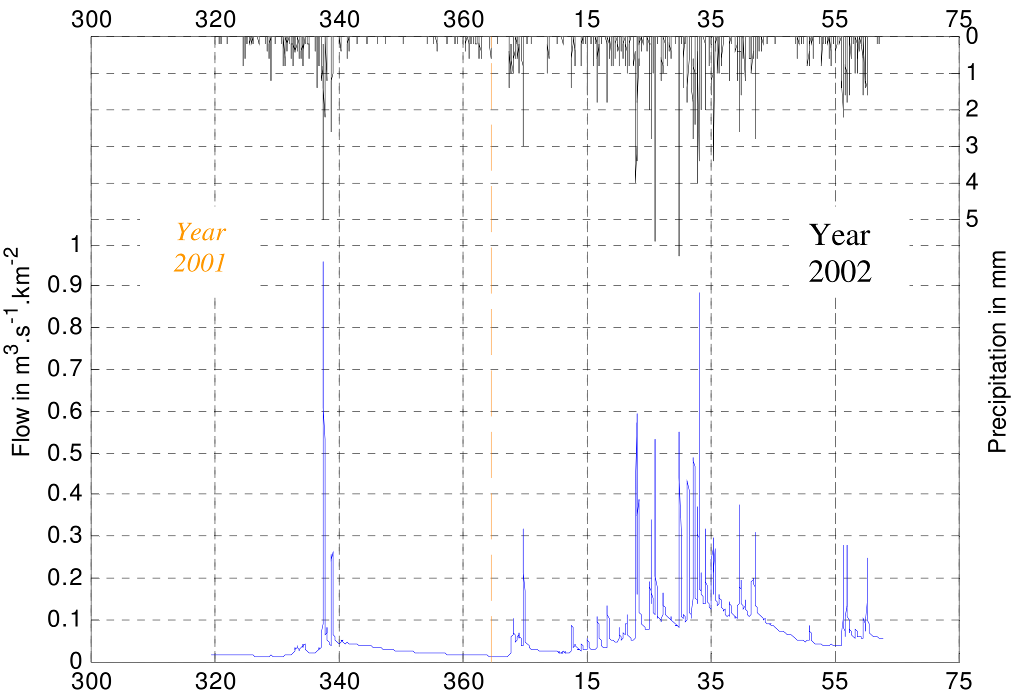

Figure 3-14 Time series of the observed runoff and precipitation (top axis) for the period on which models were tested, from November 16, 2001 to March 3, 2002.

Figure 3-14 shows the observed hydrograph for the period of test of the models. This hydrograph has interesting events in terms of testing. The high intensity rain event of day 337 appears as an isolated peak on the time series, and rainfalls after this event are limited. We can reasonably assume it is mainly generated by surface runoff. The slope of discharge observed after this rain event is characteristic of the field and will be a challenging point to reproduce for the models. Likewise the period in 2002 extending from day 15 to day 40 is very wet. Models on this period will have to reproduce the important increase in base-flow as well as the different peaks that occur.

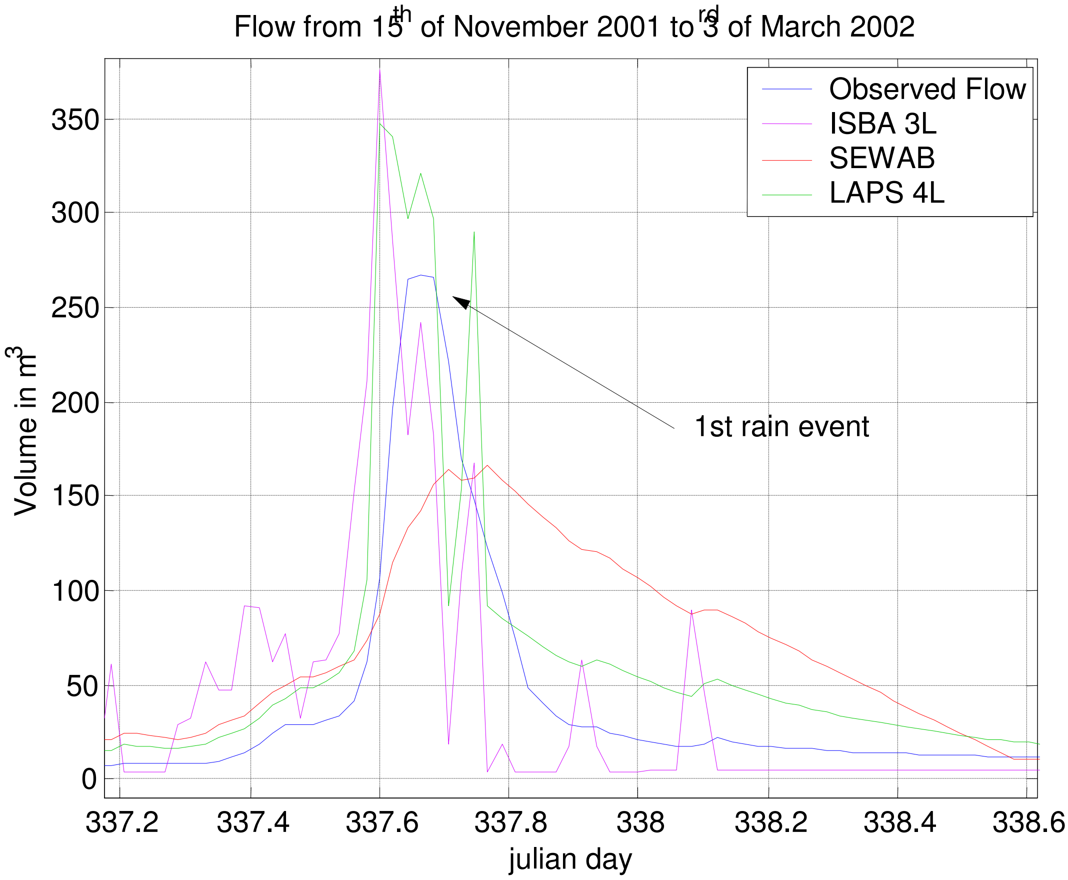

Figure 3-15 Simulation of the first peak in the hydrograph by the different models.

Figure 3-15 illustrates the general behaviour of the models. The formulation used by the ISBA for surface runoff is very sensitive to rain. It responds quickly at almost each variation in precipitation by steep peaks and a small base-flow. This may be explained by the soil moisture content during this period. The example of the hydrograph occurs between December the 3rd and December the 4th 2001, which corresponds to a very wet period of the year. The soil is saturated or close to saturation at the time of this peak (see figure 3-9). The ISBA model generates surface runoff before the entire grid cell is saturated, so that for slightly larger rainfall around this time surface runoff will occur because the soil is near saturation. Even if the peaks may be overestimated and the base-flow underestimated, globally, the volume of water produced by the simulation of ISBA seems to be correct. As for the LAPS model, it generally respects the slopes of the hydrograph peak, during the raise and fall of the hydrograph. However it overestimates the volume of water that flows to the stream and is too sensitive to rainfall. Indeed neither the ISBA scheme nor the LAPS model simulate a simple envelop for this event, as is observed. The third simulation displayed on figure 3-15 comes from the SEWAB model. Although it does not look a priori as close to the observations as the two other models, some interesting features may be noted about the SEWAB simulated hydrograph. The slope before and during the increase of flow follows the observations. But the decrease rate for this peak is too low as the flat slope after the peak indicates. However a positive aspect of this simulation is that the SEWAB model predicts a single smooth curve for this event. This is due to the definition of the ponding storage, with the water accumulating at the surface and being slowly evacuated. In this formulation the rate of discharge can be adjusted (see T_{pond} in equation (2-26)) to give a more appropriate simulation, without modifying the total discharged volume.

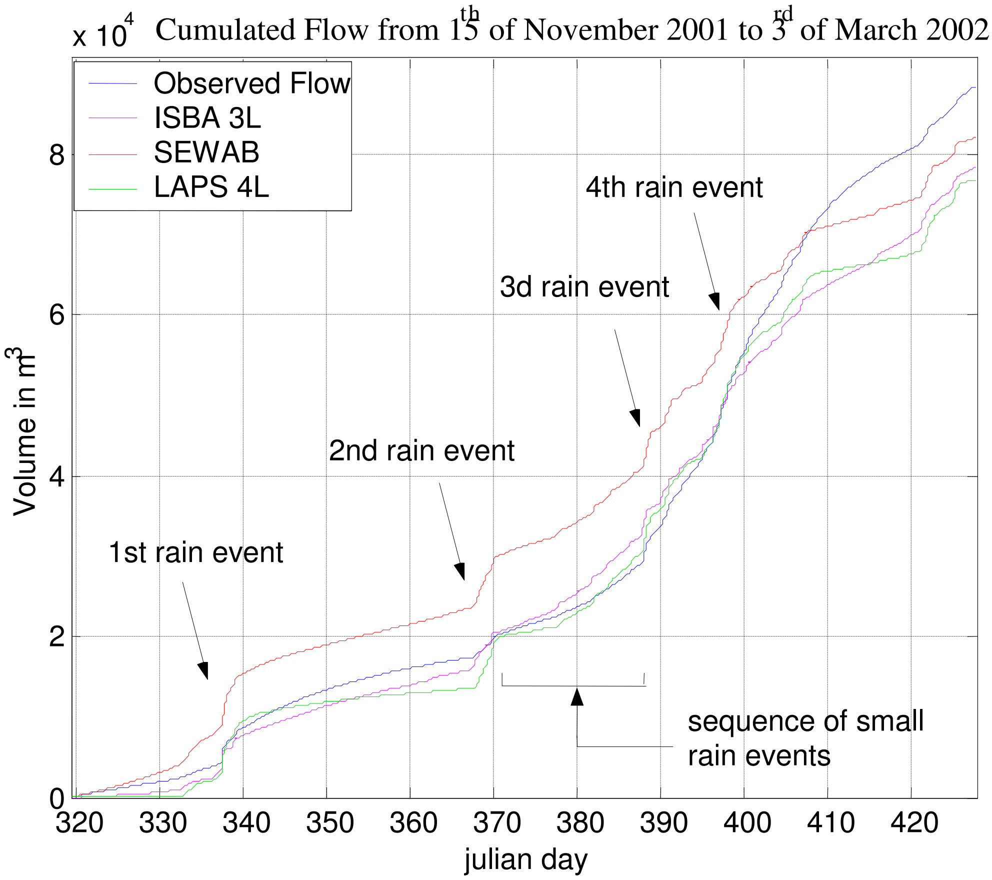

Figure 3-16 Simulated and observed cumulative flows.

The main rain events are noticeable on figure 3-16 thanks to the change in slope of the cumulative curve. Two characteristics of the different models can be read on this figure : first the total volume of water computed and so the global trend which is followed by each model, and also the behaviour of the models on a particular rain event and some time afterward. Let us consider the first rain event for example. One can notice as discussed above that the LAPS and ISBA model are near the real cumulative curve, thus showing that the predicted volumes are fairly correct, whereas the SEWAB model overestimates the volume of water in the stream. But besides the volume it is interesting to look at the behaviour of the different models, and the period after the first rain event is, in that sense, remarkable. The period between the day of year 340 and 360 corresponds to a drying period for the soil (see figure (3-9) and figure (3-14)). We can notice that the cumulative curve produced by the SEWAB model seems to be more realistic than the LAPS or ISBA. It is indeed smoother. This highlights a limit of the LAPS model whose formulation of flows are not flexible enough. A value initiates or not each runoff, and this underlines maybe the need for the ISBA model to include more components for stream-flow modelling.

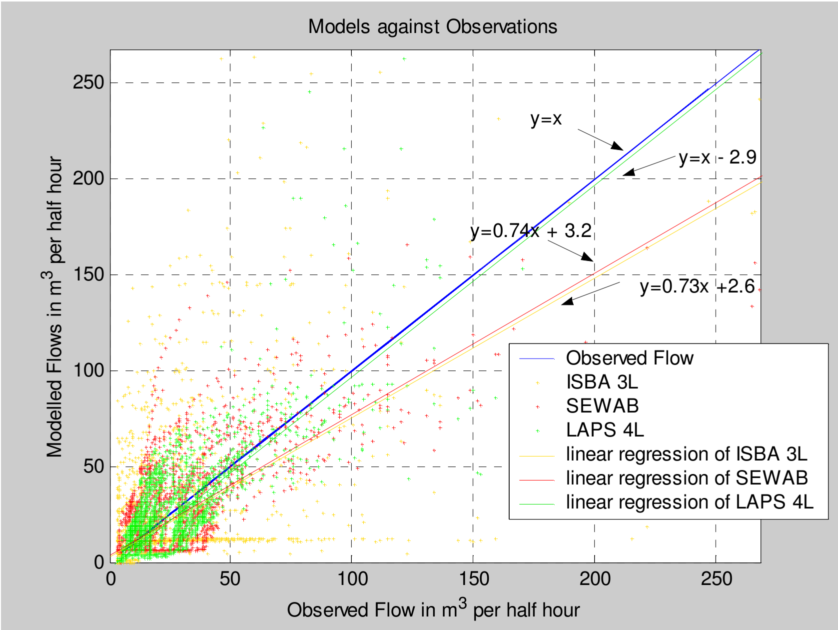

Figure 3-17 underlines the significant scattering of the models when plotted against the observations. None of them matches accurately the observations. The set of dots is quite fragmented for each model. One can notice anyway that the best regression is obtained for the LAPS, which indicates the equilibrium of data around the samples.

Figure 3-17 Scatter plot of the simulated flows, plotted against observations.

3-5-2 Analysis of the base-flow models

The base-flow is a crucial component for a good simulation of the stream-flow. On an annual budget it represents about 80 % of the volume of water for the study catchment. Although the peaks seem to occupy the major part of the hydrograph on figure 2-14, their contribution for this wet period is about 25 % of the total volume. This figure is a mean value found by a hydrograph separation method (see figure 3-18).

The different models estimate fairly well the base-flow when rain events are separated by regular drying periods. However under continuous rainfall of several days the models greatly underestimate the base-flow. This highlights the lack of water retained in their system during these events.

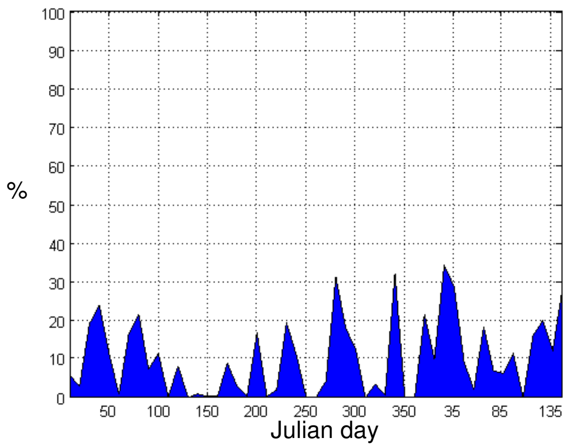

Figure 3-18 Average contribution over periods of 10 days of the surface runoff as a percentage of the total stream-flow, separated from the base-flow by a hydrograph separation technique.

The formulation of the base-flow in the ISBA model only depends on the soil moisture of the last layer. Thus a good simulation of the last layer is first required. But this is probably not enough to get a good representation of the base-flow. Since the drainage at the bottom of the last layer is the only component for the base-flow simulation, only its volume can be adjusted. But the parameters governing the drainage are closely related to the soil moisture simulation. The missing volume might have to be found in other components.

The main components of the base-flow in the SEWAB model are the slow and the fast discharge from the two reservoirs. Only little lateral runoffs are allowed through their time constants. The calibration in this model is simplified because the time constants regulating the discharge of the two reservoirs can be adjusted independently of the rest of parameters. As long as the SEWAB model includes subsurface lateral flows and drainage, the discharge slope of the hydrograph can be smoothed, each component bringing progressively less water.

The LAPS model includes several components to simulate the base-flow. The simulated slope of the hydrograph during the discharge is also smoother and more realistic than the ISBA.

In conclusion the lateral flows computed by both SEWAB and LAPS seem to provide the missing water to create a smooth hydrograph after a peak. This principle is then retained for the future work.

3-5-3 Analysis of the hydrograph peaks

This section summarizes the conclusions we drew concerning the peaks of the different models tested. This summary table aims to present the kind of response given by each formulation and thus to find the most adequate for the small grassland site.

	ISBA	SEWAB	LAPS
Principal reference	Habets et al. (1999)	Mengelkamp et al. (2001)	Mihailović et al. (1998)
Formulation for surface runoff	Variable Infiltration Capacity	Discharge from a ponding water storage.	Condition on precipitation rate and infiltration rate
Positive aspects of results	Globally the **volumes** simulated by the ISBA surface scheme are satisfactory at **large time scale**. The cumulated flow over the winter remains close to the observations curve.	The discharge follows quite well the stream-flow variations for a **time step of half an hour**. The **trend** of events is well represented, whatever they are continuous or separate, intense or moderate.	The model provides a good response in amplitude and in timing to **intense events** for which the layers below are not affected. In **summer** it corresponds to the main component of peaks in flow.
Negative aspects	Too sensitive to **small rainfalls**.	Discharge **too wide in time** but easily adjustable	Too sensitive to precipitation and so response **slopes too steep**.

	ISBA	SEWAB	LAPS
Complexity and calibration	The sub-grid runoff depends on the soil moisture w_2, on three soil parameters (w_{sat}, w_{wilt}, d_2) and on B, a shape parameter. The calibration **depends essentially on the calibration for the soil moisture** simulation. Thus it is **not possible to calibrate** runoff **alone**.	Calibration is made by adjusting the maximum ponding height, the time constant for discharge and time constant for the first layer. Because these parameters do not appear in any other formulations, the surface runoff can be calibrated **independently**, thus allowing **flexibility**.	The calibration requires a good estimate of the **soil parameters**, especially for the first layer. Thus the runoff is quite sensitive to the wet reference w_c and the hydraulic conductivity at saturation. However this makes the calibration easier because of the **small number of parameters**.
Conclusion	This scheme improves the representation of heterogeneity but is more adequate for **large scales** and **large time steps**.	The ponding process is the most **appropriate for the short time step** (1/2 hour) simulation demanded. It is well adapted for the small grassland catchment.	This parameterization does not take into account the real state of soil to generate runoff. Heterogeneity of field does not appear in the infiltration condition.

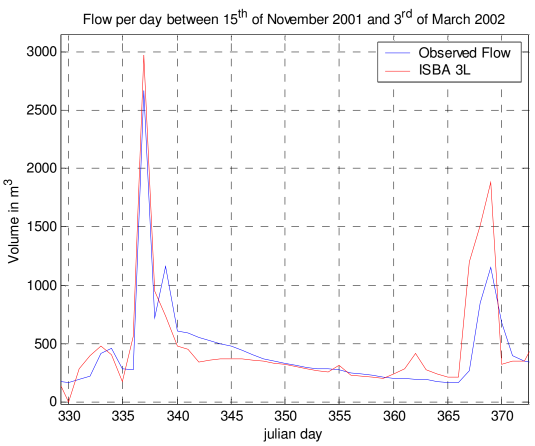

Figure 3-19 The VIC scheme is better adapted to larger time steps.

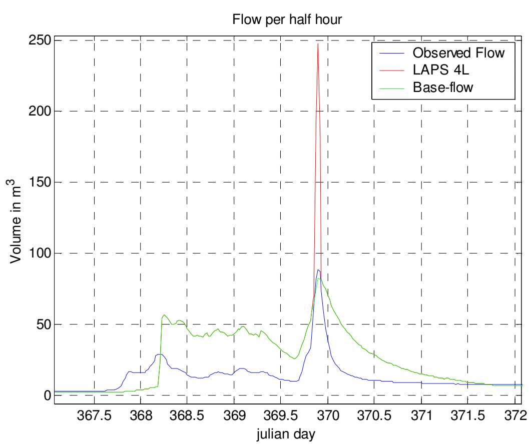

Figure 3-20 The number of components for base-flow smoothes the curve in the LAPS model

3-5-4 Conclusions about stream-flow modelling

The comparison of different parameterizations of runoff was a first approach of the stream-flow modelling. The aim of this study was not only to try to obtain a good simulation of the small catchment with a short time increment by testing these models. The implementation, the calibration and the comparison gave a better comprehension of the processes involved in each model regarding the conditions and parameters governing them, the effects and the possible problems encountered. Even if the calibration may possibly not have rendered the best of each model, the specific response of the components of the models could be assessed. Thus it could be deduced that the Variable Infiltration Capacity (VIC) scheme was not suitable for this catchment nor the temporal scale used. An equivalent result was found in an other study on the same catchment (Mengelkamp et al. 2001). The coupling between the hydrological model and the ISBA including the VIC parameterization for runoff was initially run at regional scale (Habets et al. 1996). It was also found that the principle of discharge from a ponding water storage was suitable for the small catchment. The soil moisture being well estimated by the three soil layer configuration of the ISBA scheme, it is appropriate to keep on working with this parameterization. However the drainage was found not to be sufficient in terms of volume during wet period, and lateral flow could be added. These results have been taken into account in order to achieve a parameterization of the small catchment, presented in next chapter.

Chapter 4

Final SVAT parameterization

Chapter 4
Final SVAT parameterization

4-1 Specifications of the new model

4-1-1 Introduction

The main goal of this study is to provide a suitable parameterization of the water balance of the 15 ha catchment area. The previous chapter presented the processes that led to this new parameterization. This scheme is made up of three sub-processes that compute the energy budget, the evolution of the soil moisture and the components generating the stream-flow. In this SVAT parameterization the soil moisture plays an important role in the quality of the simulation. Indeed, all the equations governing the runoffs are derived from the simulated soil moisture. The simulated volumetric water content is used as a trigger mechanism for surface runoff, or directly in the equation to calculate an outflow. For example the drainage occurring at the bottom of the deep layer. Thus the model should be more consistent since it takes into account at every 30 minute time step the physical reality of the column of soil.

The study of the different models (ISBA, SEWAB, LAPS) identify different ideas on how to generate the stream-flow, and on what components to include in the process. Several formulations have shown limitations in the capability to reproduce the quick flow. Moreover the combination of the small size of the catchment (15 ha) and a short time increment for the simulation makes the calibration difficult.

This SVAT parameterization simulates the stream-flow with a 30 minutes time increment but also tries to respect the reality of the site and the observed processes. Thus it includes a modified principle of ponding water, two components of subsurface runoff and vertical drainage. All these components are discussed in detail in section 4-3.

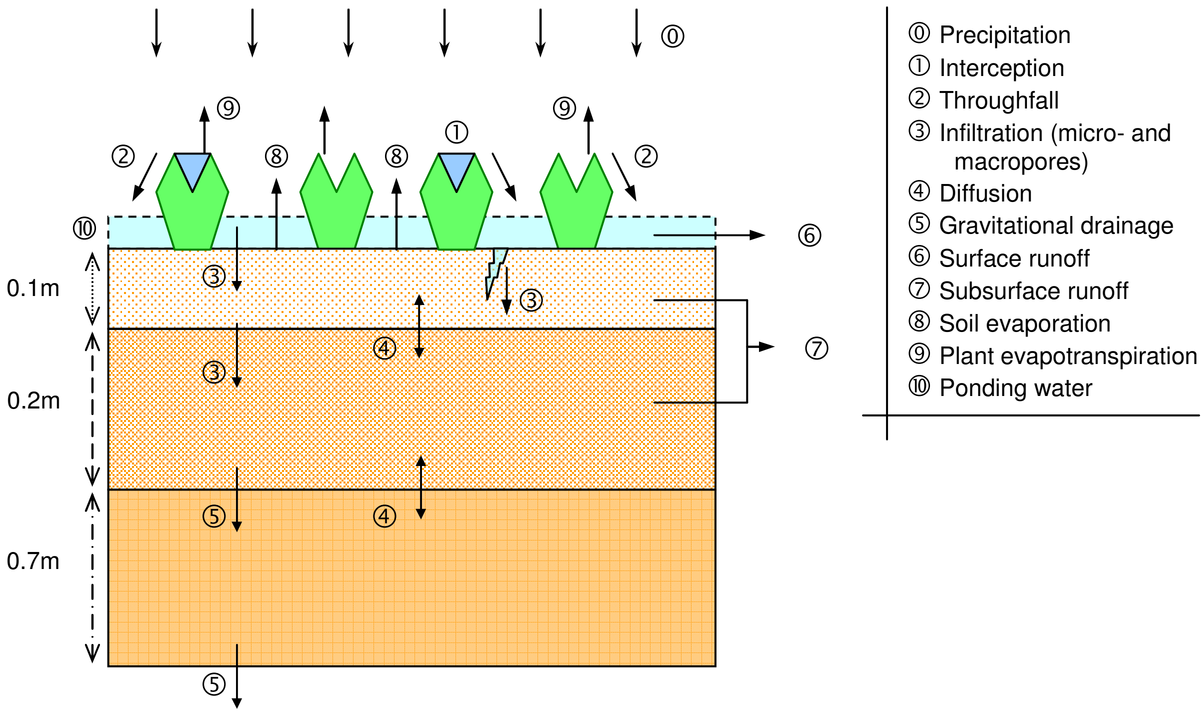

Figure 4-1 The water balance in the SVAT parameterization

4-1-2 Brief presentation

The SVAT model simulates a series of hydrological processes such as interception, evaporation from the bare ground and from the canopy, plant transpiration, infiltration into the soil matrix and into macropores, diffusion of water in the soil, surface runoff resulting from a ponding water storage, subsurface stormflow and gravitational drainage.

The main application of the model is to describe the hydrological characteristics of the hillslope during rain events. One of the main concern was to include rapid hydrological flow processes that occur during heavy precipitation, such as surface runoff, infiltration into macropores and subsurface lateral quick flow. Figure 4-1 is a schematic representation of the one-dimensional model and a list of the considered processes.

4-2 The soil moisture module

4-2-1 Review of the model

The final model used to simulate the soil moisture is the three soil layer configuration of the ISBA scheme. It is presented in chapter 2, section 3. It computes the volumetric water contents w_g, w_2 and w_3, respectively the surface layer, the root zone and the subroot layer The energy budget is solved using the equations presented in chapter 3, section 2.

We briefly recall the main equations governing the simulation of the water content at three different depths in this section.

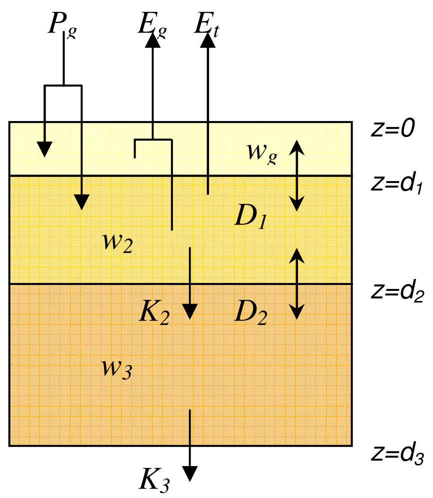

Figure 4-2 The soil layer configuration

$$\frac{\partial w_g}{\partial t} = \frac{C_1}{\rho_w . d_1} . (P_g - E_g) - D_1 \tag{4.1}$$

$$\frac{\partial w_2}{\partial t} = \frac{1}{\rho_w . d_2} . (P_g - E_g - E_r) - K_2 - D_2 \tag{4.2}$$

And for the third layer :

$$\frac{\partial w_3}{\partial t} = \frac{d_2}{(d_3 - d_2)} . (K_2 + D_2) - K_3 \tag{4.3}$$

where

$$D_1 = \frac{C_2}{\tau} . (w_g - w_{eq}) \tag{4.4}$$

$$D_2 = \frac{C_4}{\tau} . (w_2 - w_3) \tag{4.5}$$

$$K_2 = \frac{C_3}{\tau} . \frac{d_3}{d_2} . \max(0, (w_2 - w_{fc})) \tag{4.6}$$

$$K_3 = \frac{C_3}{\tau} . \frac{d_3}{(d_3 - d_2)} . \max(0, (w_3 - w_{fc})) \tag{4.7}$$

A noticeable difference of the model, compared to the one presented in chapter 3, is that the final parameterization includes the principle of ponding water. So that in equation (4.1) and (4.2) P_g is the amount of precipitation that reaches the ground after throughfall ($P_{through}$), but added to the ponding water at the surface (*Pond*). Thus P_g at time step *n* is equal to the throughfall at time step *n* plus the remaining ponding water from the previous time step (*n-1*).

$$P_g^{(n)} = P_{through}^{(n)} + Pond^{(n-1)} \tag{4.8}$$

w_{fc} is the field capacity volumetric water content. The force restore soil hydrological parameters C_1, C_2, C_3 and C_4 were in a first time estimated by the parameterization depending on the soil texture, given by Noilhan and Planton (1989), and Mahfouf and Noilhan (1996), then calibrated more precisely in a second time.

4-2-2 Parameters estimation

An estimation of the coefficients of the thermo-hydric equations can be found in Boone et al. (1999). A calibration of these coefficients have been carried out on the eleven soil types of the USDA textural classification. (see figure 2-13). (Giordani et al. 1993, 1996 ; Noilhan and Lacarrère 1995 ; Noilhan and Mahfouf 1996). However the values given can only be taken to give an idea of the range of the considered coefficient. Indeed from the field measurement of a sample of soil to the fitted regression of the value of the parameter, many sources of error can lead to a misinterpretation of the coefficient. But it is interesting to highlight this effort of modelling, thanks to which, from a simple estimation of the soil texture, many properties can be estimated. The soil coefficients regressions are presented below.

The volumetric water content at the balance of gravity and capillarity forces between the top layer and the root zone w_{eq} used in the equation of diffusion 4.4 is defined by a polynomial function :

$$\text{let} \quad y = \frac{w_{eq}}{w_{sat}} \quad \text{and} \quad x = \frac{w_2}{w_{sat}}$$
$$\text{then} \quad y = x - a.x^p.(1 - x^{8p}) \tag{4.8a}$$

where a and p are empirical parameters that can be estimated when the fraction of sand (X_{sand}) and clay (X_{clay}) are known :

$$a = 732.42 \times 10^{-3} \times X_{clay}^{-0.539} \tag{4.8b}$$

and

$$p = 0.134 \times X_{clay} + 3.4 \tag{4.8c}$$

The force-restore coefficients C_1, C_2, C_3 and C_4 can be expressed by :

$$C_1 = C_{1sat}.\left(\frac{w_{sat}}{w_g}\right)^{(b/2+1)} \tag{4.9a}$$

with

$$C_{1sat} = (5.58 \times X_{clay} + 84.88).10^{-2} \tag{4.9b}$$

$$C_2 = C_{2ref}.\left(\frac{w_2}{w_{sat} - w_2 + w_l}\right) \tag{4.10a}$$

where C_{2ref} can be estimated by :

$$C_{2ref} = 13.815 \times X_{clay}^{-0.954} \tag{4.10b}$$

$$C_3 = \frac{1}{d_3} \times 5.327 \times X_{clay}^{-1.043} \tag{4.11}$$

$$C_4 = C_4'.\frac{(d_3 - d_2)}{d_3} \tag{4.12a}$$

$$C_4' = C_{4ref}.\overline{w_{2,3}}^{\,C_{4b}} \tag{4.12b}$$

$$C_{4b} = 5.14 + 0.115 \times X_{clay} \tag{4.12c}$$

In equation (4.12b) $\overline{w_{2,3}}$ represents the interfacial water content for the layer 2 and 3. It is calculated in the SVAT model using :

$$\overline{w_{2,3}} = \left[w_2^q.\left(\frac{d_2}{d_3}\right) + w_3^q.\left(\frac{d_3 - d_2}{d_3}\right)\right]^{1/q} \tag{4.13}$$

where q is set to 6.

Formulations also describe some particular values of the volumetric water content, like the saturated volumetric water content w_{sat}, the wilting-point volumetric water content w_{wilt} and the volumetric water content at field capacity w_{fc}.

$$w_{sat} = (-1.08 \times X_{sand} + 494.305) \times 10^{-3} \tag{4.14}$$

$$w_{wilt} = 37.1342 \times 10^{-3} \times X_{clay}^{0.5} \tag{4.15}$$

$$w_{fc} = 89.0467 \times 10^{-3} \times X_{clay}^{0.3496} \tag{4.16}$$

However w_{sat} can be more accurately deduced from the observations (see figure 3-8) and its value is discussed in the next section.

Furthermore previous studies have been carried out on the same field and have required the knowledge of parameters such as w_{fc}, w_{wilt} and w_{sat}.

Thus one can find in Mengelkamp et al. (2001) :

$w_{sat} = 0.452\ m^3.m^{-3}$; $w_{wilt} = 0.18\ m^3.m^{-3}$ and $w_{fc} = 0.34\ m^3.m^{-3}$.

Albertson and Kiely (2001) used :

$w_{wilt} = 0.08\ m^3.m^{-3}$.

Table 4-1 presents the estimated value of parameters using the soil coefficients regression and the calibrated values finally used in the SVAT.

	b	a	p	C_{1sat}	C_{2ref}	C_3	C_{4b}	w_{sat}	w_{fl}	w_{wilt}
Regression with X_{clay} = 19 X_{sand} = 40	6.104	0.15	5.946	1.909	0.833	0.247	7.325	0.451	0.249	0.162
X_{clay} = 15 X_{sand} = 60	5.556	0.17	5.41	1.686	1.043	0.316	6.865	0.43	0.229	0.144
X_{clay} = 8 X_{sand} = 60	4.597	0.239	4.472	1.295	1.9	0.609	6.06	0.43	0.184	0.105
Sandy loam X_{clay} = 15 X_{sand} = 75	5.556	0.17	5.41	1.686	1.043	0.316	6.865	0.413	0.229	0.144
Calibration	4.38	0.15	5.95	0.86	0.69	0.052	7.325	0.455	0.34	0.13

Table 4-1 A comparison of some parameters values calculated with the relationships explained above and found at the time of the calibration of the SVAT model.

It is not surprising to see differences between the estimated and calibrated values. One must consider both values with the benefit of hindsight. Indeed the regression gives a linear relationship easy to apply but inevitably implies an error because of its nature. Moreover this regression has been found from a large number of calibrations, and a calibration is again a source of error. As for the values used in the SVAT model, they also come from calibration, so that a margin of error must be taken into account. According to the definition given by Franks et al. (1997), the same simulation of soil moisture can be achieved equally well by a number of parameters sets which all may be physically reasonable. This question is called the equifinality and deals with the problem of robust calibration.

4-2-3 Results and discussion

We assume that the meteorological forcing data are correctly measured so that the source of errors mainly comes from the model and the parameters. The soil water content simulated is compared to the measurements made by the in situ TDR probes. The simulated times series of the volumetric water content in the first layer is directly compared with the observations from a horizontal TDR probe set at 5 cm deep, which is in the middle of the artificial layer. The simulated time series of the soil moisture in the root zone is not directly compared to the measurements of one probe. Indeed the root zone layer overlaps the surface layer in the model. The simulated soil moisture in the root zone thus corresponds to a mean water content in soil, more representative of the column. So that a weighted average of measurements made at different depths is used as the observations. The simulated soil moisture w_2 of the root zone of assumed depth 30 cm is compared to the average soil moisture in the root zone θ_{avg} calculated by :

$$\theta_{avg} = \frac{(7.5 \cdot \theta_{5obs}) + (10 \cdot \theta_{10obs}) + (12.5 \cdot \theta_{25obs})}{30} \tag{4.17}$$

where θ_{5obs}, θ_{10obs} and θ_{25obs} are measurements at respectively 5, 10 and 25 cm deep.

Figure 4-3 presents on the same axis the time series of the surface layer and the root zone for both simulation and observation. First of all, before comparing the results of the simulation, it can be deduced from figure 4-3 that the surface layer and the root zone do not have the same texture nor properties. Indeed the volumetric water content in the surface layer is larger by 0.1 $m^3.m^{-3}$ than in the root zone. Furthermore during the period of heavy rainfall between day 370 and 410 (which is the period from January 5 to February 14, 2002) both layers reach saturation. The volumetric water content at saturation ($w_{sat,i}$) for these two layers can then be deduced from the observations. The soil moisture content at saturation in the first layer ($w_{sat,1}$) and the root zone ($w_{sat,2}$) are found to be respectively around 0.6 $m^3.m^{-3}$ and 0.46 for $w_{sat,2}$. As a consequence, the formulations used for the soil moisture computation had to be modified in order to take into account this clear difference of texture between the two layers. Thus we distinguished two values of the volumetric water content of soil $w_{sat,1}$ and $w_{sat,2}$, depending on whether it appeared in a term dealing with the first layer only or the root zone. We set : $w_{sat,1} = 0.6$ $m^3.m^{-3}$ and $w_{sat,2} = 0.455$ $m^3.m^{-3}$. The coefficient *C1* was recalculated in equation (4.9) with $w_{sat,1}$.

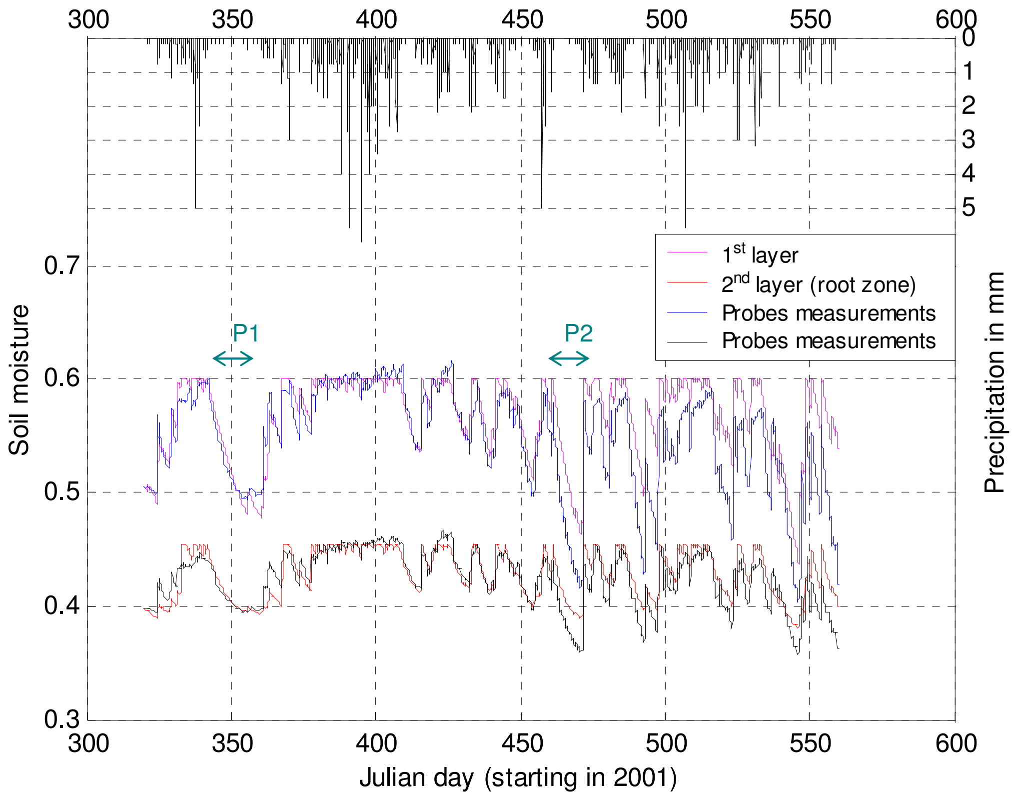

Figure 4-3 Time series of simulated and observed soil moisture content for two soil layers, from November 16 2001 to July 14 2002. Precipitation is indicated inverted on the top axis.

Globally rainfall events and drying periods are reflected correctly. The drying periods and the period of saturation are well simulated up to the day about 450 (March the 26th 2002). The soil moisture simulation of the root zone is still acceptable after this day, but the model has more difficulty fitting the observations for the surface layer. The model predicts some days of saturation in spring that do not occur. This might be because of an underestimation of the evaporation at this period.

Another explanation may come from the possible change in the soil properties with time. Indeed one can notice that after the heavy rain event of day 455 a drying period occurs with very low precipitation. This period (P2) is more or less similar to the one after day 345 (noted P1). Yet the soil moisture content in both layers decreases down to a lower value than the value to which it decreases during P1. This value corresponds, for P1 and P2, to the field capacity. Indeed the soil is in an equilibrium state. A soil is considered as being at field capacity when the downward movement of water is stopped or nearly so (Kutílek and Nielsen (1994)). The same authors insist on the fact that the field capacity is not a constant of a soil, and is a rough approximation because it depends on the previous events and on the state of soil. Then if we assumed an hypothetical variation of the field capacity, maybe a seasonality in this parameter, for P2, the model would drain more water, thus "dragging" the time series during P2 to lower values, that would fit the observations.

If the model overestimates the soil moisture, the runoff prediction will be affected. By predicting the saturation of the first layer when it is not in the observations, the model may allow water to pond and to generate surface runoff. Likewise if the soil moisture in the root zone is overestimated the subsurface runoff will be biased. The importance of a reliable and robust soil moisture simulation in the SVAT model is emphasized.

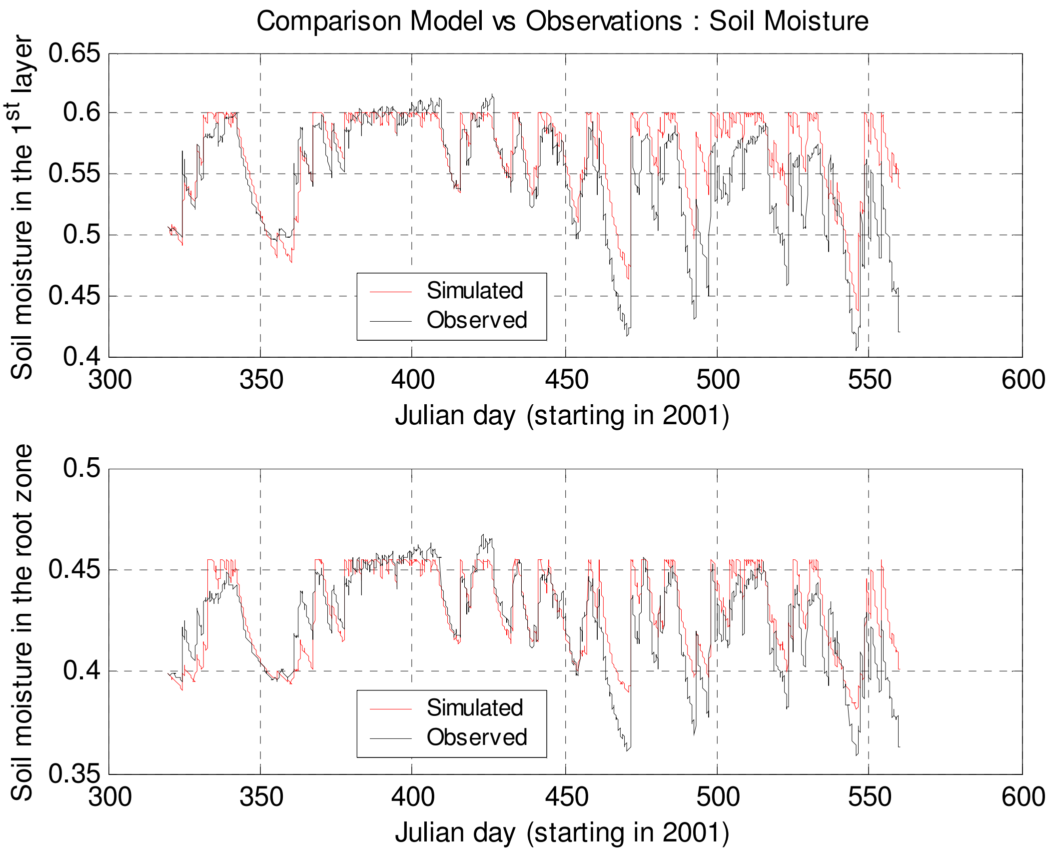

Figure 4-4 Simulated and observed time series of soil moisture content for the first layer (from surface to 10 cm deep) and the root zone (from surface to 30 cm deep)

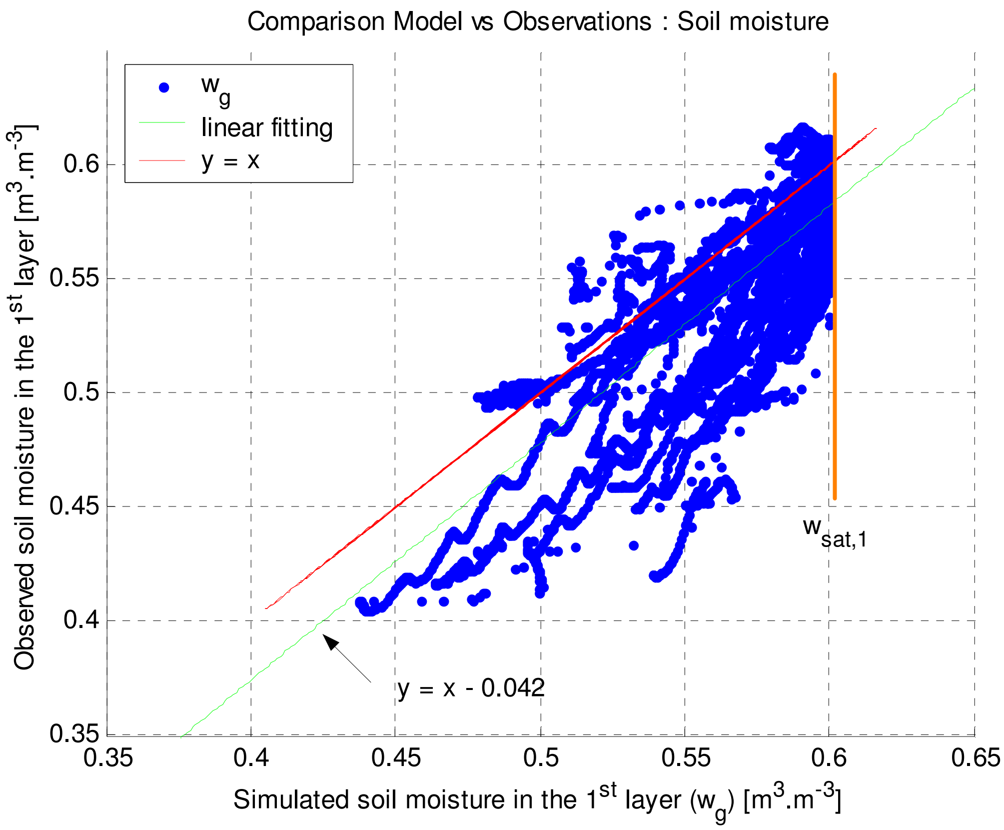

Figure 4-5 Scatter plot of the observed soil moisture in the first layer against the simulated soil moisture w_g. The upper boundary fixed in the model to trigger surface runoff is clearly noticeable. The green line shows a linear fitting of the scatter plot while the red 1:1 line is shown to mark perfect agreement.

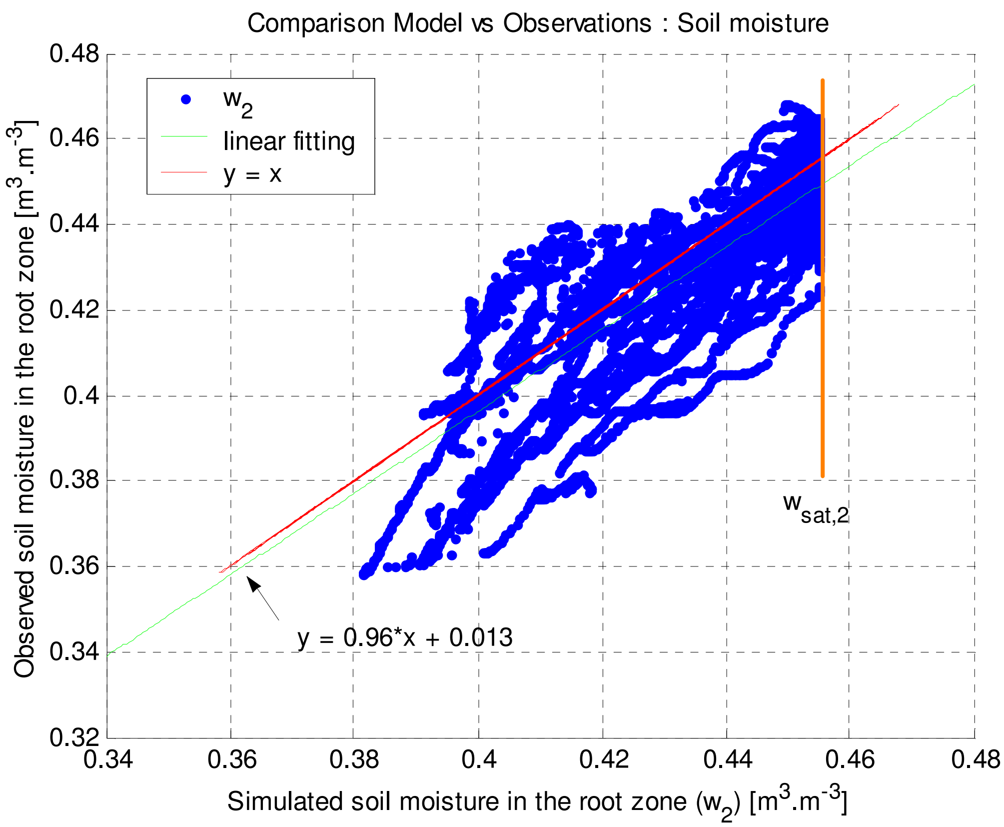

Figure 4-6 Same as figure 4-5 for the root zone

4-3 The stream-flow module

4-3-1 Introduction

The development of the SVAT parameterization has been carried out in a progressive way starting from a simple energy and water balance (Noilhan and Planton 1989). Every further step was implemented to meet a particular problem or constraint. The first objective was then to consistently simulate the peaks of the hydrograph. Indeed a hydrograph peak contains several pieces of information about a catchment area. The magnitude, the width, the lag time between the rainfall event and the peak, the attenuation compared to a previous catchment, the time of discharge, etc. characterize the catchment. A poor simulation of the peaks would probably mean a misunderstanding of some typical parameters of the catchment. The main contribution to stream water during heavier rainfall events comes from surface runoff and quick subsurface runoff (Beven and Germann 1982, Bronstert and Plate 1997, Scanlon et al. 2000).

Besides, the natural topography and soils of the site, a highly fertilized grassland, make the simulation of these two flows critical. The surface runoff is indeed a major component of the contaminants transport, so that it must be accurately and reliably modelled if management strategies of the field want to be assessed. And even though it is more difficult to observe, the same effort must be pursued for subsurface runoff.

- In the present water balance the surface runoff is modelled using a discharge from a ponding water storage. The runoff is generated only after saturation of the top soil layer (Mengelkamp et al. 2001). It is a quick response flow and is suitable for the simulation of the main part of the hydrograph peaks.

- Subsurface runoff also needed to be added. This runoff is slightly more delayed than the surface runoff and completes the discharge curve. It occurs when the root zone is saturated. In that case a lateral flow drains the excess water to the stream.

- A vertical drainage generates the base-flow (Boone et al. 1999).

- In order to generate a sufficient volume of water during heavy rainfall events, another component is computed. It deals with a subsurface stormflow as mentioned by Bronstert and Plate (1997), Scanlon et al. (2000). This quick flow takes into account rapid soil water flow processes such as infiltration into macropores. Preferential paths can be developed as a consequence of roots growth and decay, worms activity or soil reorganisation (Stephens 1996). The flow of water is transmitted through this network of macropores at velocities of the same order as surface runoffs (or overland flows) (Beven and Germann 1982). The parameterisation of the infiltration into macropores and the interaction with the soil matrix is based on Bronstert and Plate (1997).

The parameterization has been implemented with the intention of keeping the complexity low and making the calibration easier. Thus we use the term of module to indicate the relative independence of some parameters or components used in the computation of the stream-flow.

4-3-2 Description of the hydrological processes

Figure 4-7 shows how the model computes the stream water at each time step. It represents one iteration, i.e. a time increment of 30 min. :

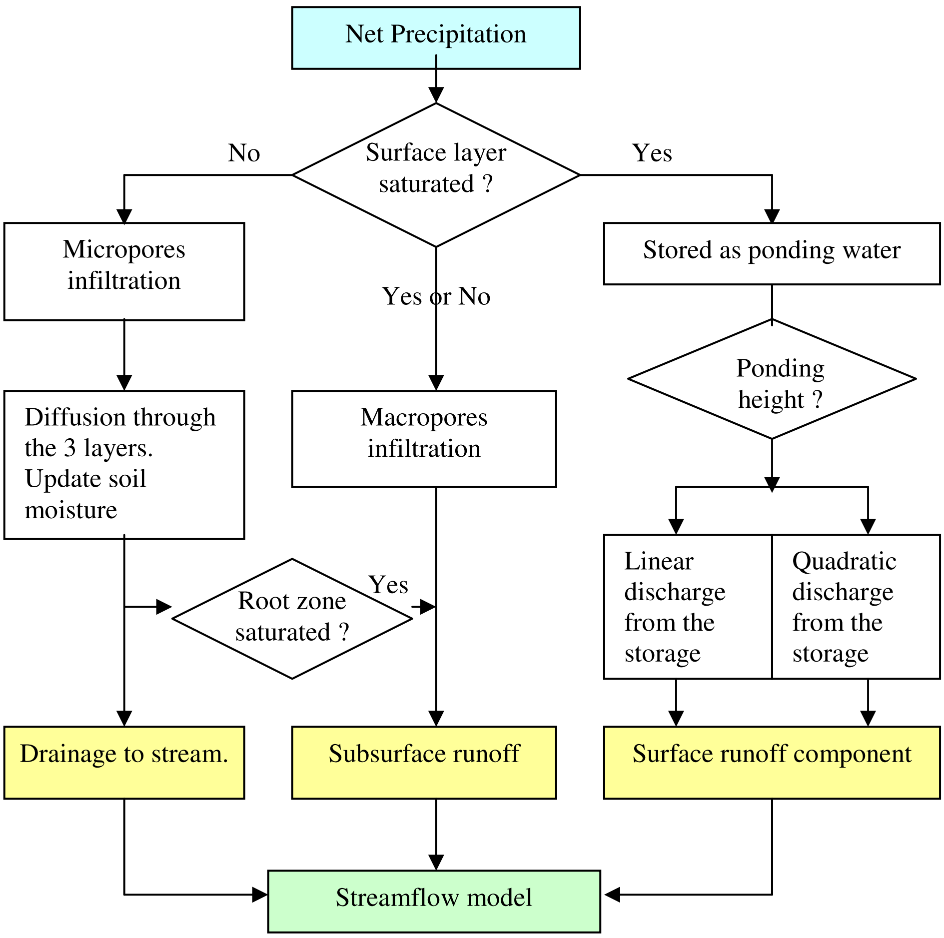

Figure 4-7 Flow chart of an iteration of the stream-flow computation module. Note : The interaction between the micropores infiltration and the macropores infiltration is not represented on this diagram.

The net precipitation at time step n is the variable $P_g^{(n)}$ defined in section 4-2 by equation (4.8) and recalled in equation (4.18) :

$$P_g^{(n)} = P_{through}^{(n)} + Pond^{(n-1)} \tag{4.18}$$

$P_{through}$ is represented as the runoff ② in figure 4-1. $P_{through}$ is the difference between precipitation, the quantity of water that is retained by the vegetation and the quantity that evaporates from the water held on vegetation.

$$P_{through}^{(n)} = Precip^{(n)} - \min[veg_3Precip^{(n)} \,;\, Wr_{max} - (W_r^{(n)} - E_r^{(n)})] \tag{4.19}$$

$veg_3Precip^{(n)}$ is the fraction of precipitation that will be in contact with the vegetation before it reaches the ground. In our case veg is set to 1 since the vegetation is composed of dense grass over the total catchment area.

Wr_{max} is the maximum amount of water that can be intercepted by the foliage. It is estimated following Noilhan and Planton (1989) from Dickinson (1984) by :

$$Wr_{max} = 0.2 \times veg \times LAI \qquad \text{[mm]} \tag{4.20}$$

$Wr^{(n)}$ is the quantity of water stored on leaves at time step n and $E_r^{(n)}$ is the evaporation from this reservoir at time step n. See equation (3.8).

Then the infiltration rate (I) is calculated to take into account the macropores infiltration (I_{mac}) and micropores infiltration (I_{mic}). (Bronstert and Plate 1997 ; Mengelkamp et al. 2001).

The total amount of water available for infiltration per time step of duration Δt is I_{max} :

$$I_{max} = P_g / \Delta t \tag{4.21}$$

The potential micropores infiltration (I_{mic_pot}) depends on the moisture of the surface layer:

$$I_{mic\_pot} = K_{sat} + D_{sat}.\frac{(w_{sat,1} - w_g)2}{d_1} \tag{4.22}$$

It is restricted by the amount of water which can occupy the empty pore space (I_{mic_free}):

$$I_{mic\_free} = \frac{(w_{sat,1} - w_g).d_1}{\Delta t} \tag{4.23}$$

The actual micropores infiltration rate I_{mic_act} is given by :

$$I_{mic\_act} = \min[I_{max}, I_{mic\_pot}, I_{mic\_free}] \tag{4.24}$$

The possible macropores infiltration rate (I_{mac_pot}) must reflect the possibility of quick absorption of excess water. It is expressed as a function of the depth of the macropores layer H_Z [m] and the volume of the macropores network V_{mac} [-]. The depth of the surface layer d_1 is taken as the depth of the macropores layer H_Z.

$$I_{mac\_pot} = \frac{V_{mac}.H_Z}{\Delta t} \tag{4.25}$$

Working on remarks found in Beven and Germann (1982) and Parlange and Hopmans (1999) an empirical equation was included to represent the hypothetical spatial evolution of the macropores system. Thus the available volume of macropores depends on the antecedent moisture conditions. More precisely, we consider that the macropores network spatially evolutes as a function of the time of saturation of the surface layer, between a lower boundary V_{mac_min} and a maximum macropores volume V_{mac_max}. The actual macropores volume V_{mac} is given by :

$$V_{mac} = (V_{mac\_max} - V_{mac\_min}).\left(1 - e^{\frac{-\ln(10)}{T_{90}} T_{sat}}\right) + V_{mac\_min} \tag{4.26}$$

where T_{sat} is a measure of the cumulative time of saturation of the first layer. T_{90} is the value of T_{sat} after which 90 % of the maximum volume of macropores is active.

The actual infiltration rate into the macropores system I_{mac_act} follows the conditions :

$$I_{mac\_act} = \begin{cases} I_{mac\_pot} & \text{, if } I_{max} > I_{mac\_pot} + I_{mic\_act} \quad (4.27a) \\ I_{max} - I_{mic\_act} & \text{, if } 0 < I_{max} < I_{mac\_pot} + I_{mic\_act} \quad (4.27b) \\ 0 & \text{, if } I_{max} - I_{mic\_act} = 0 \quad (4.27c) \end{cases}$$

Then the infiltration rate I is :

$$I = I_{mic\_act} + I_{mac\_act} \tag{4.28}$$

The soil moisture in each layer is then calculated. If the first layer is saturated after the computation the excess water is stored in the ponding storage (P_{ond}) which will discharge to generate surface runoff (Q_R). If the root zone is saturated after the computation then the water in excess is added to the subsurface component. The subsurface stormflow (Q_{storm}) is calculated from the infiltration that is routed to the stream by the mean of a reservoir (S) :

$$Q_{storm} = \frac{\ln(2)}{T_{sub}}(S + I.\Delta t) \tag{4.29}$$

where T_{sub} corresponds to the time for subsurface flow to recede to 50 % of saturation from a saturated state.

The surface runoff is calculated based on the principle of discharge from a ponding water storage (*Pond*). The equations proposed Mengelkamp et al. (2001) were implemented first. But a curve fitting applied to the scatter plot of the observed surface runoff against the computed ponding height revealed a quadratic relationship between these two variables, mainly for high values of the observed runoff. This could be explained by the variability of the shear stress with the height of ponded water. It would be interesting in further research to look at the influence of the height of ponded water on the velocity of the surface flow. An intuitive hypothesis consists in assuming that the shear stress (the Manning's roughness coefficient) decreases with the increasing height of water, because the friction due to gravel or vegetation decreases, or because the ponding height exceeds the depth of the possible compacted holes at the surface left by the cows. (Note : the surface runoff was separated from the base-flow by an automated technique of hydrograph separation. A method and a criticism of this analysis tool can be found in Nathan and McMahon (1990) and in Sloto and Crouse (1996)).

The ponding height at time n is given by :

$$Pond^{(n)} = Pond^{(n-1)} + P_{through}{}^{(n)} - I^{(n)}.\Delta t - \mathrm{E_t}^{(\mathrm{n})} \tag{4.30}$$

Discharge from the ponding storage is then calculated by :

$$Q_R = \min[Pond, \max(\, k_1 3Pond,\; k_2 3Pond^{\,2})] \tag{4.31}$$

where k_1 and k_2 are recession coefficients governing the discharge. k_1 and k_2 are found by calibration.

The base-flow is calculated following the equation of the vertical drainage as described in section 4-2, by equation (4.7). This equation is :

$$K_3 = \frac{C_3}{\tau} \cdot \frac{d_3}{(d_3 - d_2)} \cdot \max\left(0, (w_3 - w_{fc})\right) \tag{4.33}$$

However one can notice that the soil coefficient C_3 governing the vertical drainage in soil is used for both the vertical drainage from the root zone and for the deep layer (see equation (4.6)). The same coefficient is applied at two different depths. This formulation was found to overestimate the drainage at the bottom of the last layer, with C_3 chosen after the calibration of the soil moisture in the root zone. With the same coefficient C_3 applied for drainage, we do not take into account the compaction of soil with depth and the change of texture. (Kutílek and Nielsen 1994) That may be why the base-flow was overestimated. Thus we applied the same formulation with a different soil coefficient. K_3 is given by :

$$K_3 = \frac{C_{drain}}{\tau} \cdot \frac{d_3}{(d_3 - d_2)} \cdot \max\left(0, (w_3 - w_{fc})\right) \tag{4.34}$$

Finally the simulated stream-flow is the sum of the different components calculated for a time step of 30 minutes. Thus :

$$Flow = Q_R + Q_{storm} + K_3 \tag{4.35}$$

And the process is iterated.

4-3-3 Results

The hydrological processes were calibrated by comparing the measured and simulated time series of stream-flow. Calibration was performed manually and some parameters were checked using an automatic calibration algorithm based on the optimization of an objective function by an ant colony (Abbaspour et al. 2001, Gagné et al. 2001). The total data set was divided in two : the period from day 320 to 420 (November the 16th to February the 24th) was used to calibrate the model, while the period from day 420 to 560 (July the 14th) was used for the purpose of validation. One of the issues of the automatic calibration comes from the definition of an objective function whose value will be the most representative of the expected behaviour of the model. Some typical errors measurements allow nevertheless to have an idea of the quality of the simulation (see figure 4-8).

The following analysis presents the results of the stream-flow simulation with a time increment of 30 minutes. The simulated time series are compared to the continuous observations made at the weir for the period from November the 16th 2001 to July the 14th 2002. This period covers many types of forcing conditions and allows a good assessment of the behaviour of the model.

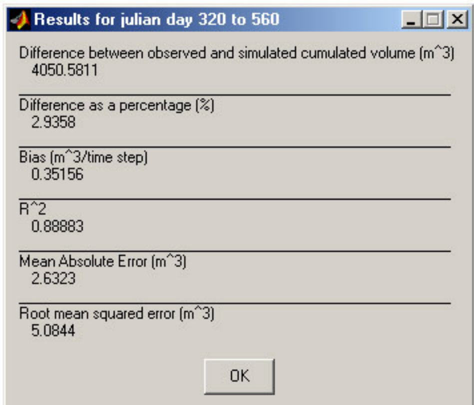

Figure 4-8 Some errors results

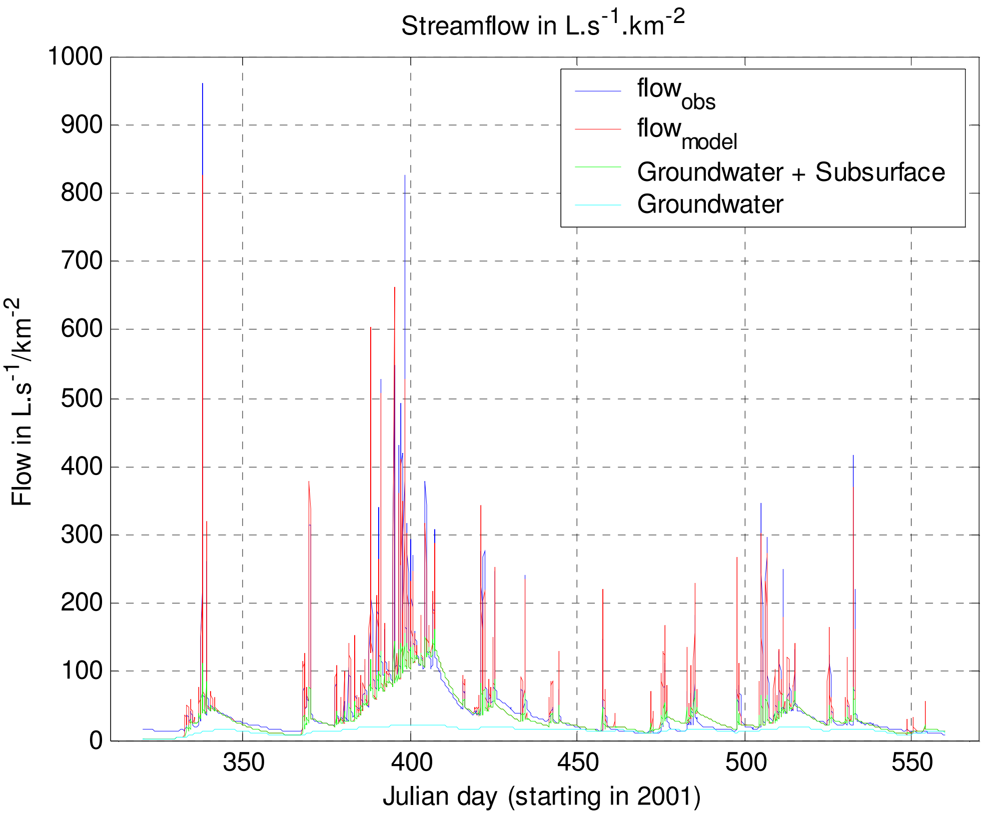

Figure 4-9 Time series of the simulated and observed stream-flow at a 30 min time increment with the indication of the different components generating the stream water. All the peaks are represented with good timing and satisfactory magnitudes. The sensitivity of the site is respected in the model as long as both responses to rain events are in good agreement.

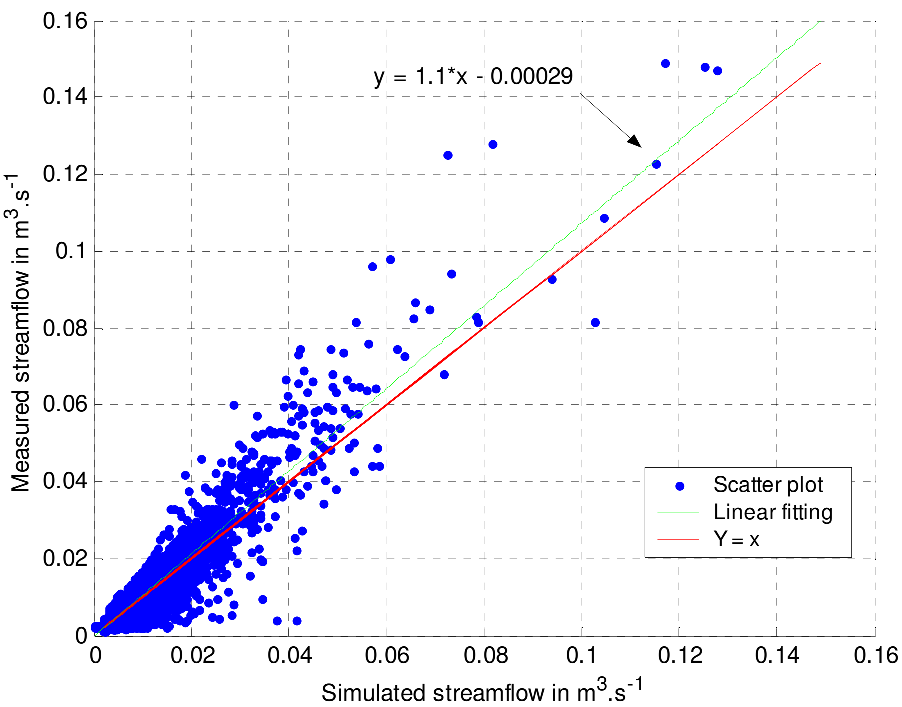

Figure 4-10 Scatter plot of the observed stream flow against the simulated flow for the whole study period. This diagram shows no unexpected trend. All the dots are concentrated along the 1:1 line that would correspond to a perfect agreement.

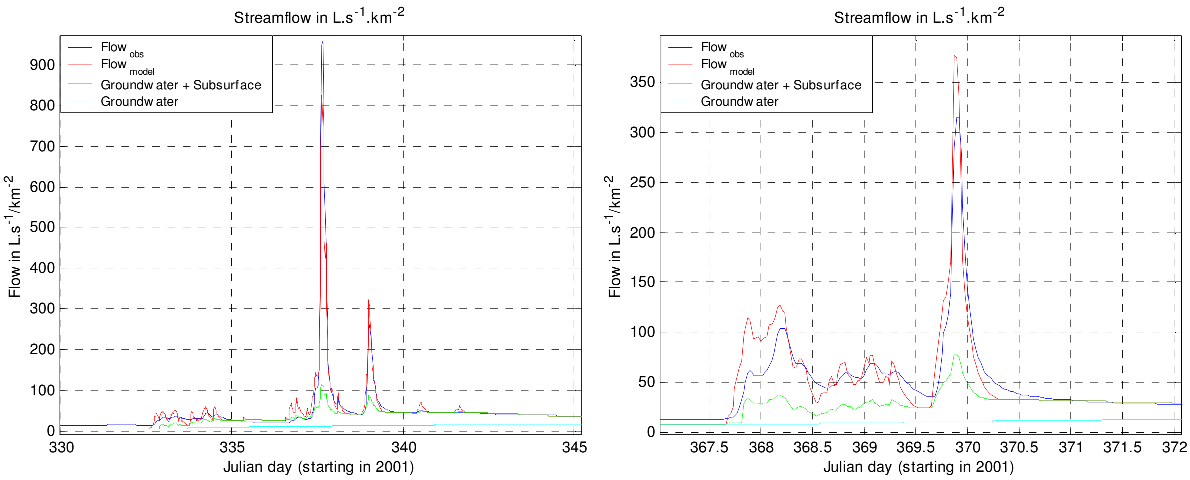

Figure 4-11 Detail of the simulation compared to the observations for some intermittent rain events. The peaks and the slopes are reasonably modelled.

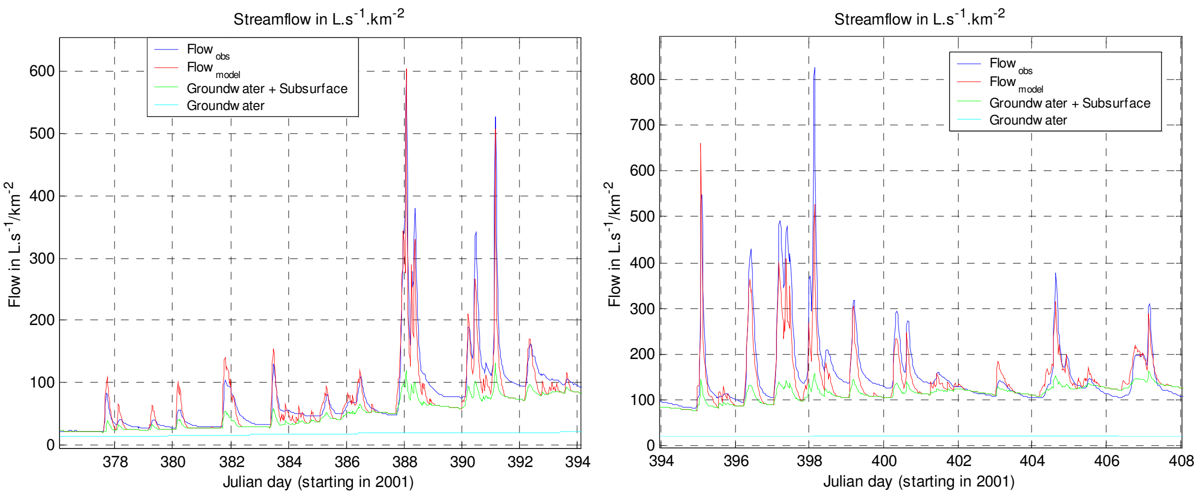

Figure 4- 12 A detail of the wettest period. This period is characterized by a sequence of heavy rain events at close intervals. The peaks are still well estimated but the end of the discharge is underestimated. This may come from a too small variation of the base-flow. The slopes predicted in particular by the storm-flow component are correct, but the simulated volume of water at the end of the discharge is too low.

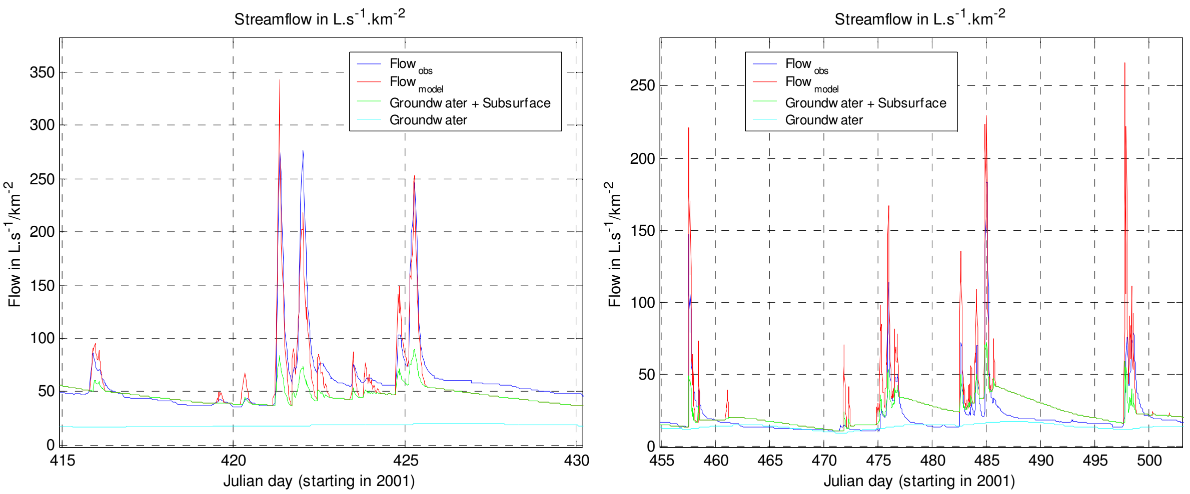

Figure 4-13 One can notice that the model predicts a small peak after day 420 or 470 that did not occur. This error comes from the soil moisture simulation which wrongly allowed water to pond. The high discharge between days 475 and 495 is also due to an erroneous simulation of the saturation of wg, thus activating more macropores and generating storm-flow.

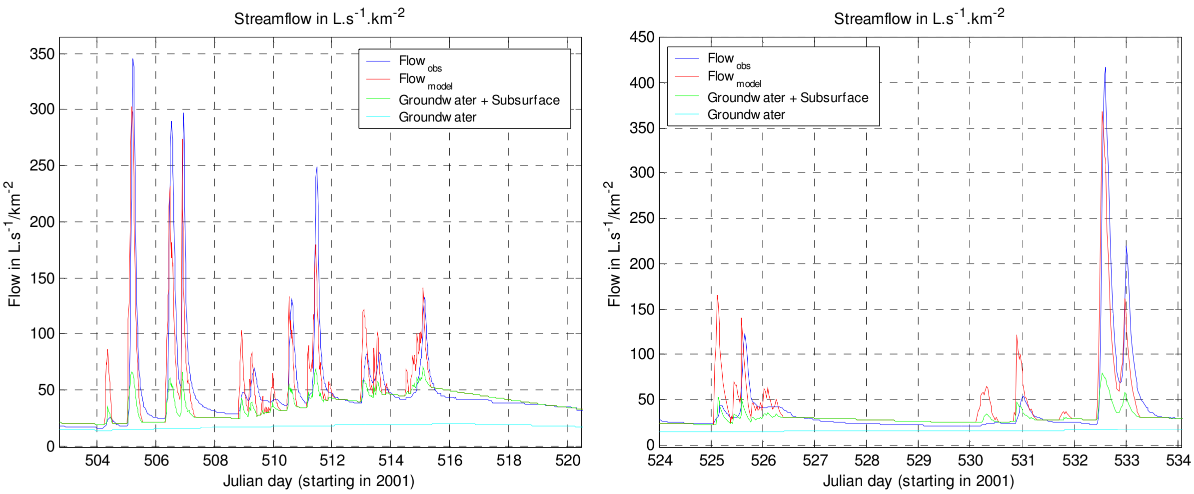

Figure 4-14 A few examples of poor simulation of surface runoff are noticeable on these figures. This highlights the tight link between the soil moisture simulation and the stream-flow computation and clearly shows the need of constant effort to improve the soil moisture simulation.

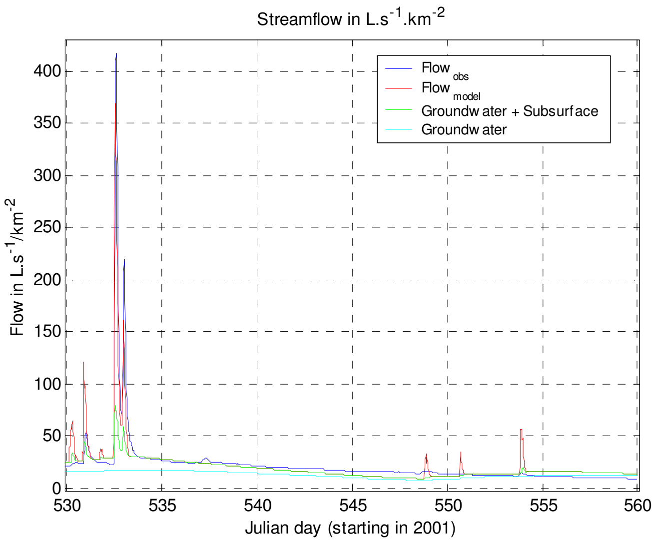

Figure 4-15 A long drying period.

Figure 4-15 illustrates again the effect of a less consistent simulation of the soil moisture, particularly for the first layer. The three very small peaks which are predicted did not occur in the observations. It is indeed surprising that after such a long drying period the model still predicts the saturation of the first layer. This might be explained by the underestimation of the evaporation during this period.

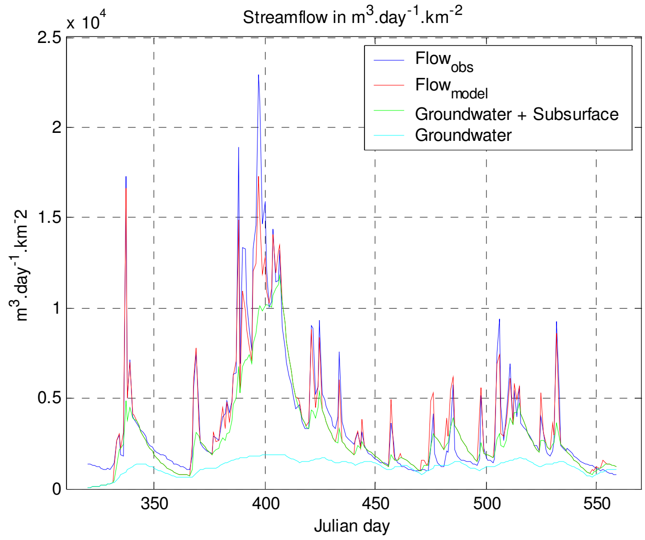

Figure 4-16 The hydrograph with a one day increment.

The temporal scale was one of the major difficulty to examine because of the sensitivity in the model it implies. But a time step of 30 min. is necessary to capture the reality of the field and the immediate response of the catchment to precipitation. One can see on figure 4-16 that if a good simulation is achieved with a short time step, the cumulated values to predict larger time increments are also correct. Whereas the contrary is not true. Daily simulation will not lead to a good simulation at 30 min time intervals easily.

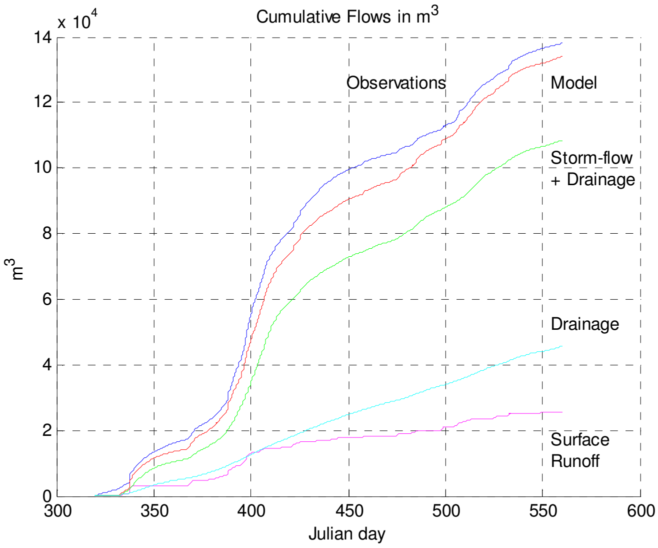

Figure 4-17 Cumulative time series of the different components of the simulated stream flow.

Figure 4-17 represents the contribution of each component that generates stream flow. Even if peaks occur very often their contributions to the total amount of water does not exceed 20 %. The quick storm flow as it is predicted in the model has a great impact on the cumulated time series. The drainage may seem slightly too low. No observations are available to confirm the relative importance of storm-flow but many authors report a great importance of this component.

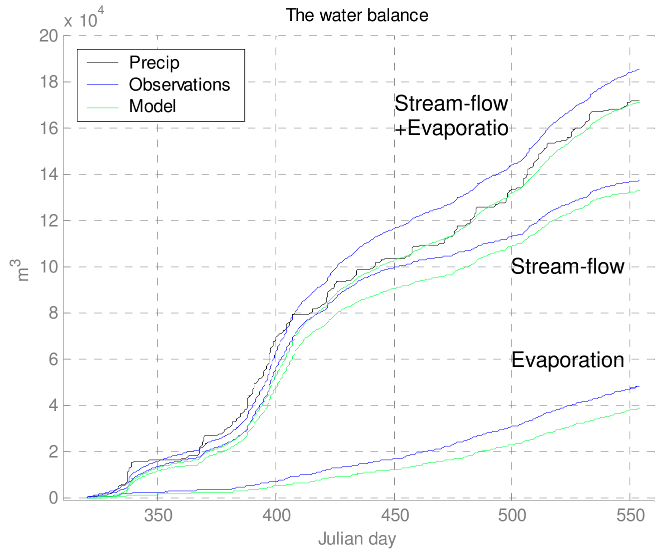

Figure 4-18 Comparison of the simulated and observed water balance without the change in soil moisture storage.

The comparison of the simulated and observed water balance in figure 4-18 indicates the inevitable possibility of error in measurements. Even though the change in soil moisture storage is neglected, the observed sum of the stream water and the evaporation is overestimated. Unless the precipitation is underestimated. We notice the high quality of measurements, since the water balance is fairly well respected.

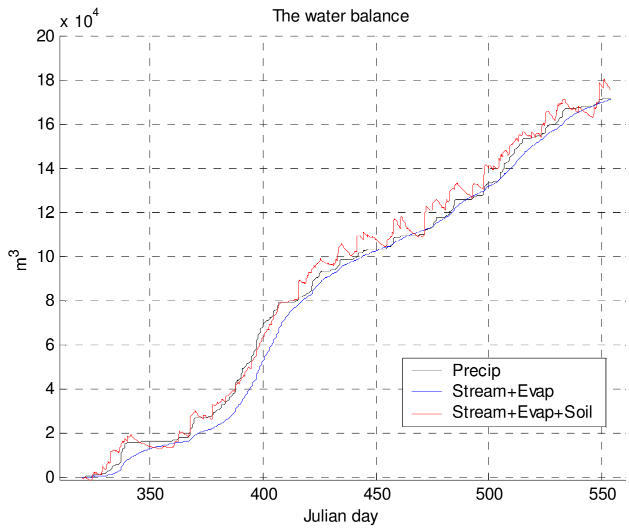

Figure 4-19 The simulated water balance.

Figure 4-19 shows the simulated water balance compared to the precipitation. It takes into account the change in soil moisture storage calculated thanks to the surface layer and root zone only (no observations are available to validate the soil moisture in the deep layer). One can notice that during drying period the effect of the storage in soil is visible (e.g. day 350 ; day 400)

4-3-4 Conclusions

The three components of stream-flow :

The simulation of the hydrograph with a short time increment of 30 minutes shows good agreement with the observed stream-flow. Although the importance of each component contributing to generate the stream water cannot be measured on the field, it seems that the predicted role of each component agrees with the literature. The different predicted outflows contribute differently to reproduce the hydrograph. The surface runoff, computed from a ponding water storage accounts for the fast response to precipitation. It constitutes the main volume of a peak. The subsurface runoff also called storm-flow is slightly delayed compared to the surface runoff. Its role is mainly to reproduce the fall of the hydrograph peaks. It creates a transition between the quick response of the surface runoff and the flat curve of the base-flow. The base-flow indeed generates a continuous discharge to the stream whose variations are very attenuated.

Validation and errors :

From a modelling point of view, the validation period reproduces the rainfall events and the drying periods as correctly as the calibration period. The errors found on the simulated hydrograph for the validation period come from the bias in the simulation of soil moisture. Since the volumetric water content in the first layer regulates the surface runoff, the errors in the simulation of the soil moisture have consequences on the simulation of flow. Even though it would be preferable to avoid these mistakes, it is a positive aspect of the stream-flow module. Indeed it means that the computation of the flow is “honest“ and reliable if the inputs are so. The errors do not combine to produce a fake good representation.

The contaminants transport : the next extension

The main water processes on the field seem to be acceptably understood and modelled. The short time step was necessary to capture the nature of the events. It has a major importance when dealing with the transport of stream contaminants such as phosphorus. As visible on figure 4-16 the hydrograph plotted with a time step of one day does not render the quick discharges. Thus a model running with a one day time increment could not assess the possible contamination of stream. Some heavy rain events could indeed wash out the soil in a few hours only carrying solutes in large quantity but in short time.

The coupling of the SVAT model with a phosphorus discharge module was then the next step in the representation of the catchment. This model of phosphorus discharge in the stream is inspired by the structure of the SVAT parameterization and uses the simulated outputs as inputs to predict the phosphorus content in water. It was developed in collaboration with Jean-Noël Vidal as a final year project for the Ecole Polytechnique in France.

4-4 The phosphorus module

4-4-1 Introduction

Phosphorus is an important factor of the quality of water. Its role in the eutrophication process of streams is abundantly documented. In Ireland, the major sources of phosphorus in streams come from the management of the grassland fields. 90% of all arable land in Ireland is grassland, most of it for cattle grazing. The concern of production over the past decades led to a general increase of nutrient fertilization. Fertilizer and slurry are in the case of grasslands the main sources of phosphorus. The consequences of repeated spreading of fertilizer are nowadays clearly identified. The concentration of phosphorus in soil has greatly increased (see table 4-2 from Whitehead (2000)) and the issue of saturation of the uppermost layers of soil nowadays arises. Indeed subsurface leaching and mostly surface runoff are critical in the solute transport. They occur close to the surface or at the surface, where the concentration of phosphorus is high, and carry large volumes of water. Thus many questions of management strategies arise with the concern of limiting the water pollution. Is fertilizer still useful ? With what frequency fertilizer should be spread ? When is the most appropriate period for fertilising ? and many others.

These questions can be addressed in the modelling effort. The model presented in the following sections joins the present need for assessment tools.

Soil horizon depth (mm)	Initial soil P (mg.kg^{-1})	Rate of application (kg P ha^{-1}.year^{-1})		
		0	16	32
0-75	710	750	930	1150
75-150	670	715	885	1010
150-225	600	625	680	740
225-300	505	500	500	510

Table 4-2 Effect of applying fertilizer annually for 35 years on the concentration of total P (mg P kg^{-1} soil) in four horizons of a grazed grassland soil in New Zealand (from Nguyen and Goh, 1992)

4-4-2 Observations and methods

Literature supplies many classification of the forms and availability of phosphorus. The idea of this model is to describe as simply as possible the transfer processes and loss of phosphorus. Being added to the SVAT model, the phosphorus module has been developed from a hydrological viewpoint. That is to say that the classification used is interested in the different sources of phosphorus whose influence on the relative contribution of the different types of phosphorus in the hydrological mechanisms is observable. Thus the model tries to describe the availability and the transport means of phosphorus, instead of trying to represent all the biochemical reactions occurring in soil. The model has then been based on simple concepts found in the literature.

Whatever its form, most of the phosphorus remains in the soil close to the surface, to a depth of about 10 cm and to a lesser extent, maybe up to 30 cm. The main part of it (about

90%) is chemically transformed into organic phosphorus which is less extractable than inorganic phosphorus. The organic phosphorus is easily available for plants uptake. The remaining 10 % of inorganic phosphorus is easily carried away by surface runoff and subsurface storm-flow. Finally slow processes occur to transform inactive phosphorus of the soil into available phosphorus. (Tunney et al.)

In the next section, we refer to Morgan's phosphorus (Morgan's P) as a measure of the available phosphorus in soil. The focus of the model is mainly on the availability of different forms of phosphorus and on the assessment of their contribution to the total phosphorus in stream.

4-4-3 The model

In order to model a simple phosphorus budget from soil to water, three phosphorus pools are used. The most active one is the soil solution, which is split between the first two soil layers of the SVAT model. A second reservoir contains Morgan's phosphorus, and a third large storage contains slowly reactive phosphorus. These pools interact by different transfers. A slow transformation occurs between the storage zone and the Morgan's P reservoir. The transfer between the soil solution and the Morgan's P follows an equilibrium law. The remaining transformation considered was between the surface layer and the root zone and deals with the soil solution. As for phosphorus uptake by plants from the root zone, this extraction is controlled by the seasonal activity of plants and the concentration of phosphorus in the soil. It occurs in the Morgan's P reservoir. The discharge in the stream is simulated by two components draining the soil solution : one from the simulated surface runoff and the other from the simulated subsurface runoff. Both are controlled by the flow intensity and the phosphorus concentration. The quantity of fertiliser spread on the field is an input for the model.

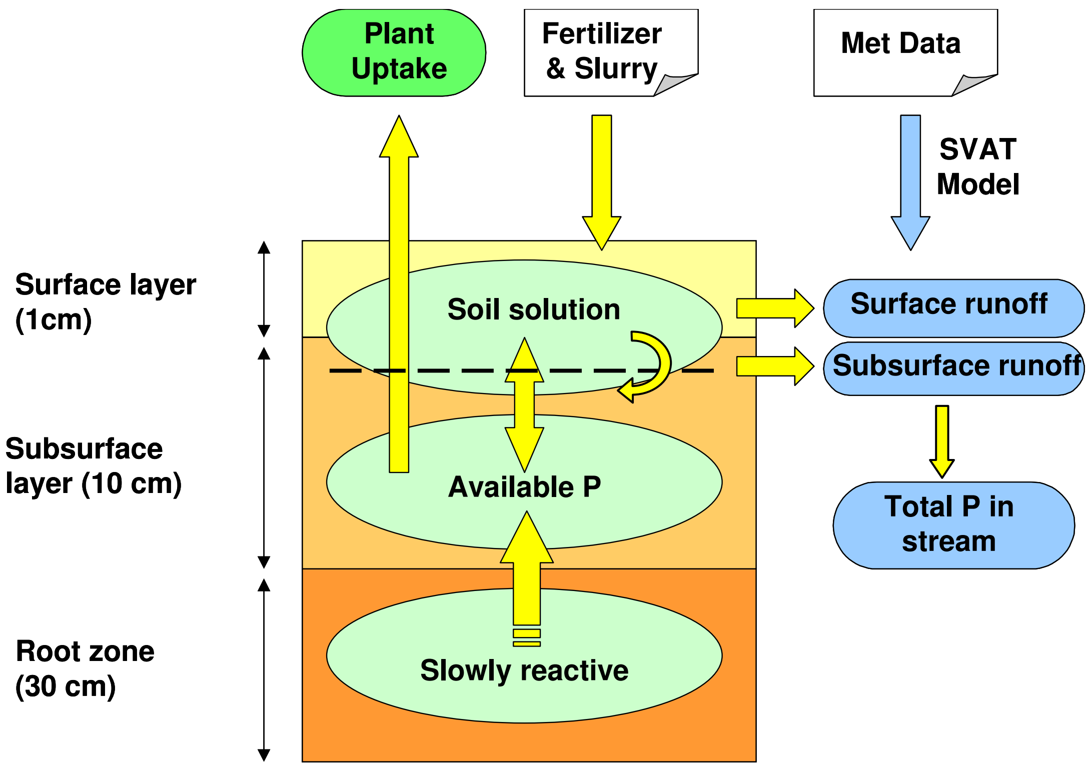

Figure 4-20 Schematic representation of the phosphorus model. The direction of the solid arrows shows the direction of the transfers.

The different transfers represented on figure 4-20 are subdivided in three categories : Input, Transfers and Outputs :

I_{load}	is the load of fertilizer or slurry.
T_{SS_AP}	is the transfer between the Soil Solution and the subsurface Available P pool.
T_{AP_SS}	is the transfer between the subsurface Available P pool and the Soil Solution. $T_{AP\_SS} = - T_{SS\_AP}$
$T_{SurfaceSS\_SS}$	is the transfer between the part of the Soil Solution in the upper layer to the total Soil Solution.
T_{slow_AP}	is the slow transfer from the deep slowly reactive reservoir to the available P pool.
$O_{SurfaceRunoff}$	is the amount of phosphorus extracted by surface runoff.
$O_{SubsurfaceRunoff}$	is the quantity of phosphorus extracted by storm-flow.
O_{Plants}	is the quantity taken by the vegetation.

The concentrations calculated by the model are :

$C_{SurfaceSS}$	the concentration in the upper part of the Soil Solution.
C_{SS}	the concentration in the Soil Solution.
C_{AP}	the concentration in the Available P reservoir.
C_{slow}	the concentration in the slowly reactive reservoir.

The fluxes are governed by the following equations :

$$T_{SS\_AP} = \frac{-1}{\tau} \cdot \left(C_{SS} - \frac{C_{AP}}{\alpha} \right) \tag{4.36}$$

where τ is a time constant governing the rapidity of transfer and α a coefficient of balance between the two pools.

$$T_{SurfaceSS\_SS} = \frac{-1}{\tau_{surf}} \cdot \left(C_{SurfaceSS} - \frac{C_{SS}}{\alpha_{surf}} \right) \tag{4.37}$$

where τ_{surf} is a time constant governing the quick transfer between the surface part of the soil solution and the lower part, and α_{surf} is a coefficient of balance between the upper part of the pool and the rest. This transfer is used to fix limit of time of the possible rapid wash out effect by surface runoff.

$$O_{SurfaceRunoff} = -(C_{SurfaceSS})^2 . K_{Surf}(Q_R) . Q_R \tag{4.38}$$

where $K(Q_R)$ is a coefficient governing the extraction. It was found from observations that K_{Surf} linearly depends on the flow. It is then defined by :

$$K_{Surf}(Q_R) = k_1 . Q_R \tag{4.39}$$

with k_1 a constant.

The same type of equation is applied for subsurface runoff :

$$O_{SubSurfaceRunoff} = -(C_{AP})^2.K_{Sub(Q_{Storm})}.Q_{Storm} \tag{4.38}$$

where $K_{Sub(Q_{Storm})}$ is a coefficient governing the extraction. It is then defined by :

$$K_{Sub(Q_{Storm})} = k_2.Q_{Storm} \tag{4.39}$$

with k_2 a constant.

The extraction by the plants from the Available P reservoir follows two variations. On the one hand it depends on the time of the year. In winter plants are much less active than in spring when new leaves grow. This seasonality is empirically modelled by another sign of the seasonal activity of plants : the net uptake of carbon dioxide. We have the great opportunity to measure this variable on the field. Thus averaging this variable on a monthly basis, and centring the variable between 0 and 1 we get a measured coefficient K_{season} of the seasonal activity of the plants. On the other hand it also depends on the concentration of phosphorus in soil. We defined after Tunney et al. () an exponential function representing the efficiency of plants depending on the concentration of phosphorus. (These coefficients are presented in figure 4-21).

$$O_{Plants} = -veg.\left[Ext_{\max}\cdot\left(1-e^{\frac{-\ln(10)}{P10}C_{AP}}\right)\right]\cdot K_{season} \tag{4.40}$$

where P10 represents the concentration of phosphorus for which the plants efficiency is around 90 %. Ext_{max} is the maximum plant yield.

The transfer from the slowly reactive reservoir to the available P is :

$$T_{Slow\_AP} = \frac{-1}{\tau_{slow}}\cdot\left(C_{AP}-\frac{C_{Slow}}{\alpha_{Slow}}\right) \tag{4.41}$$

where τ_{slow} is a time constant governing the slow transfer and α_{slow} a coefficient of balance between the two pools.

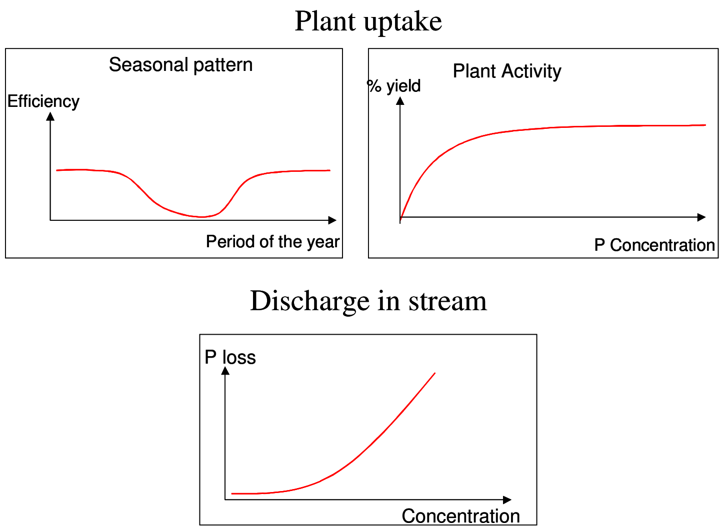

Figure 4-21 Sketch of the behaviour of some parameters controlling the P loss.

Once the transfers are defined, the expression of the concentrations at time $(n+1)$ is given by :

$$(C_{SurfaceSS})(n+1) = (C_{SurfaceSS})(n) + I_{load} + O_{SurfaceRunoff} + T_{SurfaceSS\_SS} \tag{4.42}$$

$$(C_{SS})(n+1) = (C_{SS})(n) - T_{SurfaceSS\_SS} + T_{AP\_SS} \tag{4.43}$$

$$(C_{AP})(n+1) = (C_{AP})(n) + O_{Plants} + O_{SubSurfaceRunoff} + T_{SS\_AP} + T_{Slow\_AP} \tag{4.44}$$

$$(C_{Slow})(n+1) = (C_{Slow})(n) - T_{Slow\_AP} \tag{4.45}$$

4-4-4 Results

This section presents the results of the simulation of the discharge of phosphorus into the stream. The period of simulation starts January at 1st 2002. It reproduces the P content in stream until day 140 (May the 20th 2002). At the time this study was carried out no other data were available. The model was mainly calibrated on the comparison of the observed and simulated cumulative discharge in stream.

In order to analyse the results, we must know that fertilizer was spread on day 81 that is March the 22nd.

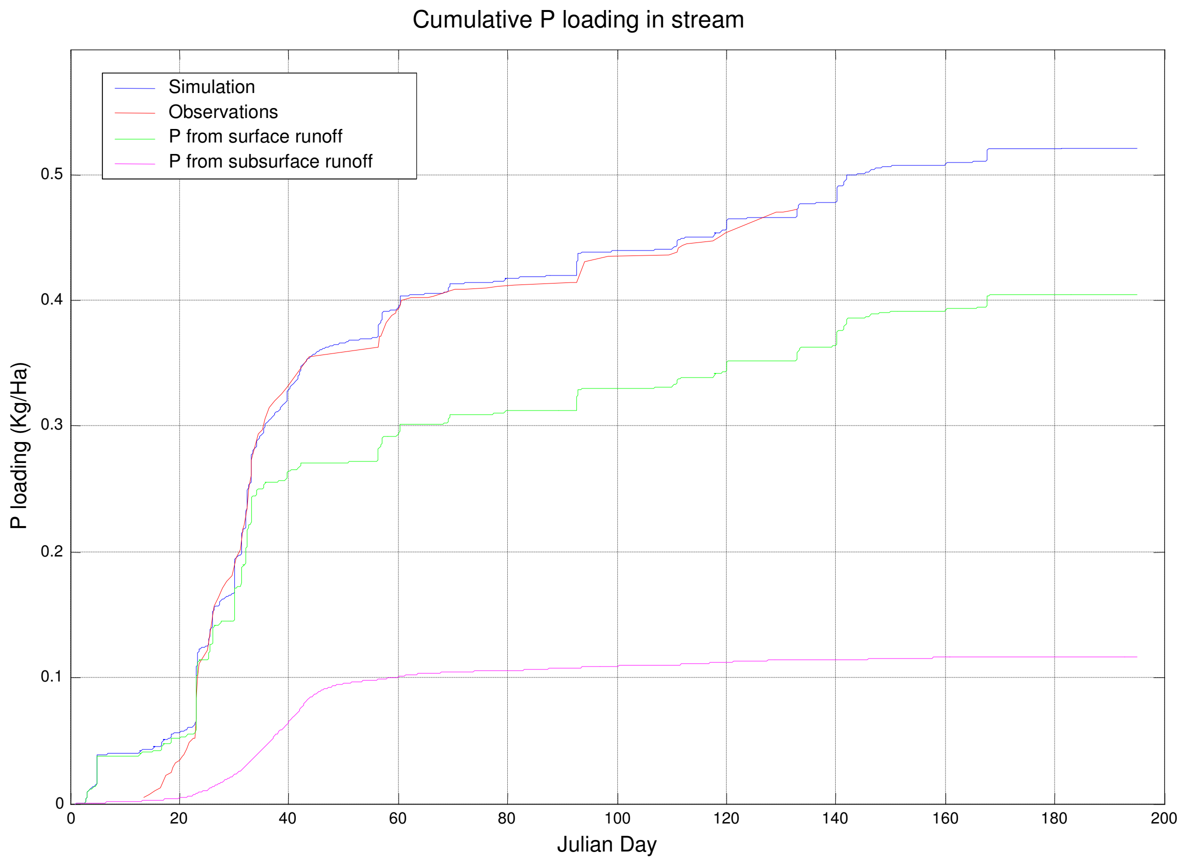

Figure 4-22 Comparison of the simulated and observed cumulative P loading in the stream. The contribution of each hydrological component shows the importance of the surface runoff in terms of pollution risk compared to the cumulative volume of water it drains. See figure 4-17.

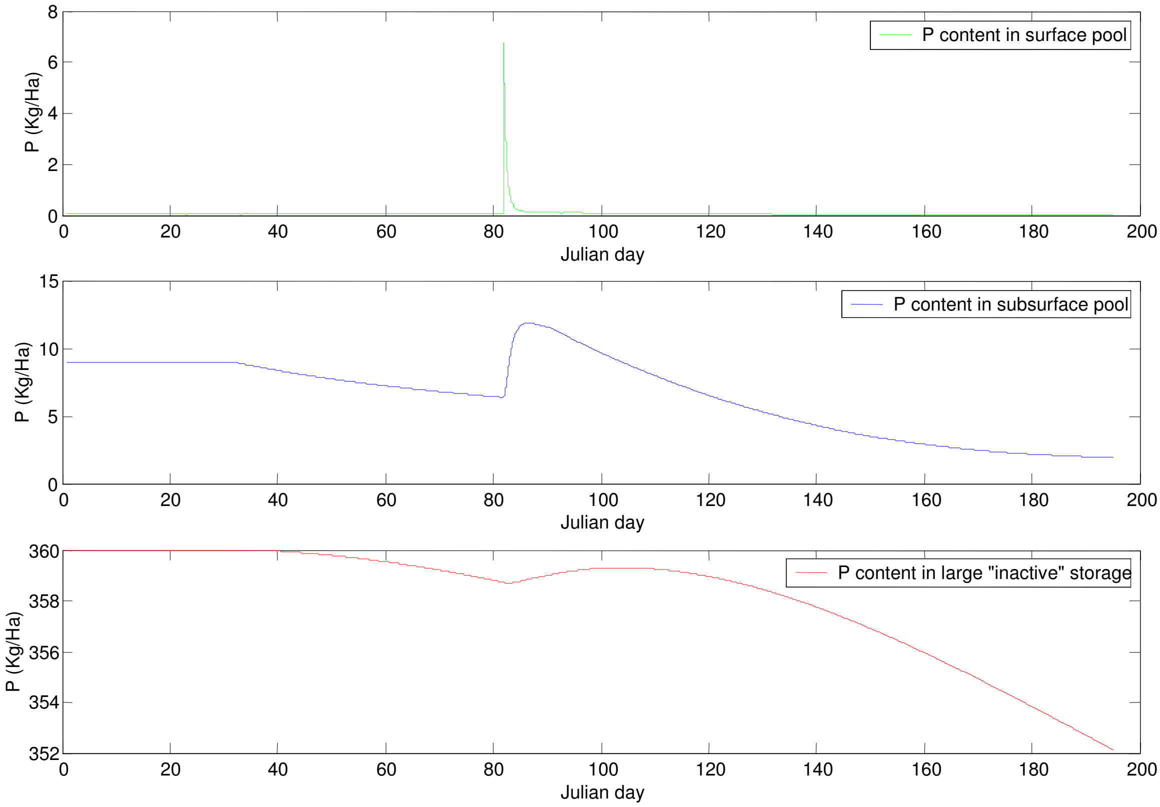

Figure 4-23 Behaviour of the three pools defined in the model. The effect of the fertilizer load on day 81 is visible for each reservoir. This figure shows the sensitivity of each pool to fertilizer. It also shows the attention that must be paid to the meteorological conditions when spreading fertilizer to avoid the rapid flush of the surface pool.

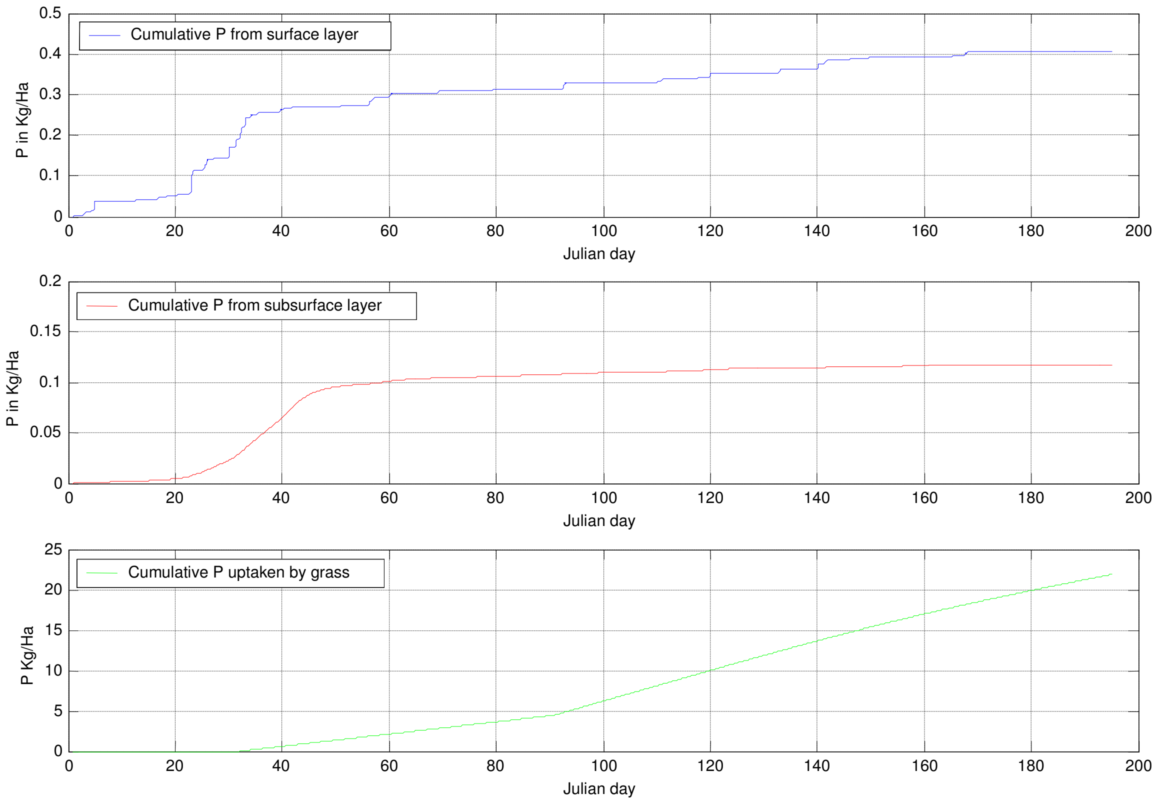

Figure 4-24 Cumulative loss of phosphorus. The three modelled ways phosphorus is extracted are shown.

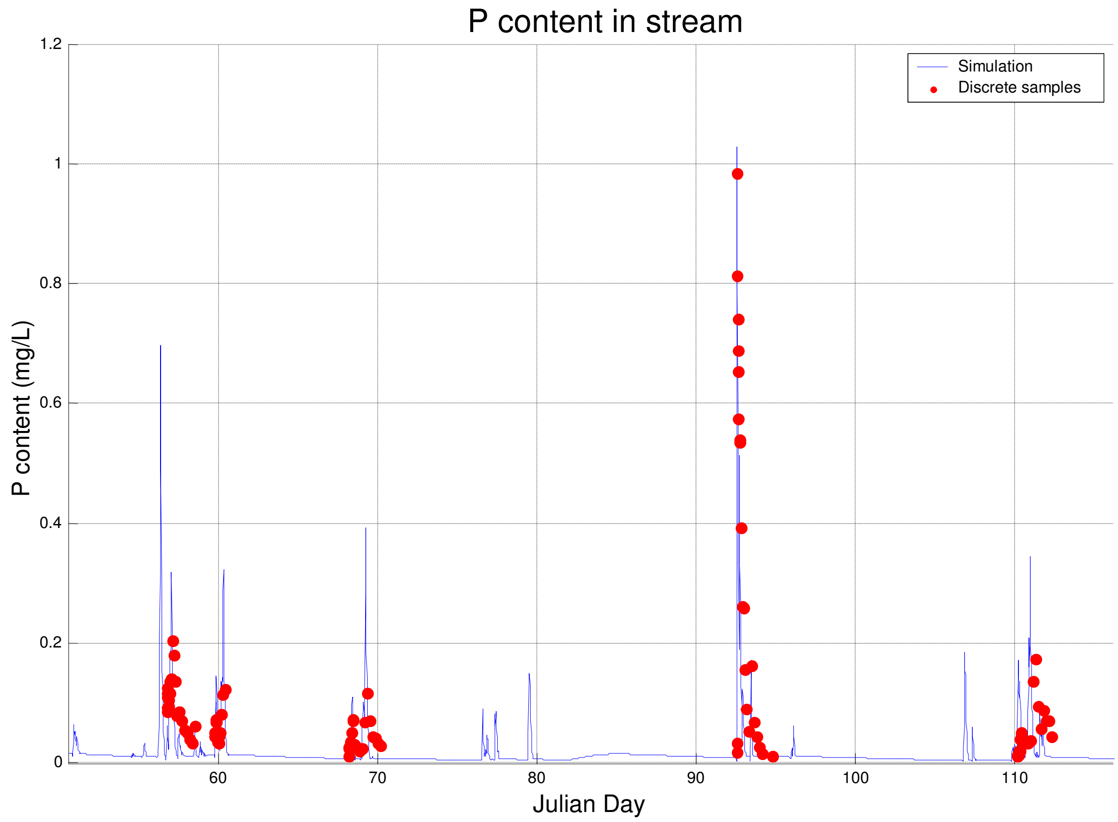

Figure 4-25 Comparison of the simulated total phosphorus content in stream with discrete samples. This set of data was used to validate the model. The good agreement in terms of magnitude and timing are encouraging.

The modelled results are encouraging. It seems that the comprehension of the main mechanisms generating a phosphorus discharge into the stream is correct, and that the equations interpret reasonably well the processes. However it would be interesting to run the model with more data. Indeed only one data set of discrete samples was used to validate the model.

If these good results were confirmed with new data, one could try to use this model as an assessment tool of management strategies. The validation data would be in that case more difficult to get. It would be difficult to convince the farmer owning the field not to fertilize his field, since it represents a risk for him in terms of grass production. But if this kind of validation was performed different scenarios of management could be tested, and the questions asked in the introduction could be answered.

An example of scenario is presented in spite of the lack of information about the reliability of the model for this kind of study in figure 4-26.

4-4-5 Scenarios

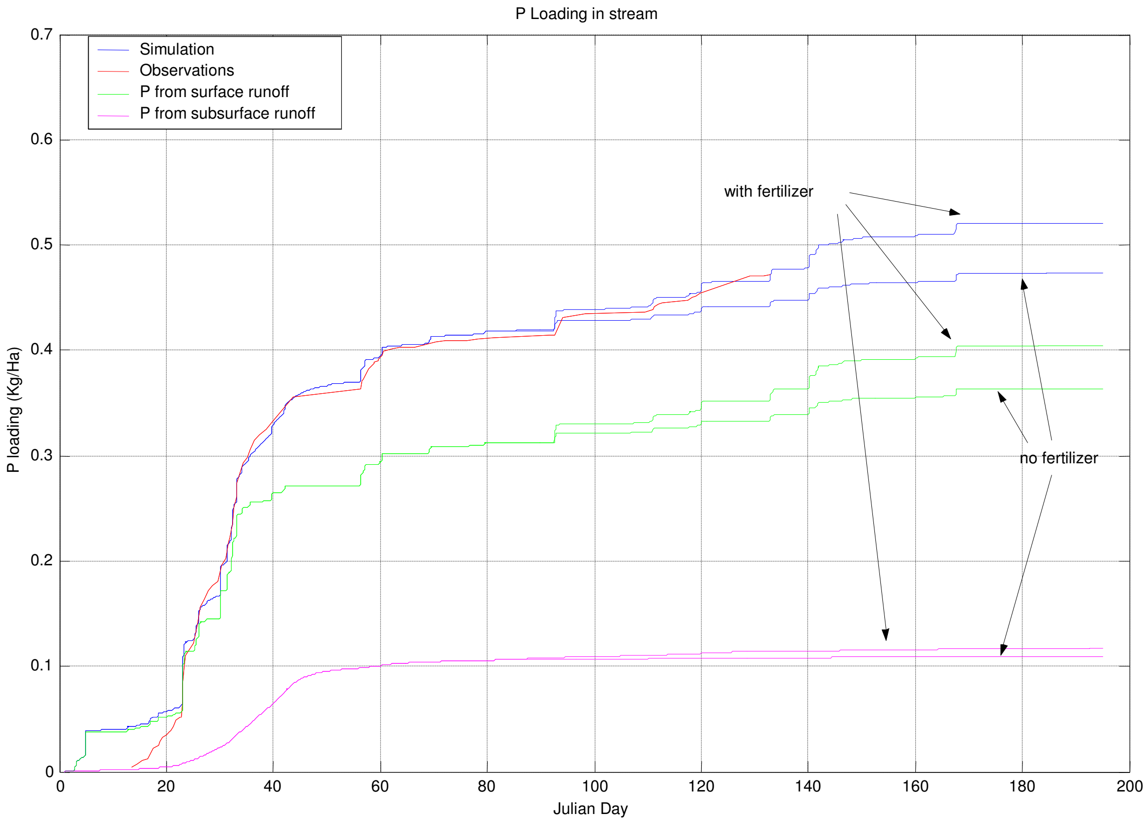

Figure 4-26 What if no fertilizer was spread on day 81 ? The model computed a possible answer for the cumulative total phosphorus content in the stream.

The results presented in figure 4-26 cannot really be discussed, as long as we are not confident in the robustness of the model.

Chapter 5

Conclusions and suggestions for further research

Chapter 5
Conclusions and suggestions for further research

5-1 Conclusions

5-1-1 Summary

A Soil-Vegetation-Atmosphere Transfers parameterization is presented in this thesis. The land surface scheme is a one-dimensional model used at the point scale. The computations are assumed to represent the whole 15 ha grassland catchment area. Indeed the study site is a small grassland considered as homogeneous with regard to the vegetation and the soil. The SVAT scheme was designed as a trade-off between an accurate description of the main physical mechanisms and the simplicity of implementation. We tried to limit the number of parameters and we designed the different flow components so as to allow easier calibration. The vegetation is simply described in terms of evapotranspiration. It acts as an interception reservoir for precipitation.

The water exchanges are computed for a thin upper layer which is 10 cm deep, a root zone layer overlapping the surface layer which is 30 cm deep, and a third layer whose depth is 1 metre. The volumetric water content in the soil is calculated using a force restore method for the three layers. The parameters governing these equations depend on the soil texture. Based on the good agreement between the observed and the simulated time series of the soil moisture for both the upper layer and the root zone, the stream-flow components have been added to the scheme.

Three components generate the stream flow. The discharge from a ponding water storage creates surface runoff, also called overland flow. The base-flow is modelled by a drainage term, controlled by the soil moisture in the third deep layer. In order to reasonably simulate the slopes of the recession limb of the hydrograph, and to include a term of quick response from the soil, a subsurface component was included. This storm-flow empirically computes the effect of macropores and preferential flow paths during heavy rain events. These components were found to give a suitable representation of the field response to rainfall. This response is characterized by sharp peaks of short duration under intermittent rain events.

The calibration was mainly performed manually, based on a first estimate of the range of parameters by using a parameterization depending on the soil textural class. But an automatic calibration was also achieved to check some parameters. This was done by the optimization of an objective function by an ant colony algorithm.

The results were compared to good continuous measurements at 30 minutes intervals. This time step was challenging in terms of modelling but is appropriate to describe the high sensitivity of the site and the rapid response of stream-flow to rain events.

In addition to the stream-flow simulation, the phosphorus discharge in the stream is also modelled. The good agreement of both the stream-flow simulation and the predicted total phosphorus content in water are encouraging for further research.

5-1-2 Conclusions about the results

Generally speaking the simulated time series are in good agreement with the observations. The simulated soil temperature follows the seasonal and daily trends. The model sometimes overestimates the range of the temperatures. The soil moisture is acceptably modelled for both the surface layer and the root zone. No conclusions can be drew about the third layer, since no observations are available at this depth. However the model overestimates the soil moisture in spring, and thus predicts surface runoff when it does not occur. This might come from the underestimation of the evaporation during this period, as seen on the simulated and observed cumulative curve (see figure 4-18). The stream-flow is correctly simulated with a time step of 30 minutes. Nevertheless one can notice that the base-flow is slightly underestimated during long and intense rain events. The comparison of the simulated and observed cumulative flow confirms this remark. The volume predicted by each component could not be assessed separately. Finally the phosphorus module seems to simulate correctly the cumulative discharge of phosphorus. However the lack of data to validate the model does not permit to claim that the phosphorus module is robust.

5-2 Suggestions for further research

5-2-1 Extension to other catchment areas

The present study is restricted to the simulation of only one small catchment area (15 ha). That means that parameters for only one type of vegetation and one soil profile have been explored. It would be of great interest to see if this model could be applied on another catchment, of approximately the same size to neglect the effect of flow routing and investigate if parameters could be fitted to represent this catchment.

If the model performs appropriate simulations for different types of vegetation or different soil textures, then a possible extension would consist in applying this SVAT parameterization on Hydrological Response Units (HRU) in order to represent a larger catchment area. An HRU is defined as a subcatchment considered homogeneous with regard to the meteorological forcing data, the vegetation and the soil (this principle is used in the SWAT model for example). The definition of a flow routing process would be necessary in that case to link the HRUs.

The model presented in this study focused on the representation of the hydrological mechanisms at point scale. Thus it does not take explicitly into account the topography of the catchment. This model could then be used as a grid cell of a 2-dimensional model integrating topography, even though it would probably increase the complexity. This kind of model would allow to work at different spatial scales.

5-2-2 On the same grassland catchment

Further research can also be carried out on the same catchment area. The continuous data coming from the field still need to be explored. Thus, a link between the SVAT model with a CO_2 fluxes model could be considered. The evapotranspiration could be simulated by an additional module based on the modelling of CO_2 fluxes. It would provide a more accurate and more detailed representation of the processes involved. Mechanisms that are not taken into account could then be modelled, like, for instance, the plant growth.

As for the soil moisture simulation the soil properties could be investigated in details. The concept of field capacity still needs to be more precisely detailed and the properties of this soil parameter remain quite uncertain. Likewise the theory of macropores is an open field for research. It requires more observations and experiments on the field. Furthermore a more robust simulation of soil moisture could be achieved by implementing the theory of assimilation. A framework is presented in Montaldo et al.(2001).

As discussed in chapter 3, the soil moisture is crucial in the water balance. Further measurements of soil moisture could be performed deeper than the current measurements to give a better comprehension of the soil moisture profile. A water table sensor could also be installed to measure the depth and variation of the water table. The definition of the depth of the third layer d_3 could then be defined more accurately (see chapter 3-3).

Further measurements also need to be achieved for the validation of the phosphorus module. As discussed in chapter 4, it would be of great interest if the model could be applied for the assessment of strategies of management of the grassland.

References

References

Abbaspour, K., C., Schulin, R., van Genuchten, M., Th., Estimating unsaturated soil hydraulic parameters using ant colony optimization, Advances in Water Resources, 24, 827-841, 2001.

Albertson, J. D., Kiely, G., On the structure of soil moisture time series in the context of land surface models, J. Hydrol., 243, 101–119, 2001.

Beven, K. J., and P. Germann, Macropores and water flow in soil, Water Resour. Res., 18(5), 1311–1325, 1982. Soc. Am. J., 46(1), 93–99, 1982.

Beven, K., J., Franks, S., W., Functional similarity in landscape scale SVAT modelling, Hydrology and Earth System Sciences, 3(1), 85-93, 1999.

Boone, A., Calvet, J., C., Noilhan, J., Inclusion of a third soil layer in a land surface scheme using the force-restore method, J. Appl. Meteor. 38, 1611–1630.

Brontsert, A., Plate, E., J., Modelling of runoff generation and soil moisture dynamics for hillslopes and micro-catchments, J. Hydrol., 198, 177-195, 1997.

Brutsaert, W., A concise parameterization of the hydraulic conductivityof unsaturated soils, Advances in Water Resources, 23, 811-815, 2000.

Brutsaert, W., Evaporation Into the Atmosphere: Theory, History, and Applications, 299 pp., Kluwer Acad., Norwell, Mass., 1982.

Brutsaert, W., On a derivable formula for long wave radiation from clear skies, Water Resour. Res., 11(5), 742–744, 1975.

Clapp, R. B., G. M. Hornberger, Empirical equations for some soil hydraulic properties, Water Resour. Res., 14, 601–604, 1978.

Deardorff, J. W., Efficient prediction of ground surface temperature and moisture, with inclusion of a layer of vegetation, J. Geophys. Res., 83, 1889–1903, 1978.

Desborough, C., E., Pitman, A., J., Irannejad, P., Analysis of the relationship between bare soil and soil moisture simulated by 13 land surface schemes for a simple non-vegetated site, Global Planet. Change, 13, 47–56, 1996.

Franks, S., W., Beven, K., J., Quinn, P., F., Wright, I., R., On the sensitivity of soil-vegetation-atmosphere transfer (SVAT) schemes : equifinality and the problem of robust calibration, Agric. For. Meteorol., 86, 63-75, 1997.

Gagné, C., Gravel, M., Price, W., L., Optimisation par colonie de fourmis pour un problème d’ordonnancement industriel avec temps de réglages dépendants de la séquence, MOSIM, 4 2001

Habets, F., Noilhan, J., Golaz, C., Goutorbe, J., P., Lacarrère, P., Leblois, E., Ledoux, E., Martin, E., Ottlé, C., Vidal-Madjar, D., The ISBA surface scheme in a macroscale hydrological model applied to the Hapex-Mobilhy area. Part I : Model and database, J. Hydrol., 217, 75-96, 1999.

Habets, F., Noilhan, J., Golaz, C., Goutorbe, J., P., Lacarrère, P., Leblois, E., Ledoux, E., Martin, E., Ottlé, C., Vidal-Madjar, D., The ISBA surface scheme in a macroscale hydrological model applied to the Hapex-Mobilhy area. Part II : Simulation of streamflows and annual water budget, J. Hydrol., 217, 97-118, 1999.

Henderson-Sellers A, McGu†e K, Pitman AJ. The Project for Intercomparison of Land-surface Parameterization Schemes (PILPS): 1992 to 1995. Climate Dynamics 1996;12:849±59.

Henderson-Sellers, A., Pitman, A.J., Love, P.K., Irannejad, P., Chen, T.H., 1995. The project for intercomparison of landsurface parameterization scheme PILPS : phases 2 and 3. Bull. Am. Meteorol. Soc. 76, 489–503.

Henderson-Sellers, A., Soil moisture simulation : achievements of the RICE and PILPS intercomparison workshop and future directions, Global Planet. Change, 13, 145–159, 1996.

Kutílek, M., Nielsen, D., R., Soil Hydrology, Catena Verl., 1994., ISBN 3-923381-26-3.

Mengelkamp, H. T., Kiely, G., Warrach, K., Evaluation of the hydrological components added to an atmospheric land-surface scheme, Theor. Appl. Climatol. 69, 199-212, 2001.

Mengelkamp, H. T., Warrach, K., Raschke, E., SEWAB - a parameterization of the Surface Energy and Water Balance for atmospheric and hydrologic models, Advances in Water Resources, 23, 165-175, 1999.

Mihailović, D., T., Description of a land-air parameterization scheme (LAPS), Global Planet. Change, 13, 207–215, 1996.

Mihailović, D., T., Rajković, B., Lalić, B., Jović, D., Partitioning the land surface water simulated by a land-air surface scheme, J. Hydrol., 211, 17-33, 1998.

Montaldo, N., Albertson, J.D., Mancini, M., Kiely, K. Robust simulation of root zone soil moisture with assimilation of surface soil moisture data, Water Resour. Res., 37(12), 2889–2900, 2001.

Nathan, R. J., and T. A. McMahon, Evaluation of automated techniques for base flow and recession analyses, Water Resour. Res., 26(7), 1465–1473, 1990.

Noilhan, J., and J.-F. Mahfouf, The ISBA land surface parameterization scheme, Global Planet. Change, 13, 145–159, 1996.

Noilhan, J., and S. Planton, A simple parameterization of land surface processes for meteorological models, Mon. Weather Rev., 117, 536–549, 1989.

Noilhan, J., Planton, S., 1989. A simple parameterization of land surface processes for meteorological models. Monthly Weather Rev. 117, 536–549.

Parlange, M., B., Hopmans,J., W., Vadose zone hydrology, Cutting across disciplines, Oxfors University Press, 1999, ISBN 0-19-510990-2.

Scanlon, T., M., Raffensperger, J., P., Hornberger, G., M., Shallow subsurface storm flow in a forested headwater catchment : observations and modelling using a modified TOPMODEL, Water Resour. Res., 36(9), 2575–2586, 2000.

Schmid, A., P., Experimental design for flux measurements : matching scales of observations and fluxes, Agric. For. Meteorol., 87, 179-200, 1997.

Sellers PJ, Mintz Y, Sud YC, Dalcher A. A simple biosphere model (SiB) for use within general circulation models. J Atmos Sci, 1986;43:305±31.

Shao, Y., Henderson-Sellers, A., Validation of soil moisture simulation in landsurface parameterisation schemes with HAPEX data, Global Planet. Change, 13, 11–46, 1996.

Singer, M., J., Munns, D., N., Soils : an introduction ; Fifth edition, Prentice Hall, ISBN 0-13-027825-4.

Sloto, R., A., Crouse, M., Y., HYSEP : a computer program for streamflow hydrograph separation and analysis, Water Resources Investigations Report 96-4040, U.S. Geological Survey.

Stephens, D., B., Vadose zone hydrology, CRC Press, 1996, ISBN 0-87371-432-6.

Wallach, R., Zaslavsky, D., Lateral flow in a layered profile of an infinite uniform slope, Water Resour. Res., 27(8), 1809–1818, 1991.

Whitehead, D., C., Nutrient elements in grassland, Soil-plant-animal-relationships, CABI Publishing, 2000, ISBN 0 85199 437 7.

Glossary of terms

Advection
- Fluid migration induced by hydraulic gradients.
- The movement of a quality, such as heat, or humidity, due to the flow of the fluid possessing that property. In meteorology, the term is usually applied to the horizontal transfer of heat (compare with convection).

Albedo
- A measure of the reflecting power of a non luminous object, such as a planet or natural satellite or a surface feature on such a body. It is the ratio of the amount of light reflected in all directions from the object to the amount of incident light. Clouds, snow, and ice have high albedos while volcanic rocks have very low albedos.
- The proportion of insolation that is reflected back from the Earth, from the tops of the clouds, and from the atmosphere, without heating the receiving surface. It averages about 30%, but varies widely according to the substance and texture of the surface, and the angle and wavelength of the incident radiation. The value for green grass and forest is 8-27% (over 30% for yellowing deciduous forest in autumn); for cities and rock surfaces, 12-18% (over 40% for chalk and light-coloured rock and buildings); for sand up to 40%; for fresh, flat snow up to 90%; and for calm water only 2% in the case of vertically incident radiation but up to 78% where there is a low angle of incidence. The albedo for cloud surfaces averages 55%, but can be up to 80% for thick stratocumulus.

Fresh snow	40-70 %
Dry sand	35-45 %
Wet sand	20-30 %
Tarmac	5-10 %
Grassland	10-20 %
Coniferous forest	5-15 %
Deciduous forest	10-20 %
Crops	15-25 %

Lighter, whiter bodies have higher albedos than darker, blacker bodies.
The total albedo of the earth is about 35%.

ARME
Amazon Region Meteorological Experiment

Baseflow (dry weather flow)
In a stream or river, the flow of water derived from the seepage of groundwater, and/or throughflow into the surface watercourse. At times of peak river flow, baseflow forms only a small proportion of the total flow, but in periods of drought it may represent nearly 100%, often allowing a stream or river to flow even when no rain has fallen for some time

Biome
A major ecological community or complex of communities that extends over a large geographical area characterized by a dominant type of vegetation. The organisms of a biome are adapted to the climate conditions associated with the region. There are no distinct boundaries between adjacent biomes, which merge gradually with each other. Examples of biomes are tundra, tropical rainforest, taiga, chaparral, grassland (temperate and tropical), and desert.

Bowen's ratio
The ratio of sensible heat to latent heat. In arid zones, β values are much greater than unity; in humid zones they are much below unity.

Bulk density
Mass of dry soil per unit volume of bulk soil.

Canopy
The uppermost layer of vegetation in a forest, consisting of the tops of trees forming a kind of ceiling. Also called crown canopy

Capillary fringe
That part of the vadose zone immediately above a water table where the media is satiated but the water is under tension.

Deep percolation
Infiltration below the root zone depth, usually in the context of irrigation.

Dew	Water droplets that are deposited on exposed surfaces during calm, clear nights, when the ground loses heat by radiation to the sky and causes the air in contact with it to become saturated. It usually forms on the tops of plants, especially the tips of grass, in places where there is a continuous vegetation cover. The water vapour is derived partly from the air and, for as long as the ground temperature remains above the dew-point, partly by evaporation from the soil. The dew-point is the temperature at which the water vapour in the air becomes saturated (the maximum amount of water vapour that the air can hold) and condenses on an available surface to form tiny droplets of dew.
Dispersivity	A characteristic of the geological medium attributed to the tortuosity and heterogeneity that affects mechanical mixing of chemicals during advection.
Eddy-correlation	In the Reynolds-averaged equations, the vertical flux of a scalar C is the average value of the correlation between the vertical velocity fluctuation and the scalar fluctuation, $\langle w'C' \rangle$. This is referred to as the eddy-correlation flux measurement.
Emissivity	Symbol ε. The ratio of the power per unit area radiated by a surface to that radiated by a black body at the same temperature. A black body therefore has an emissivity of 1 and a perfect reflector has an emissivity of 0. The emissivity of a surface is equal to its absorptance.
EOS	Earth Observation System
Fallow land	Agricultural land which is not used for crops but is left unused in order to restore its natural fertility. **Summer fallow** is the practice of leaving the ground uncultivated during a long, dry spell.
Fetch	**1**. Length of water surface over which the wind blows in generating waves. Together with wind velocity and duration, this determines wave height. Many features of coastal deposition tend to become orientated normally to the direction of maximum fetch. **2**. Distance over which an airstream has travelled across sea or ocean.
GER	Global Environment Project
GEWEX	Global Energy and Water cycle Experiment
HAPEX	Hydrological Atmospheric Pilot Experiment
Hydraulic conductivity	The ability of a soil or rock to conduct water. The conductivity of dry soil or rock is low (dry hydraulic conductivity); little water is conducted since water entering a soil must form a film of water surrounding the soil particles. Until these films are formed, little conduction occurs. Saturated hydraulic conductivity refers to the maximum rate of water movement in a soil. High values → aquifer can readily transmit water. Low values → poor transmissibility. Unit = cm/sec = ($cm^3.cm^{-2}.sec^{-1}$)
IGBP	International Geosphere-Biosphere Project
ISLSCP	International Satellite Land Surface Climatology Project

Latent heat	The energy absorbed or released by a substance when it changes its physical state (e.g. from liquid to solid) at the same temperature. The energy released as latent heat when a liquid changes to a solid is equal to the energy absorbed when such a change of state occurs in the reverse direction. Values can be large. For example, ice at 0°C absorbs almost as much energy in changing to liquid water as is needed to heat this water from 0°C to 100°C; and it takes over six times as much energy again to change water at 100°C into steam at the same temperature. Thus the latent heat of vaporization is the energy a substance absorbs from its surroundings in order to overcome the attractive forces between its molecules as it changes from a liquid to a gas and in order to do work against the external atmosphere as it expands. The specific latent heat is the heat absorbed or released by unit mass of a substance in the course of an isothermal change of state.
Leaf Area Index	The total surface area of the leaves of plants in a given area divided by the area of ground covered by the plants. In an area of dense vegetation, such as a forest, the LAI will be high.
Matric potential	- Energy required to remove water from soil grains. It results from adsorption and capillarity. It reduces free energy of water and affects water movement. The matric potential χ is always negative. - Water molecules can form hydrogen bonds with the surface of soil minerals (adsorption) as well as with other water molecules (cohesion). In soil, adsorptive forces develop between the soil mineral surfaces and the soil water. These forces exert a "pull" on the soil water. This pull between the soil and the water molecules close to the particle surface is distributed throughout the soil water by the cohesive forces between water molecules. As external forces attempt to remove water from the soil, water is restrained or held in the soil by these adhesive and cohesive forces. This places the soil water under tension. This tension or pull on the soil water causes the potential energy of the water to decrease relative to *free* water (i.e., water not held under tension). Therefore, water in soil can be held under tension because of the adsorption of water to the soil particles. Water held under tension has less potential energy per unit quantity of water than reference water (free water); therefore has a lower water potential. The decrease in water potential caused by the adsorption of water to the soil surfaces is called the Matric Potential component of the soil water potential.
Mulch	Layer of wet straw, leaves, or plastic, etc., spread around or over a plant to enrich or insulate the soil. *v.* treat with mulch.
Roughness length	The term roughness length is really the distance above ground level where the wind speed theoretically should be zero.
Stomatal resistance	Stomatal resistance is a measure of the aperture size of the stomates. As such, the stomatal resistance governs the flow of water vapor through the stomates. Since there are thousands of stomates on a leaf, the individual resistance for all the stomates are added together in parallel (the inverse of the sum of the inverse resistances for each stomate) to equal the average stomatal resistance for the leaf.
Sub-surface flow	The flow of water at a shallow depth beneath the ground surface, that occurs when rain falls faster than it can infiltrate downwards. The sub-surface flow re-emerges at the surface at or near the base of ground slopes.

Thermal conductivity	A measure of the ability of a substance to conduct heat. For a block of material of cross section A, the energy transferred per unit time E/t, between faces a distance, l, apart is given by $E/t = \lambda A(T_2 - T_1)/l$, where λ is the conductivity and T2 and T1 are the temperatures of the faces. This equation assumes that the opposite faces are parallel and that there is no heat loss through the sides of the block. The SI unit is therefore $J\ s^{-1}\ m^{-1}\ K^{-1}$.
Watershed	The dividing line, usually a ridge, between the catchment areas of two separate river systems. In the USA the term is used for the entire catchment area of the drainage basin.
Wilting point	- The point at which a plant has to supply water from its own tissues for transpiration when the soil moisture is exhausted. - The percentage of water remaining in the soil after a specified test plant has wilted under defined conditions, so that it will not recover unless it is given water.